RADC-TR-65-77
Final Report

OPTIMUM RADAR SURVEILLANCE MODE STUDY PROGRAM

Harold M. Finn

TECHNICAL REPORT NO. RADC-TR-65-77
September 1965

Techniques Branch
Rome Air Development Center
Research and Technology Division
Air Force Systems Command
Griffiss Air Force Base, New York

OPTIMUM RADAR SURVEILLANCE MODE STUDY PROGRAM

Harold M. Finn

AFLC, GAFB, N.Y., 8 Oct 65-139

FOREWORD

This is the report of the second phase of the Optimum Radar Surveillance Mode Study Program being sponsored by Rome Air Development Center under AF Contract No. 30(602)-3152. Direction of the program is provided by R. Ackley and T. Maggio of RADC.

The program is being conducted at RCA's Missile and Surface Radar Division, Moorestown, N. J. H. M. Finn, the author of the report, developed the EVSD modes and performed the reported analyses and optimizations. R. S. Johnson is responsible for the digital computer implementation of the Optimization procedures employed. C. Hughes contributed to the implementation study and to the design of the resolution-variant signal processor for pseudo-random phase-reversal code transmissions. R. Bergman, M. Cooperman, and D. Crosby provided the required high-speed digital technology for the synthesis of this signal processor. S. D. Gross is the RCA program manager.

This technical report has been reviewed and is approved.

Approved: Richard A. Ackley
RICHARD A. ACKLEY
Project Engineer

Approved: Alfred M. Starkey
THOMAS [illegible], JR.
Colonel, USAF
Chief, Surv & Control Division

FOR THE COMMANDER: Irving J. Gabelman
IRVING J. GABELMAN
Chief, Advanced Studies Group

ABSTRACT

A second-phase study of radar multiple-stage decision processors which minimize the average transmitter power and data processing costs for performing the surveillance mission are described. Energy Variant Sequential Detector (EVSD) theory is reviewed. A verification of theoretical performance predictions obtained with a digital computer simulation program reveal a deviation of simulated performance of less than 1 percent of predicted results.

A sequential detection scheme for performing high-resolution surveillance missions where relatively large time-bandwidth products are involved is described. These modes (designated as Resolution-Variant EVSD's) use the programmed control of the time-bandwidth product of the transmitted signal, the transmitted energy, and the receiver thresholds on the sequential steps employed in order to minimize both the transmitter power and the parallel signal processing costs. An active correlator system is concluded to be the most economical means for meeting the signal processor flexibility requirements for this mode, and the implementation of a Resolution-Variant EVSD where requirements include over a 150-MC bandwidth on the final sequential step is described. The resolution-variant signal processor required for efficient performance of future high-resolution surveillance missions is determined to be a critical component requiring further development.

General implementation of EVSD's are reviewed. Only in the case of the high resolution surveillance mission is a critical component involved. In general, the radar implementation of EVSD's are concluded to be well within the state of the design art, and moreover they are shown to avoid implementation problems associated with other sequential detection modes.

The optimum scan time to be used when EVSD's are employed for each scan look is developed for both the case where the target is pointing directly at the radar, and the second case where the target range is assumed relatively constant for the time duration in the surveillance volume.

EVSD modes which include an option on the time interval between sequential steps are described, and the additional power savings over the use of a conventional EVSD are computed.

TABLE OF CONTENTS

TABLE OF CONTENTS (Continued)

LIST OF ILLUSTRATIONS

SECTION 1

INTRODUCTION

1.1 SUMMARY

This report summarizes the work performed on the second phase of the Optimum Radar Surveillance Mode Study sponsored by RADC and performed at RCA Moorestown, N.J. covering the period from June 1964 to February 1965. This phase of the program has been directed toward extending the theory and application of the Energy-Variant Sequential Detector (EVSD) class of radar detection mode, obtaining a verification by means of simulation of the predicted performance of EVSD's, an investigation of the implementation of these modes, and, in particular, the determination of any critical component areas.

A basically new class of multiple-stage decision processor was evolved during the first phase of the subject program (Reference #1, 2, and 3) for the performance of the surveillance mission in modern electronically steerable-array radar systems. By properly utilizing the degrees of freedom inherent in such a radar system, these detection modes, designated as Energy-Variant Sequential Detectors (EVSD's), are specifically designed to both minimize the average transmitter power requirements without encountering the performance and implementation problems associated with the use of the Wald sequential probability ratio test.

The basic design approach has initially involved forming a multiple stage decision processor framework which is compatible with the radar requirements (the maximum number of steps is kept low, and the decision statistics are kept simple). Then the radar parameters expected to yield a 'pay off' in minimizing the average transmitter power requirements are introduced as degrees of design freedom at

each of the sequential steps. (For the basic EVSD, these degrees of design freedom are the transmitted energy, the receiver threshold, and the number of statistically independent target cross section samples. The Resolution-Variant EVSD includes the time-bandwidth product at each step as an added set of design variables.) Analytical expressions of the detection and false alarm probabilities and the average transmitter power cost are formulated for the assumed additive white noise at the receiver, matched-filter reception at each sequential step, and the selected decision-processor framework. These expressions are a function of the introduced design degrees of freedom. A classical optimization procedure is then employed to determine the 'settings' at each sequential step of the introduced degrees of design freedom which minimize the cost function and satisfy the constraint relationships--the detection and false alarm probabilities.

In this manner, practical and efficient detection modes were developed to cover a wide range of surveillance conditions. In the first phase study report (Reference #1), families of EVSD design and performance parameters are presented for the non-fluctuating target and the Swerling Cases #1 through #4 where the surveillance requirements include probability of detection in the range of 0.5 to 0.95, single-cell false alarm probabilities from 10^{-6} to 10^{-10} and where the effective number of resolution cells covered the range of one to 2000 cells. The theory and details of the optimization procedure are also presented in that report.

The significant average transmitter power savings predicted for EVSD's, coupled with other generally promising features, has motivated the broadening of the scope of the study to include the specializing of these modes for specific radar surveillance and acquisition missions, a simulation of performance in order to verify performance predictions, and a study of implementation.

An important achievement of the program has involved the development of a sequential detection scheme (the Resolution-Variant EVSD) for performing the typical high-resolution surveillance missions of the future. The typically large number

of fine resolution cells required to cover the parameter space of interest for the high resolution mission results in reduced detection efficiency and a large parallel signal processing requirement - both of these effects lead to very high implementation costs. Since the trend is toward higher resolution requirements, a significant portion of the program has been directed toward the design of a practical detection scheme overcoming these high cost factors.

1.2 CONCLUSIONS

A summary and some conclusions of the conducted second phase of the program are presented below:

1.2.1 RESOLUTION-VARIANT EVSD

The Resolution-Variant EVSD (RV EVSD) (see Section 5) is shown to overcome the major implementation problems involved in the performance of high-resolution surveillance missions of the future where relatively large time-bandwidth products are required in order to achieve a specified final resolution cell size. The large number of resolution cells involved in many high resolution surveillance missions preclude the use of more conventional sequential detection modes (even of the EVSD type) where the same resolution cell size is employed on each sequential step. This is the case since the average power saving over the use of a uniform search mode is a monotonically decreasing function of the number of resolution cells employed, and for the case, say, where a million resolution cells are involved, the savings are negligible with a conventional sequential detection mode. The implementation of the great number of parallel signal processing channels involved is an additional problem. The RV EVSD is specifically designed to overcome these problems and accomplishes a minimization of both the average transmitter power and parallel signal-processing channel requirements. The design strategy for effecting this optimization, roughly speaking, involves the introduction of the time-bandwidth product at each sequential step as an additional set of degrees of design freedom in

an EVSD framework; and the use of a 'boot-strap' operation that involves 'telescoping' to a final fine resolution cell size by stepping up the time-bandwidth product in controlled amounts on successive sequential steps. When this strategy is combined with the use of an active correlator system on reception, a commonality of equipment usage is also effected. Range-doppler coordinates of cells exhibiting threshold crossings are communicated from one sequential step to another so that the parameter space 'search' is restricted and the number of parallel processing channels reduced. The RV EVSD also enables the necessary compensation for doppler envelope compression or expansion as well as carrier frequency shifts with a minimum hardware requirement.

1.2.2 CRITICAL COMPONENT

The active correlator signal-processing system required to effect matched-filter conditions on each sequential step of a Resolution-Variant EVSD designed for high-resolution surveillance radars where the bandwidth requirements exceed 100 MC is determined to be a critical component requiring further development. Emphasizing the importance of the development of this component is the fact that most surveillance missions of the future are of the high-resolution type and that system costs would be excessive if conventional detection modes were employed. The Resolution-Variant EVSD offers the potential of economical performance of this mission. The application of high-speed digital techniques is involved in the development of the active correlator system.

1.2.3 GENERAL IMPLEMENTATION CONSIDERATIONS

Only in the case of the high-resolution mission is there a critical component program called for. In general, the implementation of EVSD's are concluded to be well within the state of the design art. In fact, these modes are designed to overcome the performance and implementation problems associated with the application of Wald's sequential probability ratio test to the radar surveillance mission, and

yet maintain comparable or greater average power savings. By using a relatively simple decision statistic rather than the likelihood ratio, data-processing requirements are alleviated; and by limiting the maximum number of sequential steps to only two or three, the 'hang-up' phenomenon associated with the performance of the sequential probability ratio test based radar modes is eliminated. The increase in energy requirements on successive steps of an EVSD can be accomplished by employing standard pulses with the number in a pulse train on a sequential step made compatible with the energy requirements of that step. Conventional radar integration techniques are involved. Indicative of the practical nature of these modes is the fact that conventional high-inertia beam steering radars can be adapted for their use.

1.2.4 EVSD SIMULATION PROGRAM

A verification of the predicted performance of specific radar surveillance missions when employing an EVSD mode has been obtained with a simulation program implemented on the IBM 7090 digital computer (see Section 4). In general, deviations of the simulated test performance were less than 1 percent of the computed results for representative EVSD's designed for the detection of each of the five target types considered in the program. This verification, coupled with the fact that the relatively simple decision processor framework of EVSD's yield closed form expressions of performance, lead to the conclusion that a relatively high degree of confidence can be placed in theoretical predictions of EVSD performance.

The simulation program is designed with sufficient flexibility so that it can be employed as a general research tool in the further development of detection modes. An indication of this flexibility, is the ability of the simulation program to check surveillance mismatch conditions (i.e., a simulation of the case where the stochastic properties of the 'actual' target encountered differs from those hypothesized in the EVSD test design).

1.2.5 SCAN TIME OPTIMIZATION

EVSD's have now been developed (see Section 6) for those applications where a number of sequential detection scan 'looks' of a target in the surveillance volume is permissible and a minimization of the average transmitter power is required for detecting the target on at least one of the scan looks with a prescribed cumulative detection probability. The target type, false alarm probability, and effective number of resolution cells are other specifications for this mission. An additional degree of design freedom which is introduced in order to obtain the desired power minimization is the scan time which determines for a given trajectory the average number of scan looks and the allowable integration time for each beam position 'look'. Optimizations have been effected for the two extreme cases of orientation of the target vector relative to the search beam. One case involves the target velocity vector 'pointing' directly at the radar. This optimization would apply for a low clutter environment acquisition phase of an area defense mission. The second one considered is a space surveillance case where the assumption can be made that the target range is relatively constant for the duration of time it is in the surveillance volume. EVSD's are concluded to be practical and efficient modes for both applications when the proper scan time is employed. This scan time is necessarily a function of the stochastic properties of the target type involved and is specified in Section 6.

1.2.6 EVSD'S WITH A CONFIRMATION DELAY TIME OPTION

The effect of introducing in EVSD designs an option on the time interval employed between sequential steps was the subject of study, and optimizations were effected with this added design strategy (see Section 7). Roughly speaking, the delay-time option EVSD mode combines the previously developed EVSD decision-processor framework for the Case #2 and #4 targets with an optional mode which is introduced when any of the N_1 first step pulses is very large, and the best policy would involve 'packing' the second-step energy immediately into a confirmation step.

For this event, the probability is assumed to be large that a target is presenting itself at a favorable (large) cross section, therefore, providing the motivation to confirm within a time interval which is small relative to the target correlation time so that the target may be 'caught' at its favorable cross section.

Additional power savings with the use of this mode over those obtainable with a conventional EVSD were determined to be less than 1/2 db for the Case #2 target; not enough for most surveillance situations to justify the use of this more elaborate mode of operation. This confirmation delay time option mode, however, may offer a greater pay-off for target types adhering to probability descriptions other than those considered in the program. The optimization achieved also demonstrates the capability of the analytical optimization procedure employed to accommodate both additional design constraints and degrees of design freedom.

1.3 PLANNED THIRD PHASE CRITICAL COMPONENT DEVELOPMENT PROGRAM

The planned third phase of the subject contract is essentially a preliminary design and development phase of a program leading to the development of a Resolution-Variant EVSD signal processor capable of meeting the flexibility requirements of an RV EVSD, and a final bandwidth requirement of over 150 MC (see Section 5). The program will also demonstrate the hardware economy and power savings of a Resolution-Variant EVSD. This planned program to develop the multiple stage resolution-variant signal-processing techniques required to efficiently fulfill the typical high-resolution surveillance missions of the future involves concurrent efforts in the systems analysis and synthesis areas and in the development of critical circuitry. High-speed digital technology will be applied to the development of the active correlator system. Since the signal processor flexibility requirements for a Resolution-Variant EVSD are similar in significant respects to those of other important high-resolution radar missions, this development program takes on added significance.

SECTION 2

EVSD DESIGN APPROACH

A relatively detailed description of the basic EVSD theory, the decision processor framework employed, and the analytical formulation of the optimization procedure is presented in Reference #1. A summary, however, of the basic approach employed in the development of efficient and practical radar surveillance modes for electronically steerable array radar systems is presented here in order to provide a needed continuity to the report.

2.1 BASIC COMPONENTS OF A RADAR SEQUENTIAL DETECTION MODE

A functional diagram of a radar as seen from the viewpoint of performing the radar surveillance mission is presented in Figure 1. It will aid in a review of the basic components of a radar sequential detection mode.

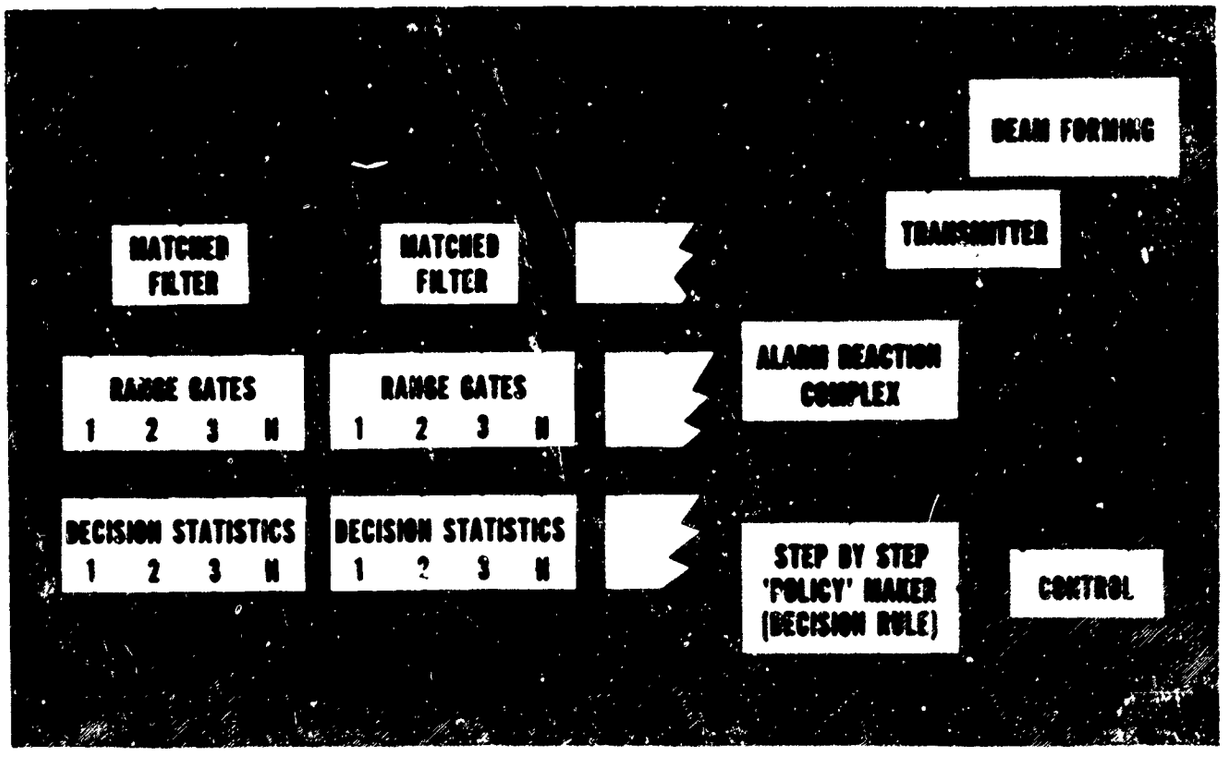

Figure 1. Radar Sequential Detection Mode

We imagine the beam of an electronically steerable array scanning the surveillance volume for the presence or absence of a target and we formalize this surveillance procedure at every beam position as a statistical hypothesis test.

What are the basic ingredients of such a test?

First — the contiguously spaced set of filters, each matched to a return signal from one of the admissible combinations of target range and range derivatives. These filters are the resolution cells, so to speak, which are examined for the presence or absence of a target. The noise samples from each of these cells are assumed to be statistically independent.

The decision statistics follow these filters and are functions of the observables (the sampled matched-filter outputs) and are employed in deciding upon the subsequent radar policy.

A decision rule is next required to determine which of the three possible courses of action to take on a sequential step.

If we decide that no target is present in any of the resolution cells, we terminated the test at that beam position and move to a new one. And if the target-present hypothesis is accepted, we invoke an alarm reaction, typically the initiation of a tracking mode.

But what if we defer the making of a decision? If Wald's sequential probability ratio test were used (Reference # 4), we would simply request another step or experiment exactly the same as in the preceding steps. Translated into radar terms, this would mean employing the same transmission and reception characteristics. Actually, however, a number of the radar parameters which influence the detection process are available for change at a sequential step, in addition to the 'zero-inertia' beam-steering capability of the array. These degrees of freedom include the transmitted energy, the time-bandwidth product, the number of statistically

independent target cross-section samples, the time interval between sequential steps, and the decision processor thresholds. So one question we seek an answer to is the following: How does one use the degrees of freedom to minimize the costs of performing the surveillance mission?

2.2 RADAR DETECTION BASED ON THE SEQUENTIAL PROBABILITY RATIO TEST

To provide a better perspective for the sequential detection modes we have developed (the EVSD Class), some aspects of a detection mode based on the use of the sequential probability ratio test are first reviewed. (Radar detection modes based on the use of the sequential probability ratio test are treated in References #5 through 9).

First — The sequential probability ratio test can be shown (Reference #10) to be an implementation, roughly speaking, of the following logic: If, at a sequential step, the expected cost can be further reduced by an additional experiment of the same type as the preceding ones — it is taken. This logic introduces questions relating to the optimum use of the radar degrees of design freedom which would permit a change of experiment at a sequential step, i.e. a change of the transmission, reception, and data processing requirements. The sequential probability ratio test is only optimum (Reference #11) for the class of tests involving the same 'experiment' at each of the conducted steps.

A second point is that, for a domain of values of signal-to-noise ratio below that employed in the test design (i.e. in formulating the likelihood ratio), the expected test length (Average Sample Number) is greater than the value for the design signal-to-noise ratio. That is to say, for lower signal-to-noise ratios, the decision statistic which undergoes a random walk between the two real numbers employed as thresholds (see Figure 2) hovers longer, on the average, in the no-decision zone. (References #5 and #9). In its pure form, this test is also one without a truncation point.

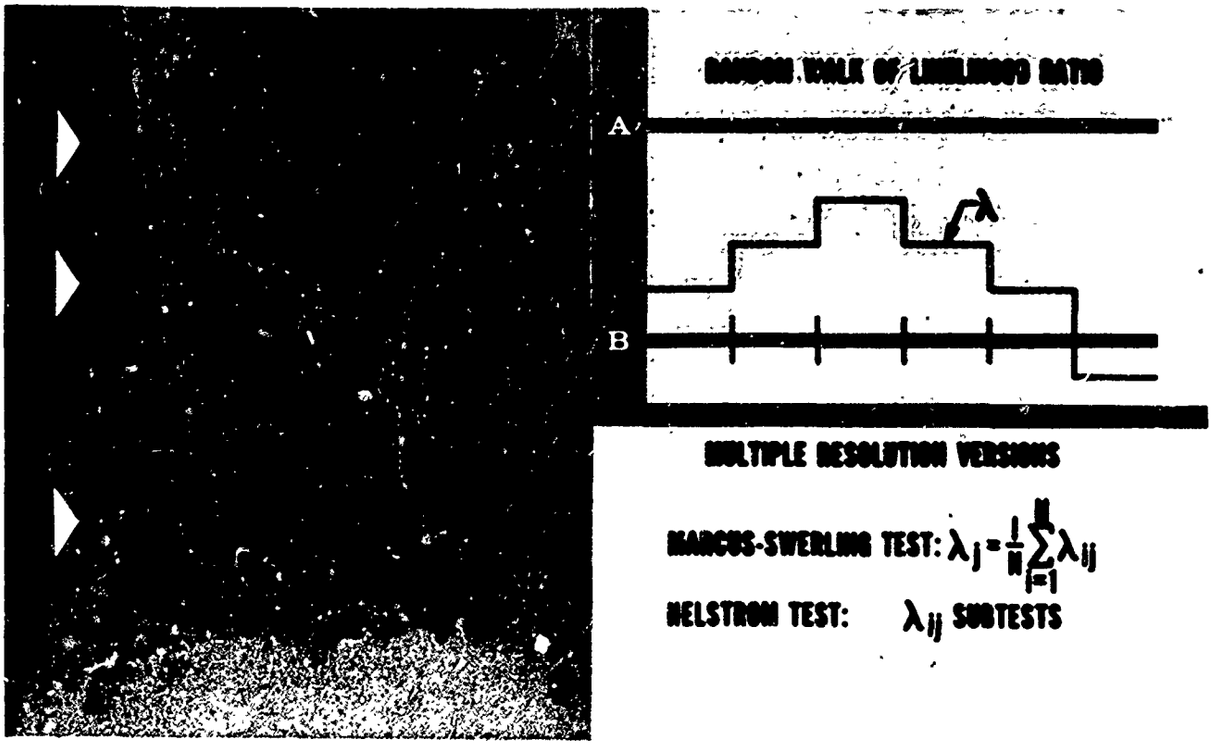

Figure 2. Radar Detection Based on the Sequential Probability Ratio Test

Another source of difficulty with this classical test involves the decision statistic employed, the likelihood ratio. The decision statistic at the i^{th} resolution element for the j^{th} step of the sequential probability ratio test (L_{ij}) is generated by forming the ratio of the conditional or posteriori probabilities of having observed the sampled receiver outputs $\{X_{ij}\}$ under the target-present hypothesis (H_1) and the noise-alone hypothesis (H_o). Two multiple-resolution cell versions of this test (See Figure 2) are the one of Marcus and Swerling — where an average likelihood is employed (Reference #9) and the Helstrom test (Reference #8) where separate sub-tests are performed at each resolution cell.

For those target types which are characterized by statistically correlated cross-section samples from look to look (for example, the Case #1 and #3 target types), the formulation of the likelihood ratio is complex and taxing on the resulting data-processing requirements. Since separate decision statistics are required for each active resolution cell and must be updated at each sequential step, the data-processing problem is multiplied.

There is an interest, consequently, in the development of detection modes which overcome some of these difficulties.

2.3 FORMING A COMPATIBLE DECISION-PROCESSOR FRAMEWORK

Rather than use the sequential probability ratio test as the starting point for the development of an effective radar detection mode, the approach which has been taken involves initially specifying a multiple-stage decision-processor framework which is compatible with overall system requirements — then introducing certain of the radar parameters as degrees of design freedom, and determining the setting of these parameters at each stage minimizing the appropriate cost function (the average transmitter power) and satisfying the specified detection and false alarm probabilities.

A list of some of the radar requirements and/or goals, and how they have influenced the developed sequential detection mode framework is presented below:

2.3.1 RELATIVELY PREDICTABLE SCAN PERIODS

The length of this test at a beam position is a random variable with a domain of values extending from one to the maximum number allowed. By limiting this maximum number to only two or three sequential steps, the possibility of an extended test length at a beam position is eliminated. From the performed optimizations, the conclusion is also reached that most of the attainable power savings over the use of a fixed sample size test is realized with a sequential procedure optimized within a framework of a maximum of two steps.

2.3.2 ECONOMICAL DATA PROCESSING

The desire to minimize the data-processing requirements for implementing the sequential detection mode has led to the use of relatively simple decision statistics in EVSD modes. Rather than use the likelihood ratio, the decision

statistic employed is simply the detected matched-filter output. The sampled linearly detected output is used for one of the target classes, the slowly fluctuating class. And the sampled square-law detector output is employed for the other class where the time interval between samples is long with respect to the correlation time of the target so that statistically independent target cross-section samples are obtained.

2.3.3 MINIMUM PARALLEL SIGNAL PROCESSING REQUIREMENTS

For high-resolution surveillance missions, where large time-bandwidth product transmitter waveforms are required and the 'covering' of the parameter space of interest with the fine resolution cell results in a large number of these cells, signal-processing costs are formidable. A design strategy specifically employed to reduce both the parallel signal-processing costs and the average transmitter power is incorporated in a class of detection modes designated as Resolution-Variant EVSD's and involves the introduction of the time bandwidth product as an added degree of design freedom. These modes are considered in detail in Section 5, and involve the increase in time-bandwidth product on successive steps in controlled amounts from a unity time-bandwidth product signal employed on the first step to the required large time-bandwidth product signal of the final sequential step. The reduction in signal-processing requirements results from a commonality of active correlator equipment usage on successive sequential steps, and by the 'boot-strap' approach which involves restricting the parameter space search on successive steps by communicating the range-doppler coordinates of cells with threshold crossings in a coarse-to fine-cell telescoping operation from one sequential step to another.

2.3.4 EFFICIENT USE OF THE RADAR PARAMETERS WHICH CAN BE CHANGED AT A SEQUENTIAL STEP, AND HAVE AN INFLUENCE ON THE PERFORMANCE OF THE RADAR SURVEILLANCE MISSION

These parameters are the design degrees of freedom of the multiple-stage processor optimization procedure and their use depends strongly on the specific radar

surveillance situation (for example, the fluctuating characteristics of the target to be detected, and the resolution requirements for this mission). In general, EVSD's are designed to minimize a cost function made equal to the average transmitter power requirement, since this power is a predominant cost factor for performing the radar mission. The signal and data processing requirements, however, have also influenced the 'setting' of these parameters on each sequential step. Implementation considerations for effecting these sequential step changes are presented in Sections 3 and 5. The optimum settings of these parameters and performance predictions for typical surveillance situations are presented in Figures 3 through 13.

These design degrees of freedom include:

a) The Transmitted Energy: The transmitted energy is a major degree of design freedom, and the sequential step control of the transmitted energy is employed with advantage for all of the surveillance situations considered.

b) Statistically Independent Target Cross-Section Samples: The number of statistically independent target cross-section samples employed on each sequential step is an important degree of design freedom for those surveillance situations which permit a time interval between pulses on a sequential step which is long with respect to the target correlation time. The minimization is a relatively 'broad' one with respect to this design degree of freedom, and a typical set of parameters for a two-step maximum procedure involves the use of three statistically independent samples on the first step and six on the second.

c) Time-Bandwidth Product: The change of the transmitter time-bandwidth product at each sequential step is an important degree of design freedom for high-resolution surveillance missions where large time-bandwidth signals are required. The use of this degree of freedom to minimize parallel signal-processing costs is discussed in greater detail in Section 5. This degree of freedom is also important in effecting a minimization of the transmitter power requirement for the high-resolution

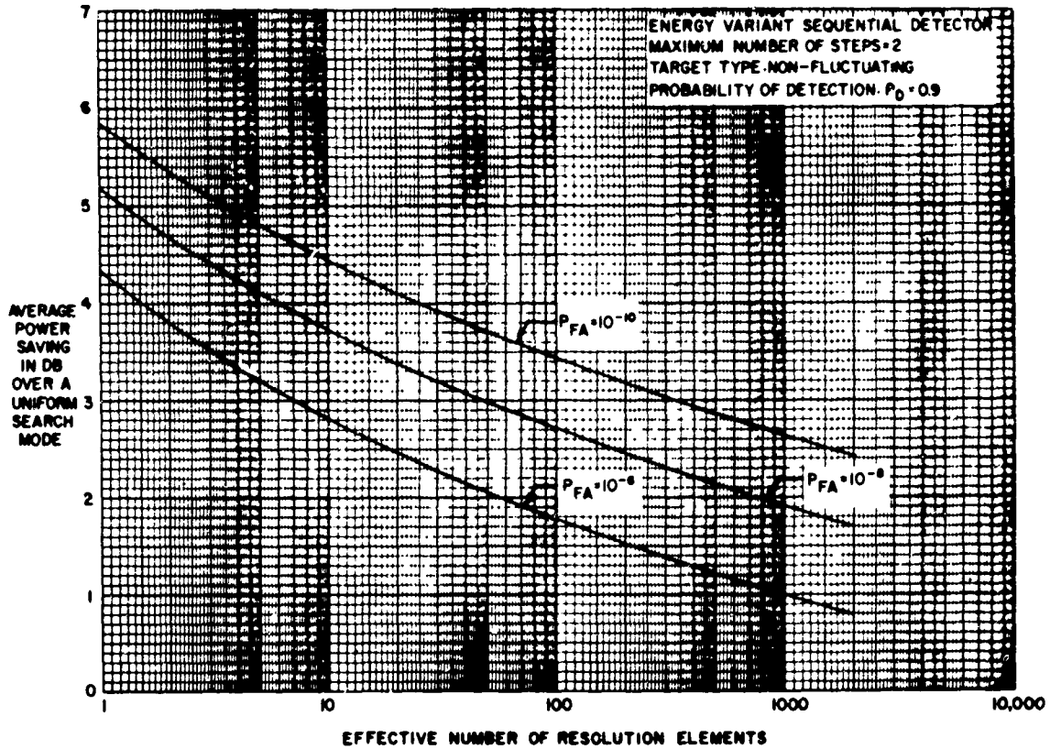

Figure 3. Average Power Saving, Non-Fluctuating Target

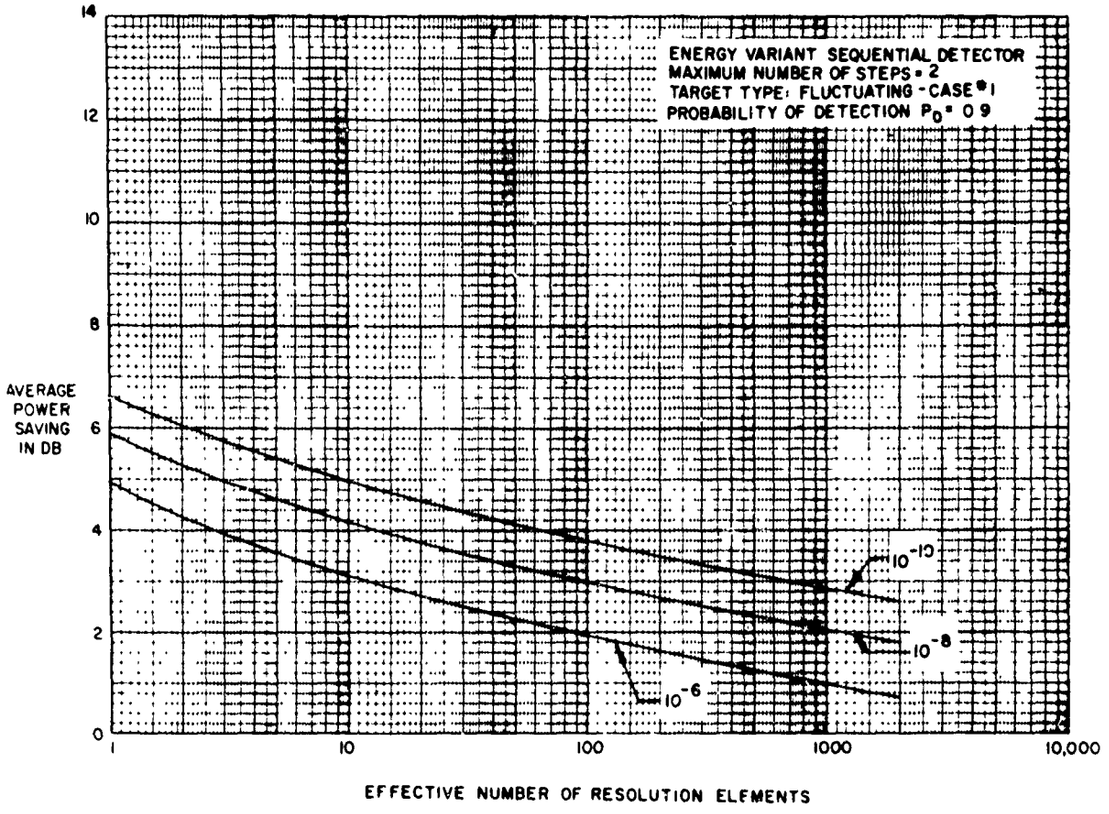

Figure 4. Average Power Saving, Case #1 Target

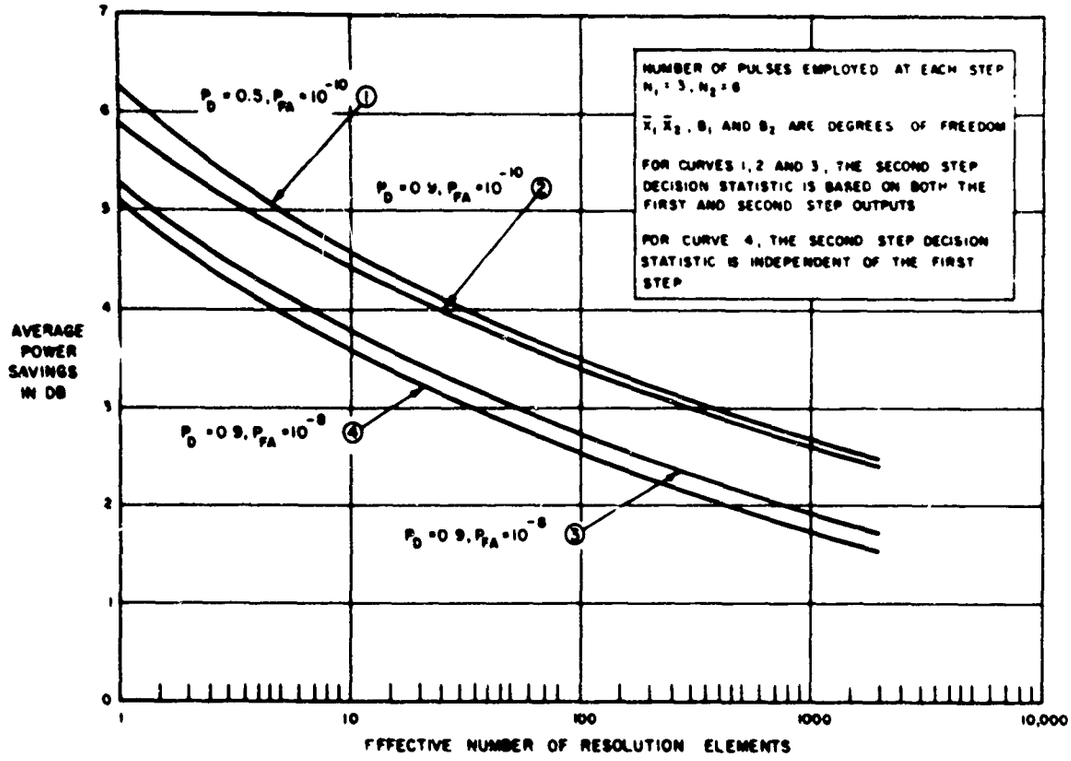

Figure 5. Average Power Saving, Case #2 Target

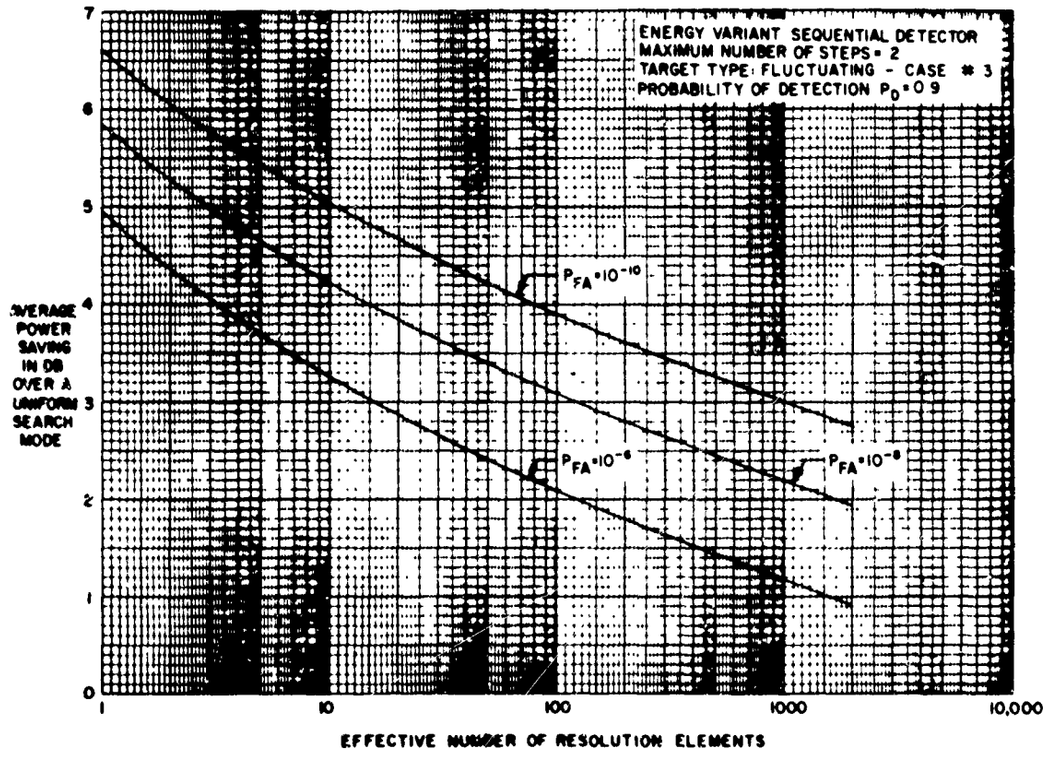

Figure 6. Average Power Saving, Case #3 Target

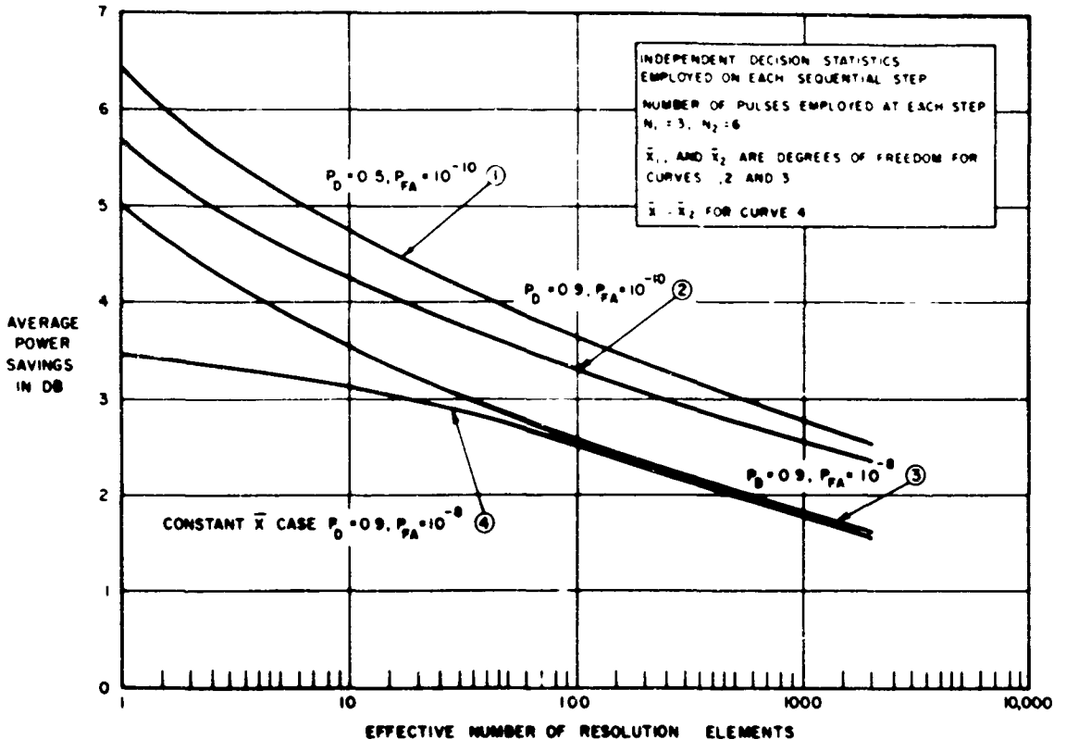

Figure 7. Average Power Saving, Case #4 Target

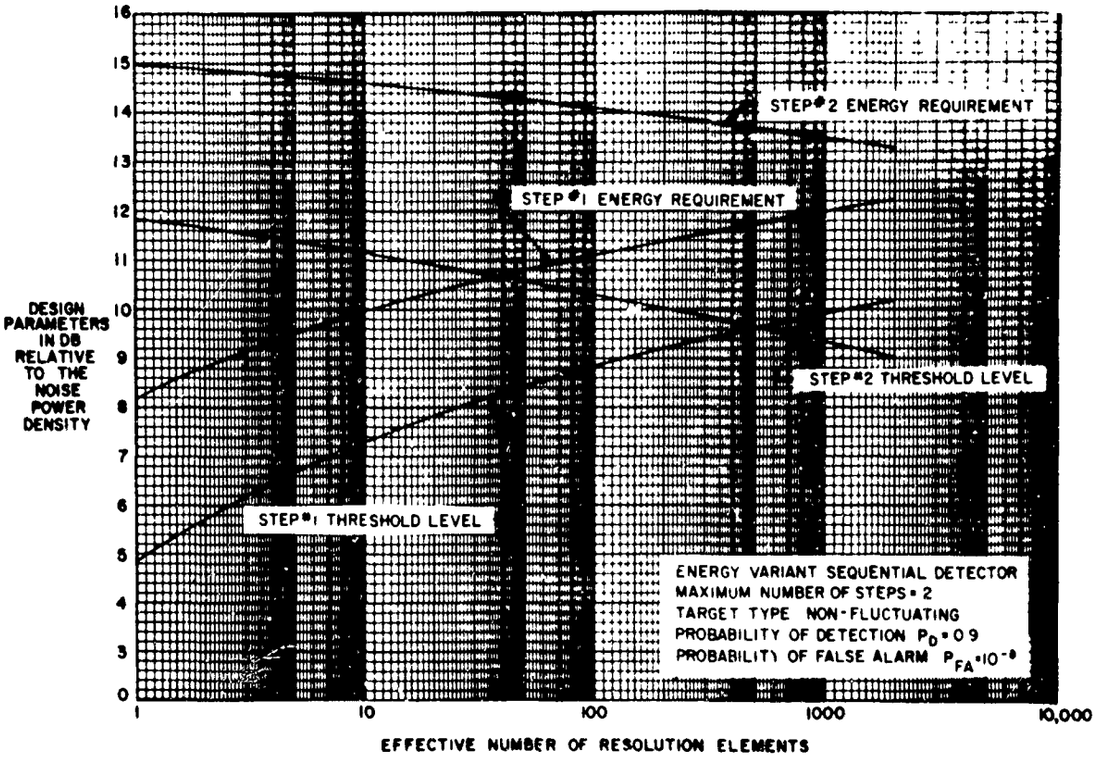

Figure 8. EVSD Design Parameters, Non-Fluctuating Target

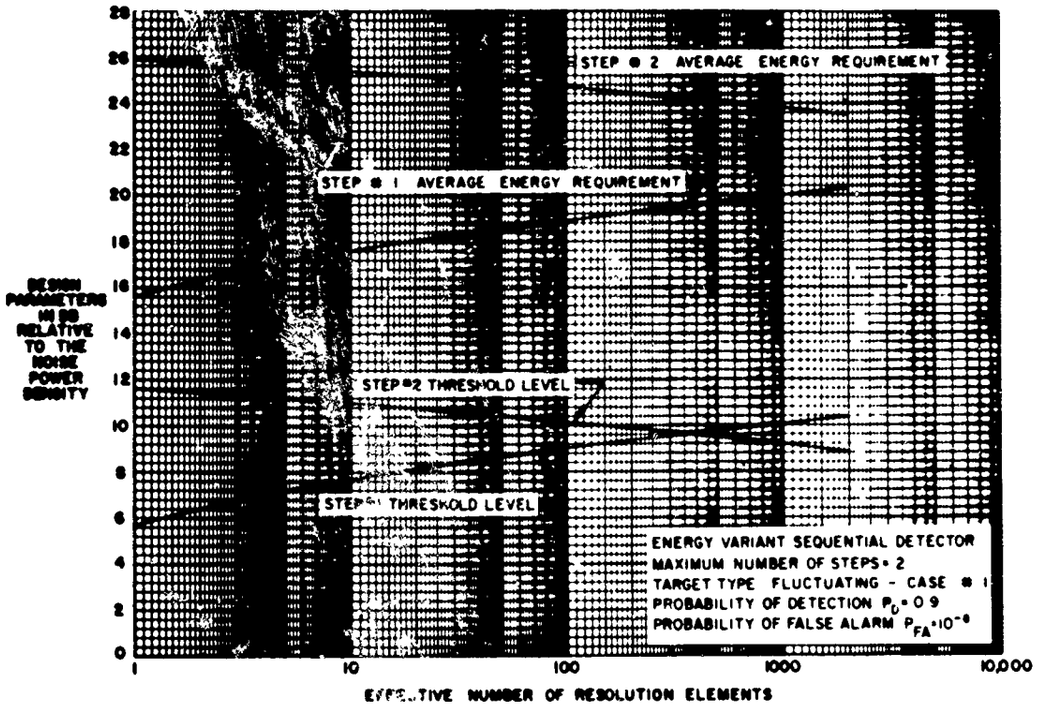

Figure 9. EVSD Design Parameters, Case # 1 Target

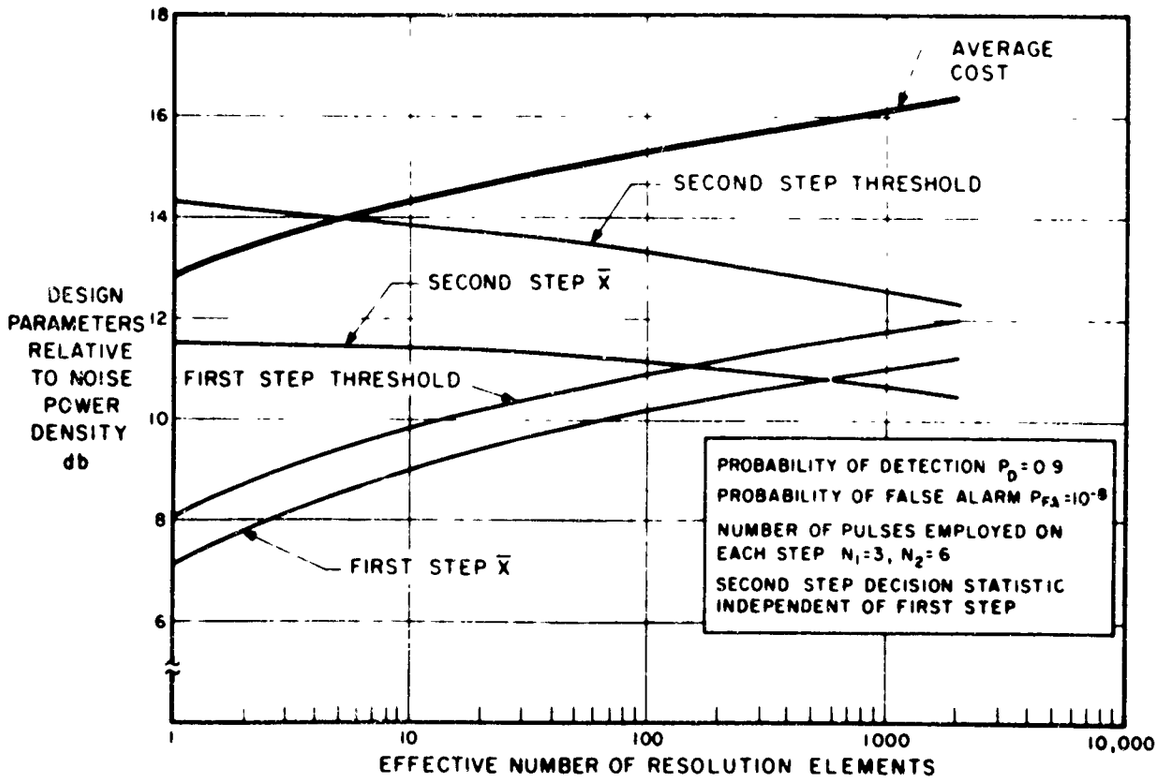

Figure 10. EVSD Design Parameters, Case #2 Target

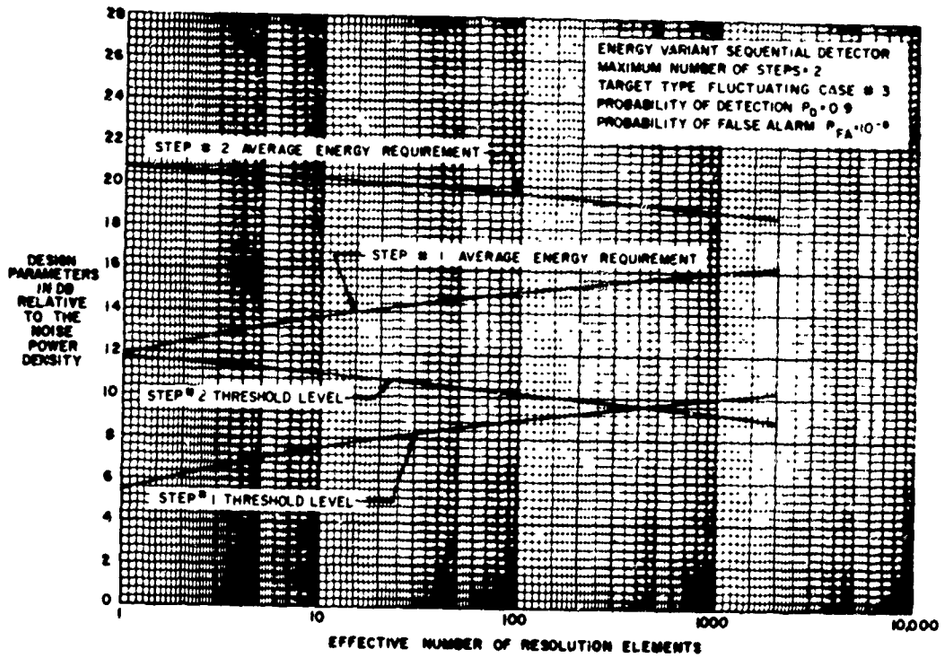

Figure 11. EVSD Design Parameters, Case #3 Target

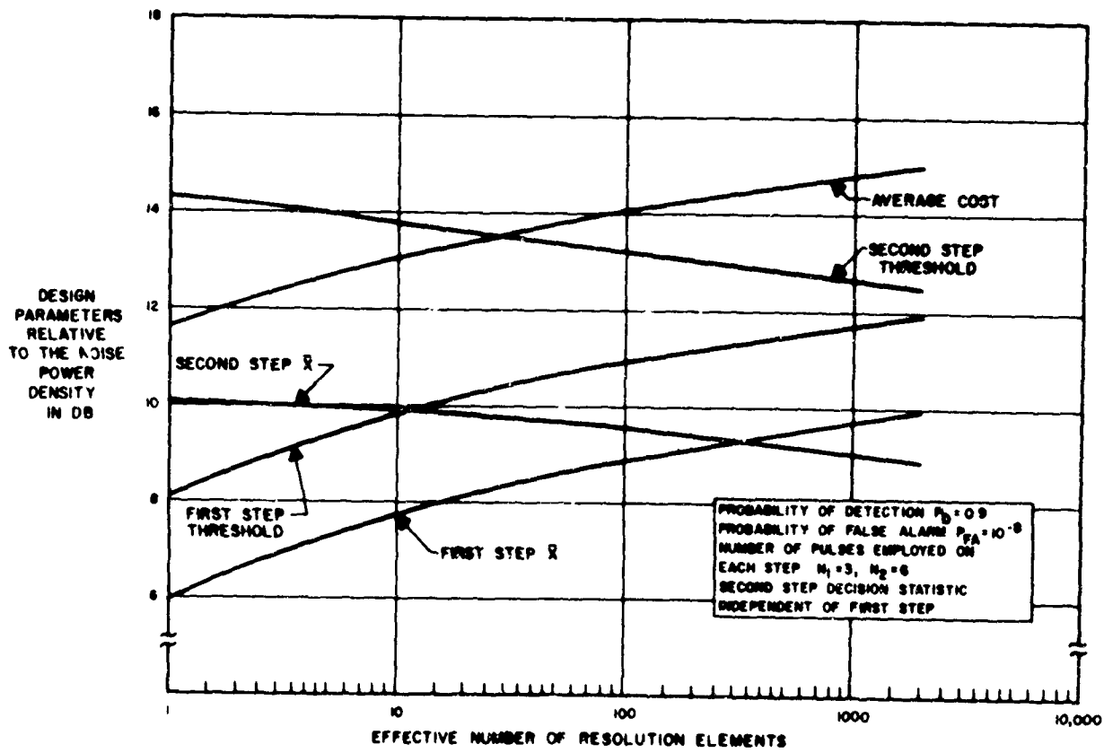

Figure 12. EVSD Design Parameters, Case #4 Target

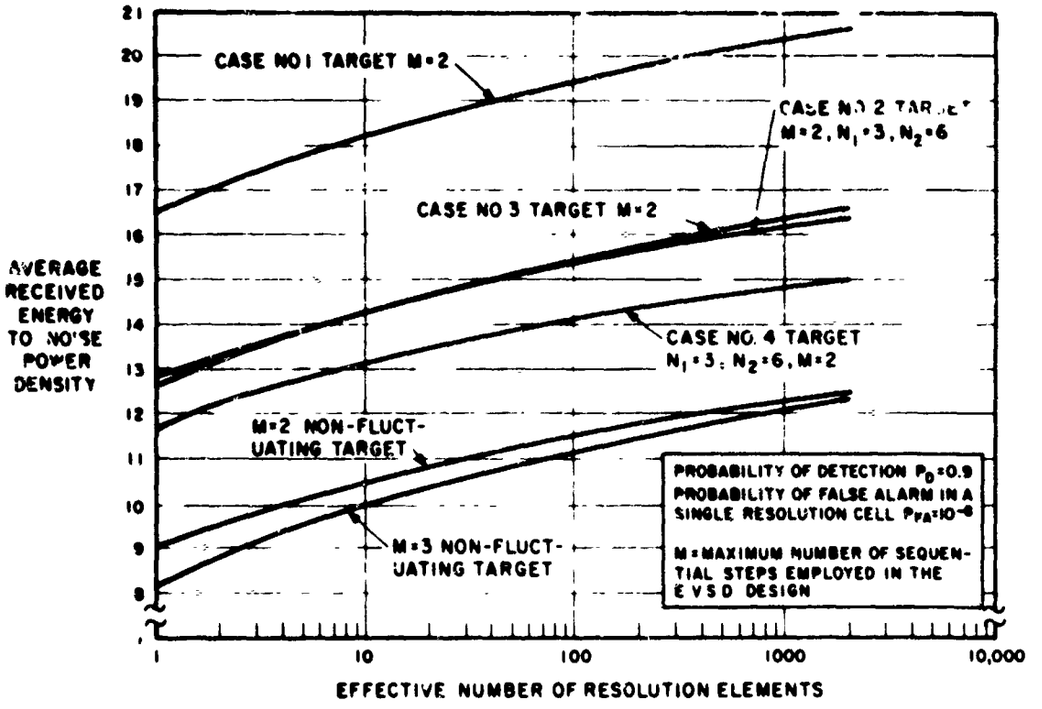

Figure 13. Comparison of Energy Requirements of EVSD's Designed for the Detection of Each of Five Target Types

mission. A theorem developed during the first phase of the program (Reference #1) states that the power requirement is a monotonically increasing function of the number of resolution cells employed on the first step of a two-step maximum procedure. This theorem, in general, leads to the strategy of 'telescoping' to the final time-bandwidth product on successive sequential steps where we start on the first step with a unit-time-bandwidth product signal.

d) Thresholds: The control of the receiver thresholds on each of the sequential steps aids in the reduction of power requirements for all of the surveillance situations considered.

2.3.5 EXTERNAL NOISE IMMUNITY AND THE DECISION RULE

For the conventional EVSD, the target present hypothesis is accepted only when threshold crossings by the decision statistics have occurred in a common resolution

cell for all sequential steps. And at the first step that this coincident requirement is violated in all resolution cells, the no-target hypothesis is accepted and the beam is moved to another position for a new test. By performing the thresholding requirement with a decision statistic based solely on the output of that step and imposing the parametric cell-coincidence requirement on successive steps, a greater degree of external noise immunity is attainable than can be provided, say, with the sequential probability ratio test where external noise variates included in the likelihood ratio on any one step are 'remembered' for the remainder of the test.

The use of independent decision statistics in an EVSD leads to a slight reduction in efficiency over the employment of a decision statistic on a sequential step which is based also on the outputs of all preceding steps. This 'loss' in efficiency is noted in Figure 5 to be less than 0.2 db for the Case #2 target. Both classes of EVSD's have been developed.

A somewhat modified decision rule is required for the Resolution-Variant EVSD since the resolution cell size changes from one sequential step to another. The groupings of cells on successive steps which allow for the acceptance of the target-present hypothesis must have the characteristic that the resolution cell on a sequential step 'embrace' or be coincident with the cell involved on the immediately following sequential step.

2.4 ANALYTICAL FORMULATION OF EVSD OPTIMIZATION PROCEDURE

The detailed optimization procedures appear in Reference #1, and some of these procedures are reproduced in Appendies 4, 5, and 6. A classical minimization is employed. The detection and false-alarm probabilities are the constraint relationships of the minimization problem; the cost function to be minimized is made equal to the average required received signal-energy-to-noise power density. The optimization involves finding the radar parameter settings at each of the sequential steps which satisfy the constraint relationship and minimize

the cost. The method of Lagrange Multipliers is used to find this minimum, subject to the constraints. A group of transcendental equations (one for each of the design degrees of freedom, for which a simultaneous solution is required result from this process. A Newton's iteration rule implemented on the IBM 7090 computer is then employed for solving these equations.

This approach is outlined here for the non-fluctuating and the slowly fluctuating target types. (Target types which are assumed to maintain a constant cross section for the duration of the sequential test.)

For this case, the probability of detection may be expressed as

$$P_D = \int_{\alpha=0}^{\infty} \prod_{J=1}^{N} Q(K_j\, \alpha, \beta_j)\, f(\alpha;\, X)\, d\alpha \qquad (1)$$

where N = maximum number of steps,

K_j^2 = ratio of the transmitted energy of the j^{th} step to transmitter energy of the first sequential step (and where $K_1 = 1$)

α = a random variable with the probability density function $f(\alpha;\bar{X})d\alpha$

$$\alpha = \sqrt{\frac{2E}{N_o}}$$

where E = received energy of the first step and,

N_o = noise power density

$\bar{X}$ = average received signal energy-to-noise power density $\left(\bar{X} = \frac{\bar{E}}{N_o}\right)$.

The density functions for the Case 1 and 3 target types are:

$$\underline{\text{Case 1}} = f(\alpha;\bar{X})d\alpha = \frac{\alpha}{\bar{X}}\, e^{-\alpha 2 / 2\bar{X}}\, d\alpha \qquad (2)$$

$$\text{Case 3= } f(\alpha;\bar{X})d\alpha = \frac{2\alpha^3}{\bar{X}^2}\, e^{-\alpha^2/\bar{X}}\, d\alpha \tag{3}$$

$$Q(K_j\alpha;\beta_j) = \int_{\beta_j}^{\infty} Xe^{-\frac{1}{2}(X^2 + K_j^2\alpha^2)} I_o(K_j\alpha X)d\alpha \tag{4}$$

The integrand of equation (4) is the conditional probability-density function of the normalized linear-detector output X of a matched filter on the hypothesis that twice the input signal energy-to-noise power density is $K_j^2\alpha^2$.

The expression $Q(K_j\alpha; B_j)$, therefore, is the probability of a crossing of the threshold β_j on the j^{th} step in one of the resolution cells.

The overall false alarm probability (P_{FO}) for the N_F resolution elements is expressed as

$$P_{FO} = 1 - (1-P_{FA})^{N_F} \tag{5}$$

where P_{FA} = the false alarm probability in an individual resolution element; and for the surveillance situations of interest where $P_{FA} << 1$, the binomial expansion can be used to obtain

$$P_{FO} \approx N_F\, P_{FA} \tag{6}$$

P_{FA} is simply the product of the probabilities of the independent noise sample threshold crossings in a common resolution cell for all sequential steps.

$$P_{FA} = \prod_{J=1}^{N} \int_{\beta_j}^{\infty} Xe^{-X^2/2}\, dX \tag{7}$$

or

$$P_{FA} = e^{-\frac{1}{2}\sum_{j=1}^{N} \beta_j^2} \tag{8}$$

The expression for the cost function C in terms of the average received signal energy-to-noise power density required for the no-target case is:

$$C = \bar{X}\left[1 + N_F \sum_{j=1}^{N-1} K_{J+1}^2 \, e^{-\frac{1}{2}\sum_{\ell=1}^{J} \beta_\ell^2}\right] \tag{9}$$

where $\frac{\alpha^2}{2}$ is employed for the non-fluctuating target instead of $\bar{X}$.

The optimization problem now involves, for the EVSD with a maximum of N steps, finding the 2N parameters ($\bar{X}$, K_2, $K_3 \ldots K_N$, β_1, β_2, $\ldots \beta_N$), minimizing the cost function C (equation 9), and satisfying the expressions for the probability of detection P_D (equation 1) and the false alarm probability P_{FA} (equation 8) for the specific values P_{FO} and P_{FAO}.

Lagrange Multipliers are employed to find this minimum, and introducing the undetermined coefficients τ_1 and τ_2, the following set of equations are formulated:

$$\frac{\partial C}{\partial \beta_j} + \tau_1 \frac{\partial P_D}{\partial \beta_j} + \tau_2 \frac{\partial P_{FA}}{\partial \beta_j} = 0 \quad j=1, \ldots\ldots, N-1 \tag{10}$$

$$\frac{\partial C}{\partial K_j} + \tau_1 \frac{\partial P_D}{\partial K_j} + \tau_2 \frac{\partial P_{FA}}{\partial K_j} = 0 \quad j=2, \ldots\ldots, N. \tag{11}$$

$$1/2 \sum_{j=1}^{N} \beta_j^2 = \ln \frac{1}{P_{FAO}}. \tag{12}$$

$$\int_0^{\infty} \prod_{j=1}^{N} Q(K_j\alpha, \beta_J)\, f(\alpha; \bar{X}) d\alpha = P_{DO}. \tag{13}$$

The partial derivatives of P_D required for this procedure are evaluated by differentiation of the integrand, and a 10-point quadrative formula is employed for accomplishing the integration with respect to α.

The simultaneous solution of these equations for the 2N unknowns for the cases where N=2 and 3 has been obtained by employing a Newton's iteration procedure implemented on an IBM 7090 computer.

2.5 TYPICAL DESIGN AND PERFORMANCE PARAMETERS

Optimizations of the type described in the previous paragraphs have been effected for the non-fluctuating target and the Swerling Cases #1 through #4. For the Case #2 and #4 target types, the added degrees of freedom are the number of statistically independent target cross-section samples employed on each step. A relatively complete catalogue of EVSD design and performance parameters is presented in Reference #1. Typical sets of these parameters are presented in Figures 3 through 13. An important part of the solution involves a comparison of the EVSD costs with those of more conventional tests. By comparing the average transmitter energy requirements of the EVSD with the energy requirements of a fixed sample-size test where the number of pulses employed is made equal to the average number used in the EVSD, a measure of the power savings is achieved for a specified set of surveillance conditions. The set of curves appearing in Figures 3 through 12 cover the five target types (the non-fluctuating and the

Swerling Cases #1 through #4) where the same detection and false alarm probabilities are specified in order to facilitate a comparison of detection requirements.

SECTION 3

GENERAL IMPLEMENTATION CONSIDERATIONS

A major emphasis of the second phase of the program has been directed toward the development of sequential detection modes suitable for the high-resolution surveillance mission where coded transmitter waveforms having relatively large time-bandwidth products are a requirement. Consequently, the general development of these modes and implementation considerations relating to them are treated separately in Section 5.

The most efficient modes for this type of mission involve programmed changes in the time-bandwidth product as well as the transmitted energy on each of a number of sequential steps, and matched filters capable of accommodating the relatively wide variations in waveform characteristics from one sequential step to another. Time-variant matched filters (i.e. active correlator systems) are concluded to present the most economical means of meeting the signal-processing requirements of a Resolution-Variant EVSD. The active correlator system fulfills both the flexibility requirements of these modes and has the advantage over time-invariant filters of permitting the same correlator hardware to be used on successive steps of the detection mode.

Some general considerations associated with the implementation of each of the design degrees of freedom of an EVSD are summarized here. Attention is given specifically to considerations which are peculiar to the realization of an EVSD mode in a radar system.

3.1 TRANSMITTER ENERGY CHANGES

The method selected for accomplishing the programmed energy change requirements is dependent on the available peak transmitter power, the resolution requirement, the required increment of programmed increase in energy, and the target type involved.

A typical increase in transmitter energy from the first to the second step of an EVSD with a maximum of two steps is noted (see Figures 8 through 11) to vary from about 7 db at one resolution element to 0 db at 2000 resolution cells, and for a radar with 100 effective resolution cells, a typical increase is 4 db. Employing transmitter tubes operating at constant peak power, the increase in energy requirement involves the selection of an ensemble of waveforms for use on each of the sequential steps which is compatible with both the system resolution and the sequential-step energy requirements.

For the relatively low time-bandwidth product requirement system, an EVSD with a maximum of two steps would be employed. For the non-fluctuating and Swerling Cases #1 and #3 target types, a single target cross-section sample is employed on each step, while for EVSD's designed for the Case #2 and #4 target types, a group of statistically independent target cross-section samples is a requirement on each sequential step - typically three on the first step and six on the second step. A non-coherent sum is employed on each sequential step. For this latter class, where the correlation time is small with respect to the interpulse spacing, two EVSD's have been developed. One involves constant-energy pulses for both steps, but where the number of these pulses employed on each step changes. (These pulses are assumed to yield statistically independent target cross-section samples.)

The second type includes, as an added degree of freedom, the single-pulse energy requirement. The typical average power savings with and without this added degree of freedom is presented in Figure 7 for the Case #4 target. And

it is noted that where the effective number of resolution cells is 100 or greater, the simpler EVSD type, which involves constant-energy samples, yields approximately the same power savings as the case where the single-pulse energy requirement is a degree of freedom. Consequently, for the Case #2 or #4 target, this EVSD type is recommended where the number of resolution cells is 100 or greater, and the implementation for this class of target typically involves transmitting three standard pulses on the first step and six more of these standard pulses when the second step is employed. A non-coherent integration is only required for each step.

The increased energy requirement of the second step for the non-fluctuating and Case #1 and #3 target types is assumed to take place coherently. However, if a single pulse is employed on the fi st step, a relatively few of these standard pulses can meet the increased energy requirement on the second step; and since the non-coherent integration loss is relatively small where a few pulses are involved and occurs on the infrequently used second step, the effective non-integration loss for the sequential procedure is negligible if non-coherent rather that coherent integration is employed. For this non-coherent integration case, the same resolution cell size is employed on each sequential step, and no modification of the decision rule is involved.

For the case where the second sequential-step energy increase is obtained coherently, and assuming the use of a single pulse on the first step, the duration of the first-step pulse could be increased, and a matched filter employed on the second step to accommodate this changed waveform requirement; or a coherently integrated train of pulses can be employed to accomplish the energy increase. For both coherent schemes, the resolution cell dimensions are changed from the first to the second sequential step, and consequently a modification of the decision rule must be made to allow the acceptance of the target-present hypothesis when overlapping resolution cells exhibit threshold crossings on each of the two sequential steps.

An indication of the effective resolution requirements of such a system is obtained by superimposing, on a common coordinate system, the signal ambiquity function contours of the waveforms employed on each sequential step. Schematic representations of this type for both the increased pulse duration case, and the coherently integrated pulse train case, are presented in Figure 14. It is noted that, for the increased time-duration single-pulse case, the intersection of the first and second-step resolution cell maintains the higher range resolution of the first step pulse of duration τ_1, and the higher doppler resolution of the second step $1/\tau_2$. The effective doppler resolution increase is τ_2/τ_1, or the ratio of the second-step energy E_2 to that of the first step E_1.

For the case where coherent integration of a train of n pulses is employed with an interpulse spacing of T_o, the increase in doppler resolution of the second step to that of the first step where a single pulse of duration τ_1 is used, is the ratio nT_o/τ_1. For this example, illustrated in Figure 14, the uncoded pulses of the second step are of the same duration as the single pulse employed in the first step so that the range resolution is the same for each step. If the difference between the maximum admissible target doppler frequency (f_D max) and the minimum doppler frequency (f_D min) is large relative to the required doppler resolution Δf_D, a significant reduction in the total number of doppler filters can be obtained with the coherent pulse train second step, and the use of a voltage-controlled local oscillator. In this scheme, the doppler region ($f_{D\ max} - f_{D\ min}$) is covered with the relatively coarse doppler resolution first-step filters where the doppler resolution is $1/\tau$ and the bank of contiguously spaced doppler cells would be approximately

$$m_1 = \frac{f_{D\ max} - f_{D\ min}}{\frac{1}{\tau_1}}$$

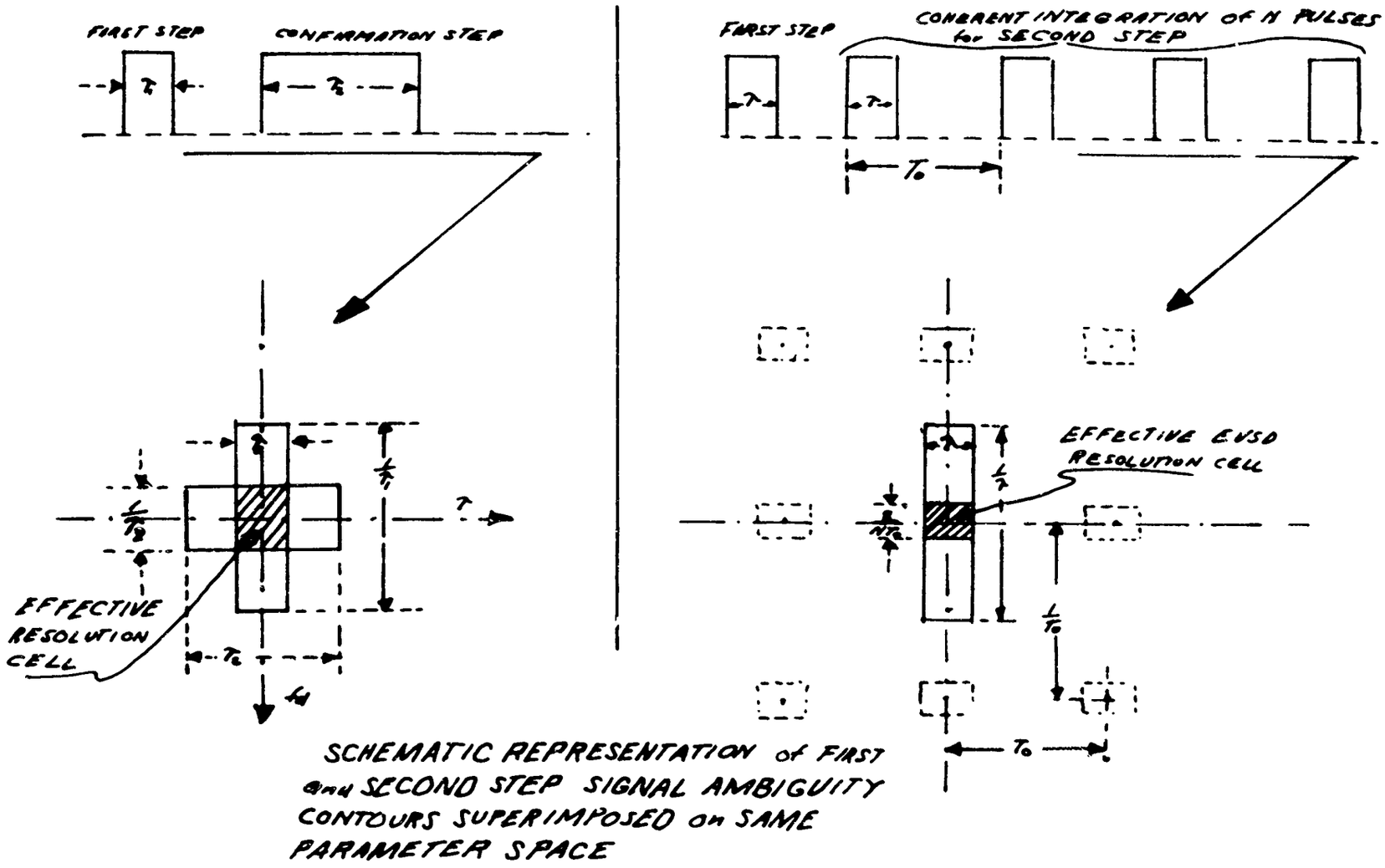

Figure 14. Resolution Characteristics of EVSD with Second-Step Energy EVSD

A relatively small bank of doppler filters with doppler resolution $1/nT_o$ is then required to cover the domain of doppler frequencies embraced by a single coarse cell of the first step. The number of these fine cells would be

$$m_2 = \frac{\frac{1}{\tau_1}}{\frac{1}{nT_o}} = \frac{nT_o}{\tau_1}$$

A voltage-controlled local oscillator would be employed in this EVSD scheme to effectively shift the fine bank of second-step doppler filters to the doppler frequency region where a first-step threshold crossing was recorded. So the total number of doppler filters employed is $(f_{D\ max} - f_{D\ min})\ \tau_1 + nT_o/\tau_1$. In a conventional detection scheme, a covering of the whole doppler space of interest with the fine doppler cells would be required (that is, the number required would be $m_o = (f_{D\ max} - f_{D\ min})\ nT_o$). The coarse-fine resolution scheme implicit in this EVSD implementation involves matched-filter processing on each of the sequential steps, and should not be confused with previously proposed coarse-fine resolution schemes which involve a single step of transmission. In these schemes, a significant mismatch is tolerated upon reception for the coarse-cell processing. In addition, no attempt at achieving the increased efficiency of a sequential detection mode is attempted in these other schemes. The unique features of a resolution-variant sequential detector in increasing the detection efficiency are discussed in the following paragraphs.

3.2 SEQUENTIAL STEP TIME-BANDWIDTH PRODUCT CONTROL

A theorem developed during the program (See Reference #1) states that the transmitter power requirement of an EVSD is a montonically increasing function of the number of resolution cells employed on the first step of a two-step maximum procedure. This is the case since the use of the second sequential step in a no-target environment depends directly upon the number of false-report inducing

possibilities of the first step. So the obvious strategy in general for a two-step maximum procedure involves the use of an uncoded (unity time-bandwidth product pulse) on the first sequential step and employing the coded waveform meeting the system resolution requirements on the second sequential step. To achieve the predicted efficiency, it is necessary to accommodate in the receiver signal processor the change in transmitted time-bandwidth product so that matched-filter operation is approximated on each sequential step. The previous catalog of families of EVSD design and performance parameters appearing in Reference #1 are still applicable for resolution-variant EVSD's with a maximum of two steps. These EVSD's were designed for the case where the same resolution cell size was employed on each step. To use these data for the resolution-variant EVSD with a maximum of two steps, it is simply necessary to interpret the effective number of resolution elements as the number of resolution cells employed on the first sequential step. The single-cell false-alarm probability P_{FA} employed as a fixed requirement for this data is now interpreted as the false-alarm probability in a two-step coarse-fine parameter cell pair. The total false-alarm probability at a beam position P_{FO} is expressed as

$$P_{FO} = m_1 \frac{T_2}{T_1} \frac{W_2}{W_1}$$

where m_1 is the effective number of resolution cells used on the first step, and T_1W_1 and T_2W_2 are the time bandwidth products of the first and second sequential steps respectively. The interprtation of detection probability remains the same.

For the case where the needed surveillance resolution imposes very large time-bandwidth product requirements (say greater than 10,000), it is desirable, for a number of reasons, to "telescope" to the final resolution cell size in more than two sequential steps. An optimization for such a high-resolution requirement has been effected and is considered separately in Section 5.

No special problems are encountered in implementing the sequential-step threshold control requirements of an EVSD.

3.3 EVSD IMPLEMENTATION FOR HIGH-INERTIA BEAM-STEERING RADAR SYSTEMS

A particularly interesting feature of the Energy-Variant Sequential Detector is its adaptability for use with high-inertia beam-steering antenna systems. For example, if an EVSD with a maximum of two steps were employed for a radar with an antenna of the parabolic reflector type, two beam positions, separated a few beam widths apart, can be effected with offset waveguide feeds to the antenna. Operating at a constant rotation rate, the lead beam position would be in continuous use for the first sequential step with transmitted energy E_1. Threshold crossings of this first sequential step would be memorized, and when the second or lagging beam (which normally would not be powered) was in the beam position of a first-step threshold crossing, a waveguide switching system would program a second-step energy requirement to this lagging or confirmation beam system. In this manner, the appreciable power savings of an EVSD over the use of a uniform search mode can be achieved with a high-inertia beam-steering system.

SECTION 4

EVSD PERFORMANCE SIMULATION

A verification of predicted performance of the developed EVSD modes is accomplished with a simulation implemented on a digital computer (IBM 7090).

The developed EVSD simulation program has been designed with sufficient flexibility so that it can also be used as an effective research tool enabling mode evaluations, which would be difficult to perform analytically.

In general, however, the relatively simple decision processor framework of the Energy-Variant Sequential Detector leads to correspondingly less complicated probability distributions describing system performance than those, for example, encountered in sequential modes based on the adaptation of Wald's sequential probability ratio test to the radar surveillance mission.

Performance predictions for the sequential probability ratio test based detection modes hinge upon the solution of a relatively complicated random walk problem, the one involving the random walk of the likelihood ratio from one sequential step to another between the upper and lower thresholds of this test. In general, only relatively crude bounds on performance can be obtained for this detection mode. On the other hand, EVSD's employ a maximum of only two or three steps and employ relatively simple decision statistics, so that closed-form solutions are attainable (for example, see Section 2 and also reference 1).

Consequently, a relatively high degree of confidence can be placed on the accuracy of the theoretical predictions of EVSD performance for the assumed target types and matched-filter receiver conditions. And the excellent correlation obtained between

the analytically predicted results and those obtained by the simulation program verify the original computations of performance. In general, the simulation results deviate by less than 1% from the analytical predictions.

4.1 BASIC LOGIC OF PERFORMANCE SIMULATION

A fundamental aspect of the developed EVSD simulation program involves effecting an authentic simulation of the sequence of sampled linearly detected matched-filter outputs $\{y_n\}$ both within a sequential step and from one sequential step to another, and all within a common resolution cell. This simulation, moreover, is required for all of the five target types considered in the program, the non-fluctuating and the four fluctuating types of Swerling (Cases #1 through #4). The probability density function of n sampled outputs $\{y_n\}$ jointly with the sampled signal variates $\{\alpha_n\}$ may be expressed as:

$$f(y_1, y_2 \ldots y_n, \alpha_1, \alpha_2, \ldots \alpha_n)\, dy_1\, dy_2 \ldots dy_n\, d\alpha_1, d\alpha_2 \ldots d\alpha_n$$

$$= \prod_{i=1}^{n} f(y_i/\alpha_i)\, dy_i \; f(\alpha_1, \alpha_2, \ldots \alpha_n; \bar{X})\, d\alpha_1\, d\alpha_2 \ldots d\alpha_n \tag{14}$$

where the conditional probability density function

$$f(y_i/\alpha_i)\, dy_i = y\, e^{-\frac{y_i^2 + \alpha_i^2}{2}}\, I_o(\alpha_i X_i)\, dy_i \tag{15}$$

is the well known Rice or modified Rayleigh distribution where $\alpha_i = \frac{\sqrt{2E_i}}{N_o}$. ($E_i$ is the received energy on the i^{th} pulse and N_o is the noise power density.) The joint density function of the sampled target cross sections, or correspondingly, the received signal energy variates to noise power density is the quantity

$f(\alpha_1, \alpha_2, \ldots \alpha_n, \bar{X})\, d\alpha_1\, d\alpha_2 \ldots d\alpha_n$ where $\bar{X}$ is the ratio of average received energy E to noise power density N_o. The basic logic of the simulation is presented in Figure 15 for a single resolution cell. A variate y_i representing the sampled

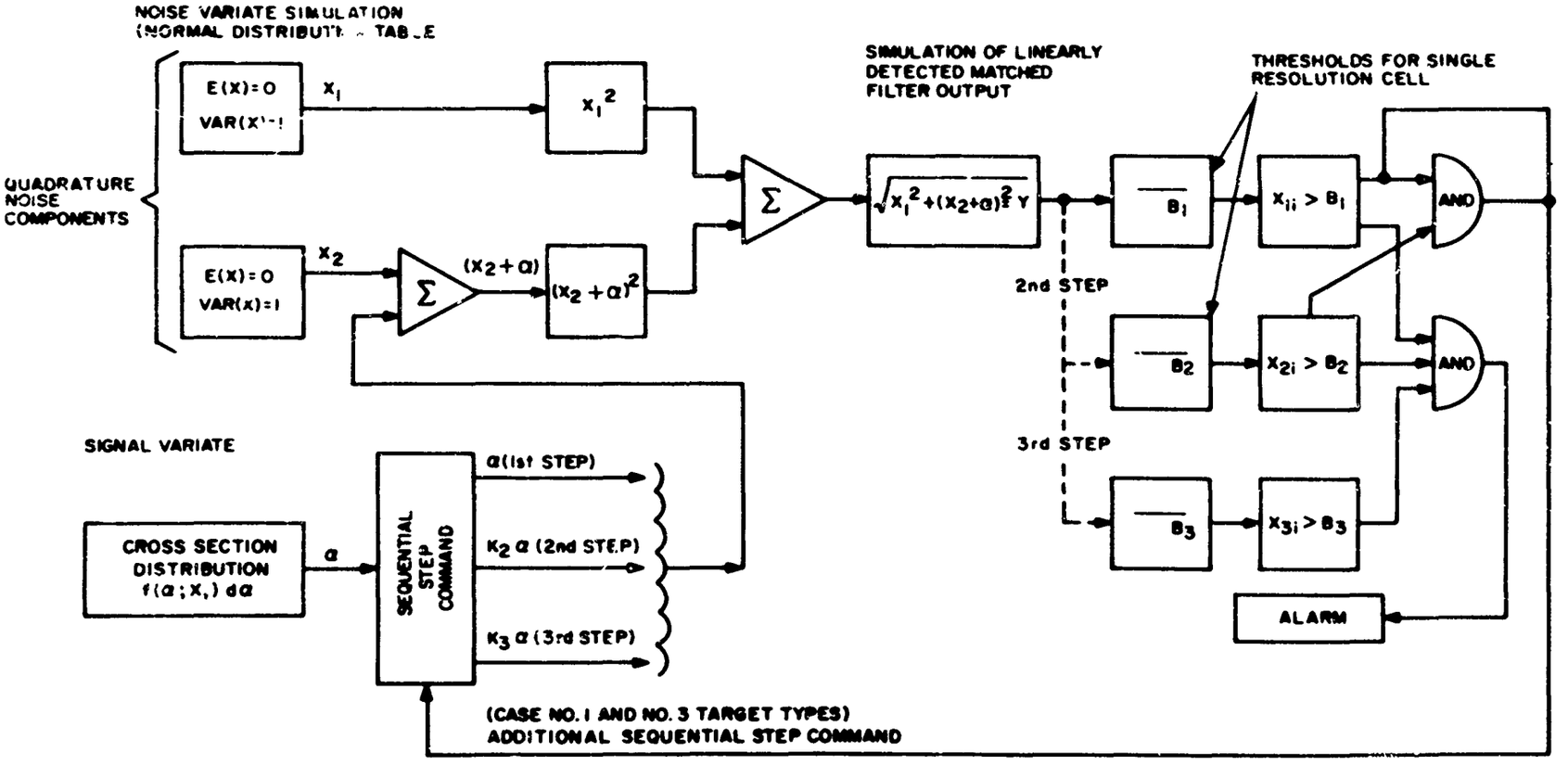

Figure 15. Basic Logic for Simulating EVSD Performance

matched-filter output at the i^{th} sampling is simulated by first selecting two independent samples (X_1 and X_2) from a normal distribution (mean values of zero and variance of unity). These values represent the normalized quadrature noise samples in the predetection section of the receiver. The signal variate α_i is then selected from a random-number program simulating the probability density function of the target type of interest. (Two spectral characteristics are considered; for the Case #1 and #3, only one signal variate sample α is selected and is employed for the duration of the test on all sequential steps. Increases in transmitted energy from one sequential step to another are then effected for this slowly varying class of targets by simply multiplying the selected α by an appropriate constant. For the Case #2 and #4 target types, independent selections of target cross-section samples are made for each pulse within a sequential step and from step to step.)

The quantity $y_i = \sqrt{X_{i1}^2 + (X_{i2} + \alpha_i)^2}$ is then formed, and the set of $\{y_i\}$ formed in this manner can be shown to represent the set of sampled matched-filter outputs with the joint distribution defined by equations 14 and 15. The decision statistic for effecting a threshold comparison with the threshold β_i at the i^{th} step is simply the matched-filter output y_i for the Cases 1, 3, and 5 target models, and for the Cases #2 and #4 target, the sum of the squared outputs at a sequential step. A program option allows the use of a decision statistic at a sequential step which includes the summed outputs of preceding steps. The decision rule logic for the EVSD under test is then introduced and the test proceeds until a decision is made on the acceptance of the target-present hypothesis. Threshold crossings of the decision statistics are required at each of the sequential steps in a common resolution cell in order to accept the target-present hypothesis.

For each surveillance situation simulated, the test is repeated about 2000 times in order to effect statistically significant estimates of the detection probability and this estimate is simply the ratio of the count of the number of times the target-present hypothesis was accepted to the total number of replications. Verification by simulation of false alarm probability was not considered necessary since the analytical

expressions of false alarm probability for the target models considered are relatively simple and computed values of this probability can be assumed to be relatively error free. A simulation of these typically low values of probability would also involve a prohibitively large number of replications of the test procedure in order to effect statistically significant values of this error probability.

A typical set of results for the performance check of EVSD detection probability is tabulated below. The case considered here is an EVSD designed for the detection of a case #3 target, and where the single-cell false alarm probability is 10^{-8} and 10 resolution cells are involved. The first column presents the theoretical predictions for the thresholds and energy levels employed, and the second column presents the estimated values. For each set of predicted error probabilities, the threshold settings and the received ratios of signal energy to noise power densities are made equal to the optimum quantities minimizing the average energy requirements. So that a verification of detection probability is, in effect, an implicit verification of these minimum energy designs.

The number of replications for this test was 1000 and the average deviation from the predicted values is noted to be less than 1 percent.

P_D (Predicted Values)	$\hat{P}_D$ (Estimated Values)
0.5	0.48899
0.6	0.60399
0.7	0.70400
0.8	0.80400
0.9	0.89399
0.95	0.93800

4.2 TABULATION OF EVSD SIMULATION PROGRAM INPUTS

A list of the program inputs and outputs is presented here, and it demonstrates some of the program flexibility making it useful as a general evaluation tool. One feature

noted in this tabulation is that provision is made for creating a surveillance mismatch situation. That is to say, one where the 'actual' target present differs from the one employed in the design of the sequential test. The sensitivity of an EVSD to such mismatch conditions can thus be evaluated.

I. Program Inputs

a. Target Type Design
- D1 - Case 1 Fluct.
- D2 - Case 2 Fluct.
- D3 - Case 3 Fluct.
- D4 - Case 4 Fluct.
- D5 - Non-Fluctuating (Case #5)

Actual Target Type
- A1 - Case 1 Fluct.
- A2 - Case 2 Fluct.
- A3 - Case 3 Fluct.
- A4 - Case 4 Fluct.
- A5 - Non-Fluctuating (Case #5)

b. Maximum Number of Sequential Steps M

c. Thresholds - $\beta_1, \beta_2 \ldots \beta_M$

d. Required signal energy to noise power density on each sequential step. (Single-Pulse Specification) $\overline{X}_1, \overline{X}_2 \ldots \overline{X}_M$ (Input will be specified in db (10 log $\overline{X}$))

e. Design Performance:
   1. Probability of Detection (P_D)
   2. Probability of False Alarm (P_{FA})
   3. Effective Number of Resolution Cells (N_F)

f. Number of statistically independent target cross-section samples on each sequential step. ($N_1, N_2, \ldots N_M$)
(For the non-fluctuating and Cases #1 and #3 target models $N_1 = 1$ and $N_2 = N_3 \ldots N_M = 0$)
(That is to say, there is only one independent sample for the duration of the test. Each step involves a single pulse of energy of the specified values for this class of target types.)

g. Decision Statistic at Each Sequential Step

(1) Non-fluctuating and Case #1 and #3 target models.

Decision Statistic - Linearly Detected Matched-Filter

(Y_i) a i^{th} step.

$$Y_i = \sqrt{X_1^2 + (X_2 + \alpha_i)^2} \tag{16}$$

where X_1 and X_2 are statistically independent samples of a normal distribution with mean value of zero and variance of unity.

$\alpha_i = K_i \alpha_o$ where K_i^2 is the ratio of the energy employed on the i^{th} step to that employed on the first step; α_o is obtained from the density function.

For Case #1 Target:

$$f(\alpha_o; \overline{X})\, d = \frac{\alpha_o}{X_1} e^{-\frac{\alpha_o^2}{2X_1}} d\alpha \quad . \tag{17}$$

$$\left(K_i^2 = \frac{\overline{X}_i}{\overline{X}_1} \right)$$

For Case #3 Target:

$$f(\alpha_o; \overline{X})\, d\alpha = \frac{2\alpha^3}{X^2} e^{-\alpha^2/\overline{X}} d\alpha \tag{18}$$

(2) Case #2 and #4 Target Models

Decision Statistic at i^{th} step $\left[\sum_{j=1}^{N_i} \frac{Y_{i_j}^2}{2} \right]$

(Independent Case)

where

$$\overline{Y}_{i_j} = \sqrt{X_1^2 + (X_2 + \alpha_{i_j})^2}$$

and α_{i_j} is a statistically independent sample obtained from the appropriate probability density function.

For Case #2 Model:

$$f(\alpha_{i_j}, \bar{X}_i)\, d\alpha_{i_j} = \frac{\alpha_{i_j}}{\bar{X}_i} e^{-\frac{\alpha_{i_j}^2}{2\bar{X}_i}} d\alpha_{i_j} \tag{19}$$

For Case #4 Model:

$$f(\alpha_{i_j}, \bar{X}_i)\, d\alpha_{i_j} = \frac{2\alpha_{i_j}^3}{X_i^2} e^{-\frac{\alpha_{i_j}^2}{\bar{X}}} d\alpha_{i_j} \tag{20}$$

(3) Independent vs. Dependent Case

Independent Case - implies that the i^{th} step decision statistic is simply based on the outputs of the i^{th} step. (This is the general case as previously specified.)

Dependent Case - For some EVSD designs with a maximum of two steps, the second-step decision statistic is a function of both the first- and second-step outputs.

For the non-fluctuating and Case #1 and #3:

Decision Statistic at 2nd Step $(Y_1 + Y_2)$

For the Case #2 and #4 Target Types:

Decision Statistic at 2nd Step

$$\left[\sum_{i=1}^{N_1} \frac{Y_{1i}^2}{2} + \sum_{j=1}^{N_2} \frac{Y_{2j}^2}{2}\right] \tag{21}$$

h. Number of Replications

i. Quantization Specifications - Provisions for Quantizing Y_i or $\frac{Y_{i_j}^2}{2}$ or (Y_i or $X_{i_j}^2/2$) can be specified as analog.

II. Program Outputs

a. Estimated Detection Probability -

$$E(P_D) = \frac{\text{Number of Registered Alarms}}{\text{Total Number of Replications}}$$

b. Use of Each Step -

Number of times i^{th} step is employed.

SECTION 5

OPTIMIZATION OF THE HIGH RESOLUTION SURVEILLANCE MISSION-RESOLUTION VARIANT EVSD

Special consideration has been given during the study to the development of sequential detection modes which minimize the cost of performing typical high-resolution surveillance missions. The radar missions in the class considered involve the use of coded high time-bandwidth product waveforms (pulse compression systems) for obtaining the required resolution of say a small cluster of targets. The environment is assumed to be relatively free of clutter targets so that the major false report inducing events are due to the receiver thermal noise.

Two major problems arise in the implementation of a radar for effecting this high-resolution mission. First, it is noted (for example, see Figures 3 through 8) that the average power saving of a constant resolution sequential detection mode over the use of a uniform search mode decreases as the number of resolution cells increase. So for example in a radar with a million resolution cells, the power savings would be less than 1/2 db for an EVSD employing the same time-bandwidth product waveform.

The second major problem with high-resolution missions is the cost of implementing the receiver signal-processing requirements. The signal-processing costs are an increasing function of the number of resolution cells, so that for a million resolution cell radar, the costs are formidable for implementing the parallel signal-processing requirement.

5.1 RESOLUTION-VARIANT DETECTION THEOREM

An important theorem developed during the program (see Reference #1) states that with the introduction of time-bandwidth products of the transmitted signal as a degree

of design freedom, the average transmitter power requirement is a monotonically increasing function of the number of resolution cells employed on the first sequential step of an EVSD with a maximum of two steps. The proof of the theorem is relatively simple and is based on showing that the expressions for the detection and false alarm probabilities in a final resolution cell are the same as for the constant resolution cell EVSD, but that the cost function is noted to be a monotonically increasing function of the number of resolution cells employed on the first step.

This theorem provides a clue to the design strategy for minimizing average power requirements. It suggests the use of an ensemble of transmitted waveforms for the sequential test which involves the use of a unity time-bandwidth product signal on the first step and the final large time-bandwidth product signal on the final step. An optimization program with the time-bandwidth product as a degree of freedom at each sequential step has been developed which verifies this strategy.

5.2 COMPATIBLE STRATEGY FOR MINIMIZING AVERAGE TRANSMITTER POWER AND SIGNAL PROCESSING COSTS

The maximum number of sequential steps to be employed, and the time-bandwidth product used on the intermediate steps are strong functions of the requirement for a minimization of signal-processing costs. Briefly, the strategy involved in minimizing the number of parallel signal-processing channels involves the use of the same set of active correlator signal-processing channels on successive steps, but where the effective resolution cell size of each channel becomes progressively smaller from one sequential step to another. By controlling the increase in time-bandwidth product on each sequential step, and communicating from one step to another the range and doppler coordinates of threshold crossings, the 'telescoping' or 'boot-strap' operation of programming the active correlator channels to represent a set of fine resolution cells embracing the target on the final step is accomplished.

A representation of this commonality of signal-processing equipment is presented in Figure 16, and a schematic representation of the signal ambiguity diagram for a

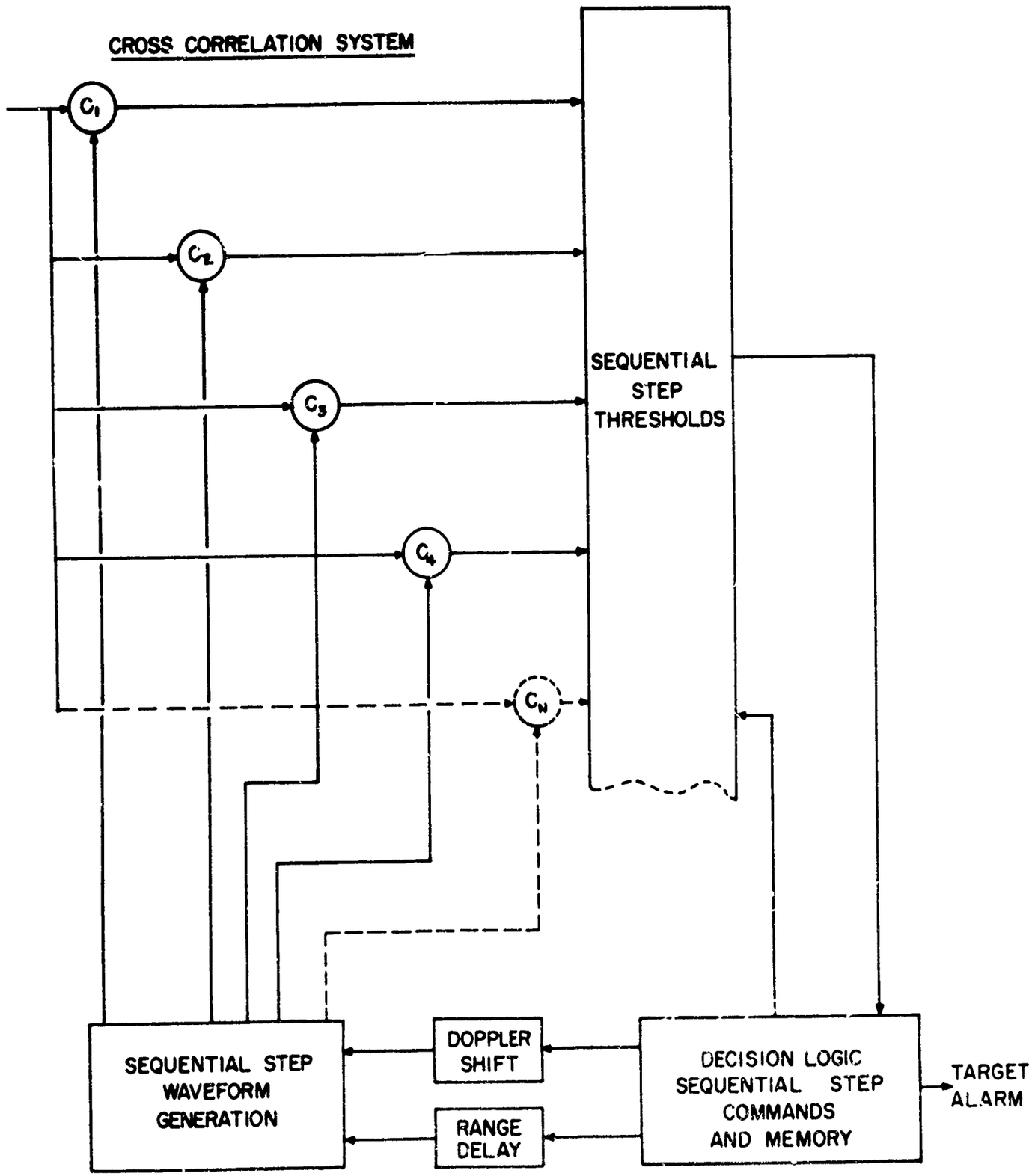

Figure 16. Resolution-Variant Signal Processor Conceptual Diagram Introducing Economy of Equipment Utilization

three-stage resolution-variant sequential procedure is shown in Figure 17. The 'dissecting' of the resolution cell containing a target on successive steps with an N-channel active correlator system is schematically illustrated in Figure 18. For this case, the factor of time-bandwidth increase is the same for each step so that for a sequential mode with a maximum of N steps and a final time bandwidth requirement of TW, the factor of increase on each step would be $(TW)^{1/N}$.

As an example illustrating the effectiveness of this resolution-variant strategy for reducing signal-processing equipment costs, consider a million resolution cell radar. That is to say, a radar which would require a million resolution cells to cover the parameter space of interest with the required fine-resolution cell. Assume a time-bandwidth product of 10,000, and that a 'covering' of the target range-doppler uncertainty space if a unity time-bandwidth product signal were used, would be 100 cells. Now consider a resolution-variant sequential mode employing a maximum of three steps, a unity time-bandwidth product pulse on the first step, and coded waveforms on the second and third steps with increases in the time-bandwidth product of 100 on each of these latter two steps. A 100-channel active correlator system can now be programmed for use on each of these three steps, and assuming the use of a few 100-channel units to accommodate various multiple target clusters, the million parallel processing channel requirement has been reduced to that of a relatively few hundred!

A common design strategy has thus been evolved which effectively minimizes both the required average transmitter power and the receiver signal-processing costs. The sequential detection modes developed with this resolution-variant strategy have been designated as Resolution-Variant EVSD's. These modes also include the transmitter energy and receiver threshold on each sequential step as design degrees of freedom as in the more conventional EVSD's.

5.3 RESOLUTION-VARIANT EVSD DECISION RULE

The decision rule for the Resolution-Variant EVSD involves the acceptance of the target-present hypothesis only when threshold crossings have occurred in successive

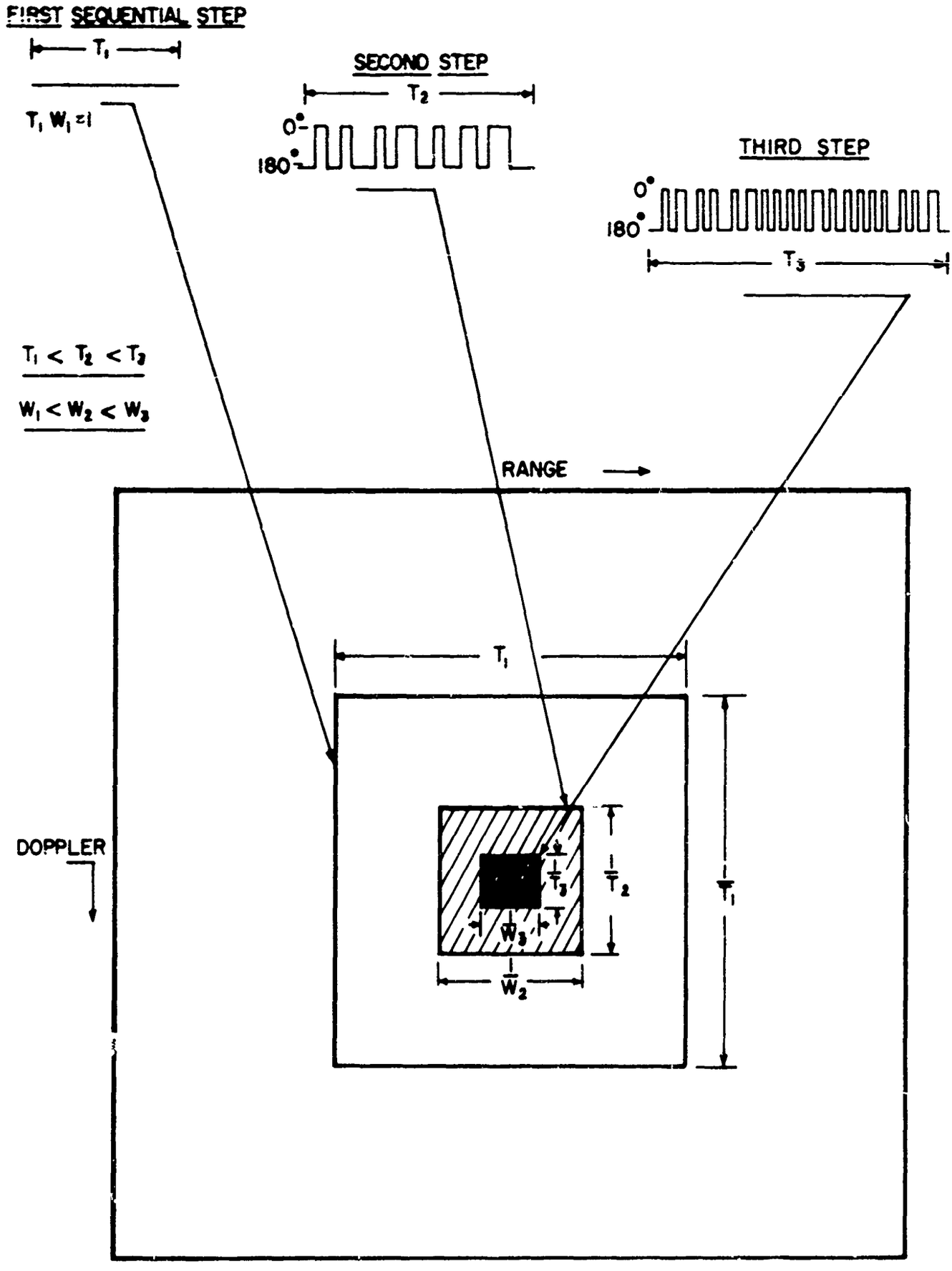

Figure 17. Resolution-Variant EVSD (Maximum of Three Steps) Schematic of Signal Ambiguity Space (Phase-Reversal Code Signal Ensemble)

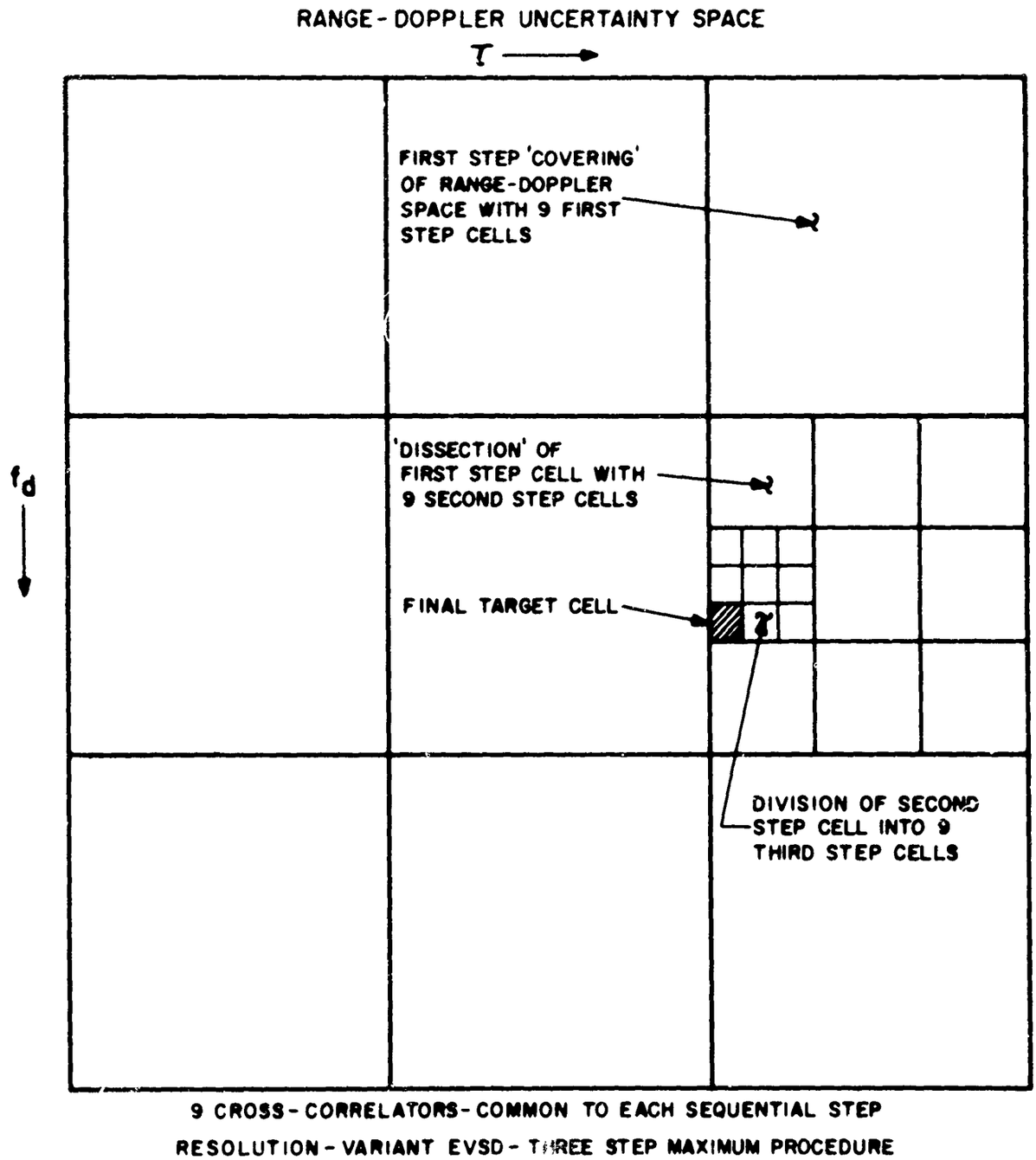

Figure 18. Illustration of the 'Telescoping' Operation on Successive Sequential Steps in a Range-Doppler Parameter Space

step resolution cells which form what may be described as a composite cylindrical resolution cell grouping. Figure 17 indicates such a grouping. That is to say, the resolution cell involved at each step must embrace or be coincident with the cell involved on the immediately following sequential step. For the first sequential step where this composite cylindrical resolution cell requirement is violated, the no-target hypothesis is accepted and the beam is moved to a new position.

For the case where the same resolution-cell size is employed on each of the sequential steps, the decision rule reduces to that of the regular EVSD's and is defined in Section 2.

5.4 ANALYTICAL FORMULATION OF THE RV EVSD OPTIMIZATION PROCEDURE

The analytical procedure for selecting at each sequential step the transmitter energies and receiver thresholds minimizing the average transmitter power requirements for a specified set of surveillance conditions, and where the time bandwidth product changes are specified, is similar to the one developed for the more conventional EVSD's. An outline of this procedure is presented here for the detection of a non-fluctuating target and where a maximum number of steps of N is employed.

The expression for the probability of detection P_D is:

$$P_D = \prod_{i=1}^{N} Q(\alpha_i, \beta_i) \tag{22}$$

where the Q function and the parameters α_i and β_i have previously been defined in Section 2.

The probability of a false alarm in at least one of the cylindrical resolution sets of cell combinations (P_{FO}) may be expressed as:

$$P_{FO} = P\left\{ \bigcup_{i=1}^{n_1} \left[X_{1,i} > \beta_1 \bigcap \left(\bigcup_{J=1}^{F_2} X_{2,J} > \beta_2 \right) \right.\right.$$
$$\left.\left. \bigcap \left(\bigcup_{K=1}^{F_3} X_{3,K} > \beta_3 \right) \bigcap \cdots \bigcap \left(\bigcup_{\ell=1}^{F_N} X_N > \beta_N \right) \right] \right\} \quad (23)$$

where the X's refer to the detected outputs on successive steps in cylindrical resolution sets of cells. The factor F_i is the ratio of the time-bandwidth product of the i^{th} step $(TW)_i$ to that of the $(i-1)$ step $(TW)_{i-1}$:

$$F_i = \frac{(TW)_i}{(TW)_{i-1}} \quad (24)$$

n_1 equals the number of resolution cells [illegible] range-doppler uncertainty space with a unity time-bandwidth product signal.

The total false alarm probability P_{FO} (equation 23) may be approximated as:

$$P_{FO} \approx n_1 \left[\prod_{i=2}^{N} F_i \right] e^{-\sum_{j=1}^{N} \frac{\beta_j^2}{2}} \quad (25)$$

by making use of the binomial expansion, and in general that the quantities $e^{-\beta_j^2/2} << 1$. The development is similar to that employed in the resolution-variant theorem.

The product $\prod_{i=2}^{N} F_i$ is equal to the time-bandwidth product of the last stage $(TW)_N$ since the time-bandwidth product of first stage is unity and the intermediate stage TW's are cancelled in the product of ratios. This last stage time-bandwidth product $(TW)_N$ yields the resolution required of the mission and, therefore, the factor in equation (25)

$$n_1 \prod_{i=2}^{N} F_i = n_1 (TW)_N = N_F \tag{26}$$

where N_F is the number of the fine last-stage resolution cells which would be required to cover the total parameter uncertainty space. The expression

$$e^{-\sum_{j=1}^{N} \frac{\beta_j^2}{2}}$$

may be given the interpretation of an equivalent single-cell false alarm probability (P_{FA}) where the single-cell dimensions are those of the final sequential step. Equation (25) may now be expressed as

$$P_{FO} = N_F P_{FA} \tag{27}$$

where

$$N_F = n_1 \prod_{i=2}^{N} F_i \text{ and } P_{FA} = e^{-\sum_{j=1}^{N} \frac{\beta_j^2}{2}} \tag{28}$$

By using the equivalent cell interpretation of equation (27) and (28), a single-cell false alarm probability basis of comparison with fixed sample size tests and EVSD tests with constant resolution is achieved.

The cost function, here again as for the conventional EVSD design, is made equal to the average received energy to noise power density required to perform the specified surveillance mission and may be expressed as:

$$C = \frac{\alpha_1^2}{2} + \frac{\alpha_2^2}{2} n_1 e^{-1^2/2} + \sum_{J=3}^{N} \frac{\alpha_J^2}{2} \left(n_1 \prod_{K=2}^{J-1} F_K \right) e^{-\sum_{i=1}^{J-1} \frac{\beta_i^2}{2}} \tag{29}$$

The optimization problem now involves determining the design parameters $\{\alpha_i\}$ and $\{\beta_i\}$ minimizing the cost ($\bar{C}$) (equation 29) and satisfying the detection probability (P_D) (equation 22) and the total false alarm probability (P_{FO}) (equation 25). The final resolution cell size, and consequently the time-bandwidth product is an additionally specified quantity. Using this time-bandwidth product, and the admissable range-doppler parameter space of the target, the number of final resolution cells required to cover the admissable target parameter space N_F can be computed, and the false alarm requirement can be made in terms of (P_{FA}), the equivalent single-cell false alarm probability (equation 25). The time-bandwidth increase on successive steps $\{F_i\}$ are inputs to this energy minimization procedure, and are mainly a function of the signal-processing scheme for effecting a commonality of equipment usage on successive steps.

The minimization of $\bar{C}$ is now obtained using the method of Lagrage Multipliers as for the conventional EVSD's (See Section 2 and Appendix II). The expression for P_D and P_{FA} are the constraint relationships for this procedure.

Design and performance parameters for a typical surveillance situation obtained with this procedure are presented in Figures 19 and 20. A Resolution-Variant EVSD with a maximum of three steps is considered with the required time-bandwidth product of 10,000 obtained by stepped-increases of 100 on the second and third step. An indication of the significantly increased average power saving of an EVSD with the same time-bandwidth product on each step is displayed in Figure 19. (It is assumed that the unity time-bandwidth signal of the first step covers the target range-doppler uncertainty space in 10 resolution cells.) In this figure, the power savings over the use of a fixed sample size test or uniform search mode are presented for both a conventional EVSD, and the Resolution-Variant EVSD for the same P_D and equivalent single-cell false alarm probability P_{FA}. It is important to note in this figure that the scale of the abscissa represents the total number of resolution cells for the 'constant resolution' EVSD, and only the first-step resolution cells for the Resolution-Variant EVSD. The two curves are noted to be practically

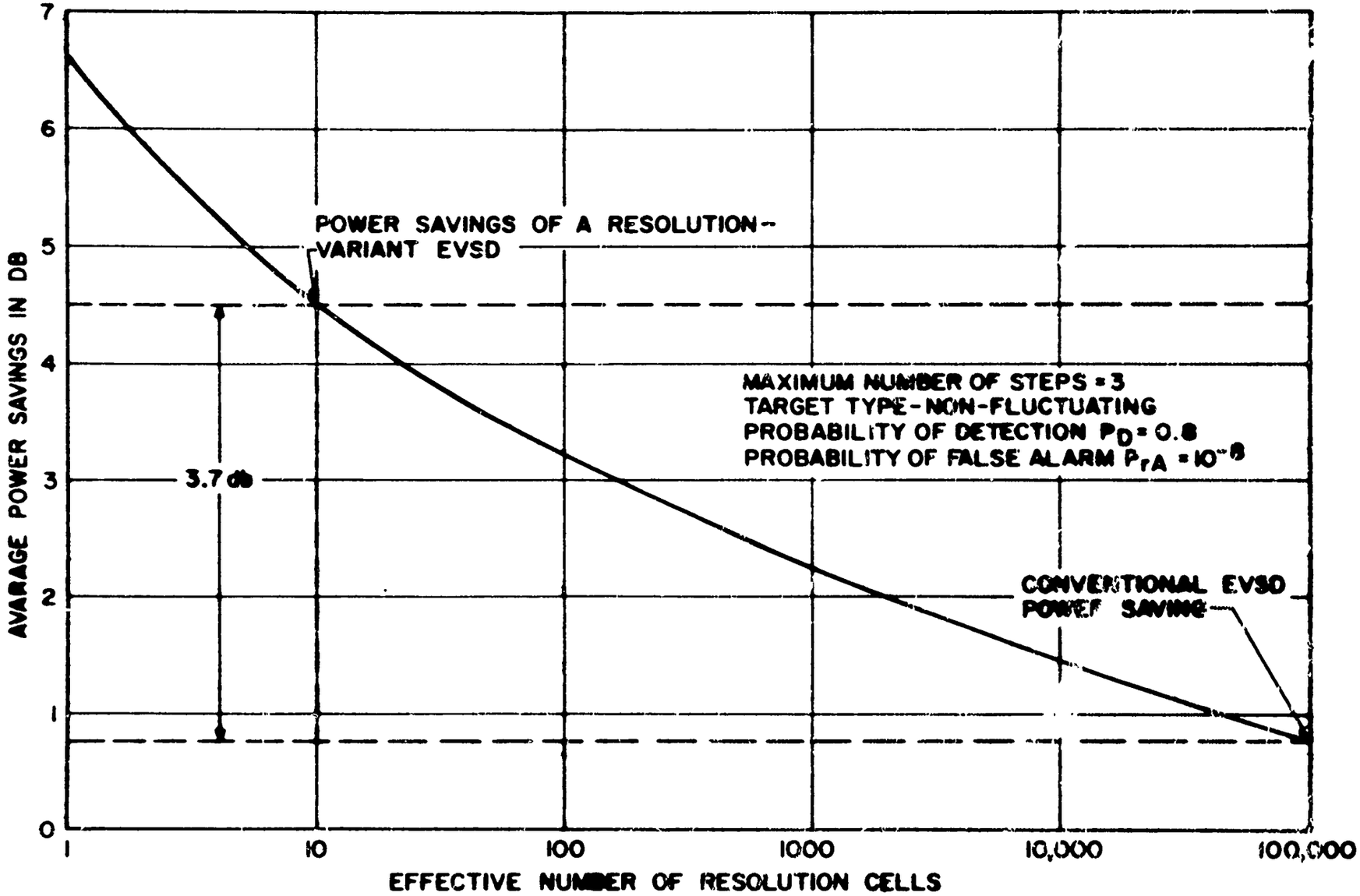

Figure 19. Average Power Saving of a Resolution-Variant EVSD

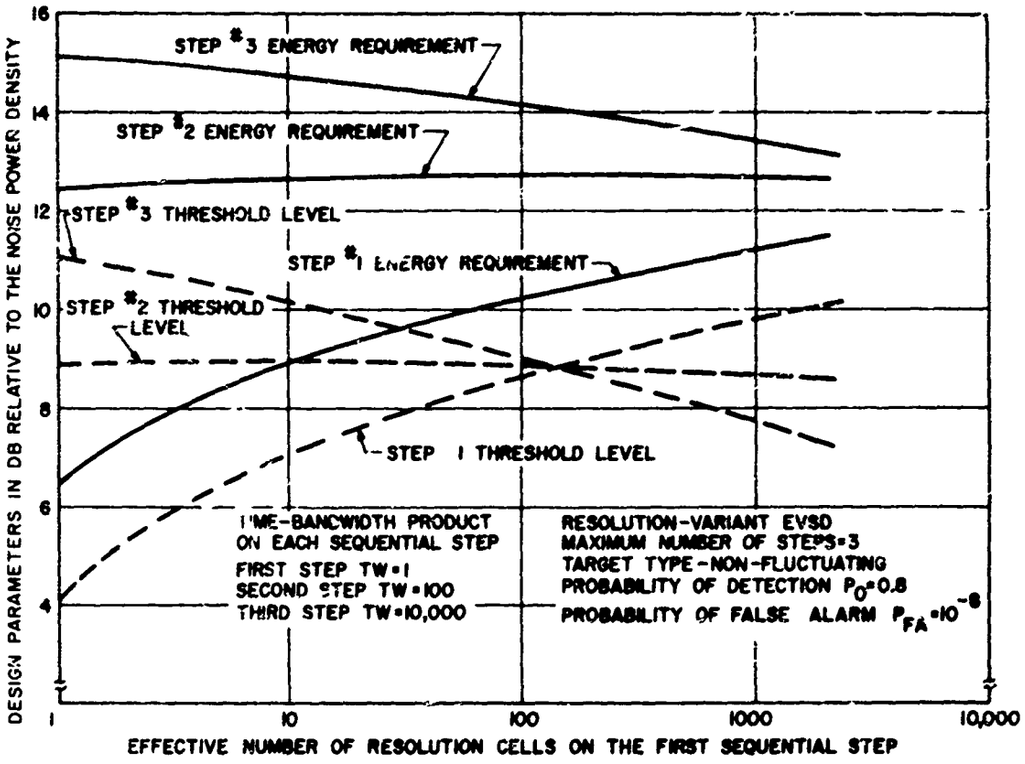

Figure 20. Design Parameters of a Resolution-Variant EVSD

coincident, so for example, if it is assumed that the first step covers the range-doppler uncertainty space in 10 resolution cells, the power saving of the Resolution-Variant EVSD over the use of a constant resolution EVSD is noted to be 3.7 db, approximately the difference in power requirements of a 10 resolution cell radar over the use of a 100,000 resolution cell radar.

Design parameters for this Resolution-Variant EVSD are presented in Figure 20. For the sake of comparison, the energy and threshold requirements of a conventional EVSD adhering to the same set of surveillance requirements are shown in Figure 21.

5.5 TRAFFIC HANDLING IN A RESOLUTION-VARIANT EVSD

The commonality of usage of one or two sets of active correlator channels to handle the signal processing of a Resolution-Variant EVSD on all sequential steps imposes a need for a multiple target-handling priority logic. For example, if the pseudo-random phase-reversal coded waveform and active correlator system described in

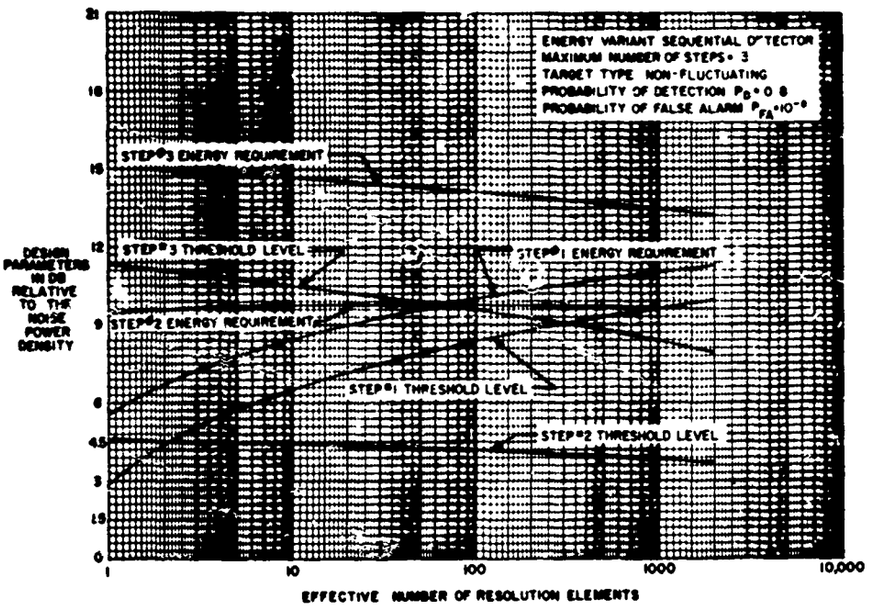

Figure 21. EVSD Design Parameters for a Three-Step Maximum Procedure, $P_D = 0.8$, $P_{FA} = 10^{-8}$

Section 5.11 is employed, all multiple-target report combinations can be handled with one set of correlators with the exception of a combination of target reports that involve the same range bin but different doppler channels. For this case, a maximum likelihood or 'greatest of' procedure can be used for selecting range-doppler bins to search on subsequent steps.

An important question to be answered when this type of 'greatest of' logic is used is the following: What is the degradation of performance due to mistakes made in selecting a noise-alone channel rather than the channel containing the signal on a sequential step? The conducted analysis shows that for the case where a signal channel is competing with 10 noise-alone channels, the reduction in detection probability for a three-step maximum procedure is less than 0.1%.

The computations are based on the developed expression of the probability that with n + 1 channels, n of which contain noise alone, and one contains the return of a non-fluctuating target plus noise, the matched-filter output of the signal channel will be

both greater than that of the n noise channels and of the threshold β. This probability is:

$$P_{D_i} = \sum_{P=0}^{n_i} (-1)^P \binom{n_i}{P} \frac{e^{-\frac{P\alpha^2}{2(PH)}}}{P+1} Q\left(\frac{\alpha_i}{\sqrt{P+1}}, \beta_i \sqrt{P+1}\right) \quad (30)$$

where $Q(\alpha, \beta)$ is the Q function defined in equation 4 of Section 2.4, $n_i + 1$ is the number of target bins involved in the priority assignment of the i^{th} sequential step, and $\alpha_i^2/2$ and β are the receiver signal energy to noise power density and the threshold, respectively, of the i^{th} step. The probability of detection of the sequential mode is the product of single-step detection probabilities of equation 30 for each of the N steps. The development of equation 30 is presented in Appendix 1.

5.6 ENVELOPE AND FINE STRUCTURE DOPPLER

In conventional radars employing low time-bandwidth product signals, the affect of envelope compression due to target doppler is neglected. Uncompensated-for envelope compression does not significantly degrade system performance if the inequality

$$\frac{V}{C} << \frac{1}{2TW} \quad (31)$$

is true. (For example, see Elspace, Reference #12 for a development of this inequality) where V is the target doppler velocity, C is the speed of light, and T and W are the time duration and bandwidth of the transmitted signal. This inequality is based on assuming a constant velocity target, and for this case, the return signal at delay τ (t) can be shown to be:

$$\psi\ (t - \tau(t)) = u\left[\frac{1 - V/C}{1 + V/C}\ (t - \tau_o')\right] e^{J2\pi\ (t_o - V)\ (t - \tau_o')} \quad (32)$$

where the complex modulation function is $u\left[\frac{1 - V/C}{1 + V/C}\ (t - \tau_o')\right]$

where $\tau_o' \approx \frac{2R_o}{C}$, and the factor $\frac{1 - V/C}{1 + V/C}$ appearing in the argument of the modulation function is indicative of the compression or stretching of the returns signal modulation time scale.

For a transmitted signal of duration T, the compression increment or error in the argument of u (t) is:

$$\left(1 - \frac{1 - V/C}{1 + V/C}\right) T = \frac{2\ V/C}{1 + V/C}, \quad T \approx \frac{2V}{C} T, \tag{33}$$

and the criterion of keeping this time increment small with respect to 1/W leads to the inequality of equation (31),

$$\frac{V}{C} << \frac{1}{2TW} \tag{34}$$

For those high resolution radars, where the relationship of target doppler velocity and time-bandwidth product is such that the inequality of equation (31) is violated, considerable hardware complications are introduced if the envelope compression is to be compensated for the full range of possible doppler shift in a fixed sample size test.

The Resolution-Variant EVSD employing time-varying matched filters, or active correlators, provides a good method for introducing the required compression in the receiver signal processing with a minimum hardware requirement. In general, the procedure involves a compensating compression or expansion of the cross-correlation signal time base at a sequential step employing doppler information obtained from the immediately preceding sequential step. For example, consider the pseudo-random phase-reversal coded waveform ensemble of Section 5.11. To compensate for an estimated doppler shift V, say estimated on the second sequential step, the new 0-180 degree phase-reversal frequency would be $\frac{1 + V/C}{1 - V/C}$ times the transmitted phase-reversal modulation frequency. This boot-strap operation from one sequential step to another significantly reduces the number of parallel channel compensations which would be required if a 'single shot' mode were employed.

5.7 ACTIVE CORRELATION SYSTEM

A marked reduction in the number of parallel processing channels required is accomplished by the dual measures of programming a gradual increase of the time-bandwidth product on successive steps of the multiple stage decision processor, and employing an active correlation system as the basic signal processing scheme for approximating matched filter requirements on successive sequential steps. The signal processor must accommodate changes in the transmitted signal time duration, bandwidth, and the waveform 'density' and other fine-structure waveform details.

A general conclusion reached from the implementation investigation which has been conducted is that an active correlation system represents the most effective way of meeting the signal-processing flexibility and economy demands of an efficient high-resolution surveillance mode. That is to say, a basic choice must be made between time-variant and time-invariant filtering systems; and for the RV EVSD the time-variant processing or active correlation systems is most compatible with system requirements. A conceptual diagram of such a multiple-stage cross-correlation system is presented in Figure 16.

A commonality of equipment usage in the active correlator system is effected by a 'boot-strap' operation that involves both a controlled gradual increase of time-bandwidth product on successive steps of the multiple-stage processor, and a communications to the programmer of the parameter coordinates of the resolution cells exhibiting threshold crossings at a sequential step so that the parameter space surveillance on subsequent steps can be limited. In this manner, the same correlation and signal generation equipment can be employed on successive steps representing different resolution cell sizes. In effect, each sequential step is employed to accomplish a dissection of a resolution cell of an immediately preceding step.

(The target-present hypothesis is only accepted when threshold crossings occur in an admissable combination of successive sequential step parameter cells.)

Flexibility in the active correlation system is achieved by a digital control (and for some waveform ensembles - the generation of modulation) of the delayed and frequency-shifted correlation signals employed as the 'guesses' of the return signal.

5.8 SIGNAL AMBIGUITY DIAGRAM OF RESOLUTION-VARIANT SIGNAL PROCESSOR

A schematic representation of the signal ambiguity space for a three-step maximum procedure is presented in Figure 17. A pseudo-random phase-reversal code is used to illustrate this telescoping to a final resolution cell size in three sequential steps. The target is declared present only when threshold crossings occur in an admissable combination of 'coarse' - 'medium' - 'fine' cell combinations at each of these three sequential steps. Such a combination is illustrated in Figure 17. The sidelobe levels are also, of course, a function of the waveform and time-bandwidth product employed on each of the sequential steps. A task of the next phase of the program will involve a more detailed analytical treatment of the multiple-stage target resolution process which would include computation of side-lobe characteristics at each of these stages for specific waveform ensembles. A statistical analysis of errors in the decision processor will then be conducted as a function of these more detailed resolution models.

5.9 WAVEFORM ENSEMBLES FOR THE RESOLUTION-VARIANT EVSD

The waveform design of the successive steps following the conventional unity time-bandwidth product initial step will be influenced by both the anticipated target environment and implementation considerations. Examples of signal ensembles which may be employed in a Resolution-Variant EVSD are presented in Figure 22 for a

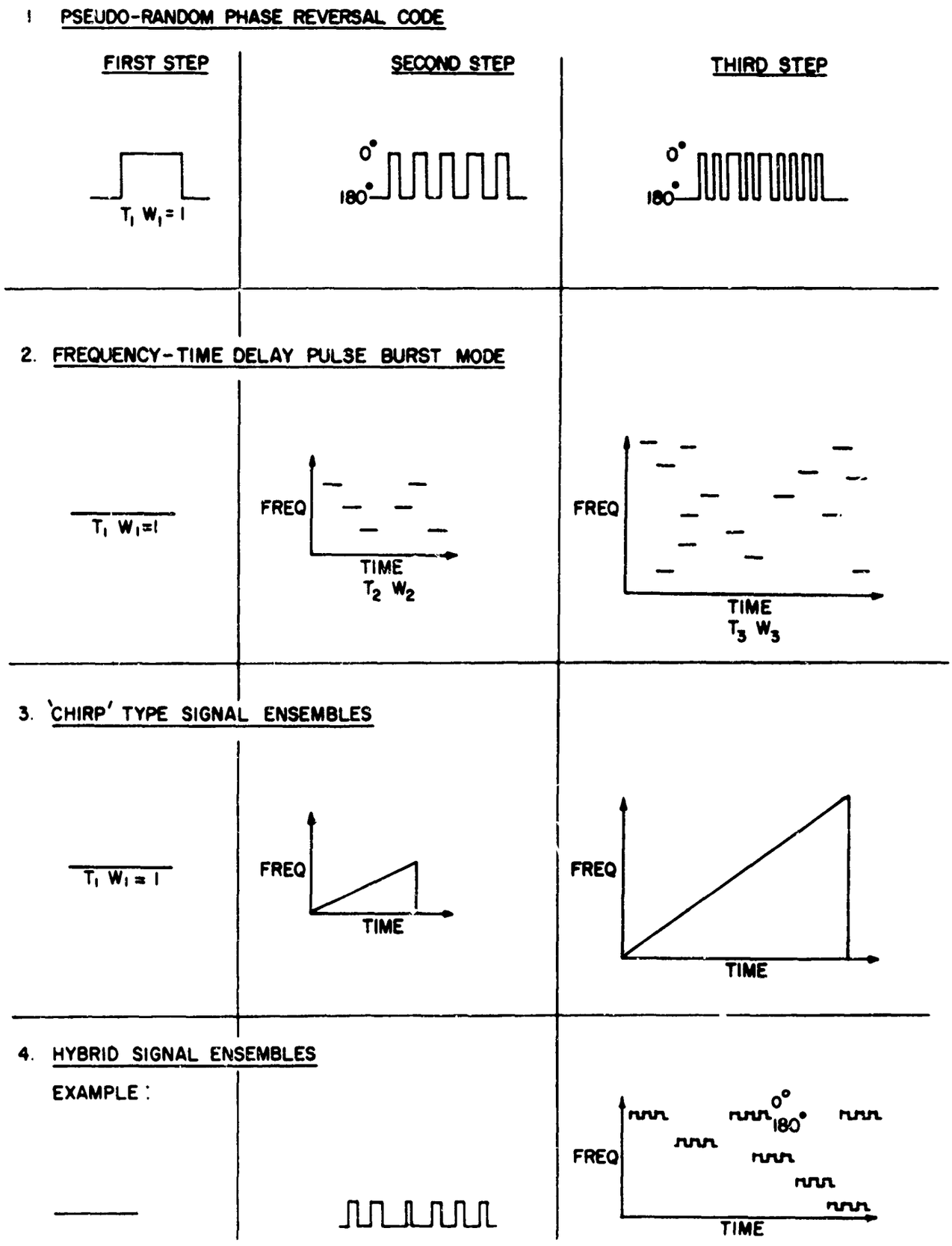

Figure 22. Typical Waveform Ensembles for Resolution-Variant EVSD

three-step maximum procedure with coded waveforms employed on the last two steps. These include: (1) the pseudo-random phase-reversal coded waveform, (2) the frequency-shift time-delay pulse burst waveform, and (3) the chirp type of waveform ensemble which would include both linear and non-linear frequency modulations. The increased time-bandwidth product on successive steps is noted in Figure 22.

Six other hybrid waveform ensembles for a three-step maximum Resolution-Variant EVSD are also derivable from the three ensembles listed above. These 'hybrid' waveform ensembles are generated by employing one waveform type on both the second and third step with a common bandwidth and then achieving the additional frequency spread of the transmitted energy of the third step by superimposing one of the modulation techniques not previously employed. (That is to say, one of the two remaining modulation techniques.) Such a hybrid ensemble is illustrated in Figure 22. In this example, a phase-reversal code is employed on the second step, and on the third step, a frequency-shift time-delay pulse burst mode is employed with the phase-reversal code superimposed on each of the subpulses.

5.10 TYPICAL DESIGN PARAMETERS

A typical set of design parameters for a Resolution-Variant EVSD which are significant for the design of the signal-processor unit are presented here in order to provide a vehicle for discussion of the active correlator in greater detail.

The representative set of parameters tabulated below is noted to include changes in both the bandwidth and time duration on successive steps. For the three-step maximum procedure, a unity time-bandwidth product signal is employed on the first sequential step, and the bandwidth increases are in steps of 125 to 1, increasing from 10 KC on the first step, to 1.25 MC on the second step and finally to 156 MC on the third step. The corresponding range resolutions are 8.1 nautical miles for

the first step, 400 feet for the second, and 3.2 feet for the final step. An increase in the duration of the signal from 100 usec. on the first step to 200 usec. on the second and third steps is also included in this example. The time-bandwidth product increases from unity on the first step to 250 on the second step, and to over 31,000 on the final step.

TYPICAL PARAMETERS FOR RESOLUTION-VARIANT SIGNAL PROCESSOR

Sequential Step	Bandwidth	Time Duration	Time Bandwidth Product
First Step	10 kc ΔR = 8.1 n.m.	100 μsec. Δfd = 10 kc	Unity
Second Step	(125) 10 kc = 1.25 mc ΔR = 400 feet (0.8 μsec.)	200 μsec. Δfd = 5 kc	250
Third Step	$(125)^2$ 10 kc = 156 mc ΔR = 3.2 feet (6.4 nano seconds)	200 μsec. Δfd = 5 kc	(250) (125) = 31,250

5.11 RESOLUTION-VARIANT SIGNAL PROCESSOR EMPLOYING A PSEUDO-RANDOM PHASE-REVERSAL CODE SIGNAL ENSEMBLE

To illustrate an active correlator system for meeting the resolution-variant requirements, a functional diagram of such a signal processor with a maximum of three steps and based on the employment of a pseudo-random $0\text{-}180^{o}$ phase-reversal code ensemble is presented in Figure 23.

A conventional unity time-bandwidth product first stage signal processor is employed. The commonality of equipment usage is demonstrated in the second and third stages which involve stepped increases in signal bandwidth. The same pseudo-random code signal generator and associated shift register and phase reversal correlators are employed for the latter two steps. Each stage of the correlator shift register represents a 400 foot range bin on the second step, and a 3.2 foot range bin on the third step, using as an example the parameters of the previous

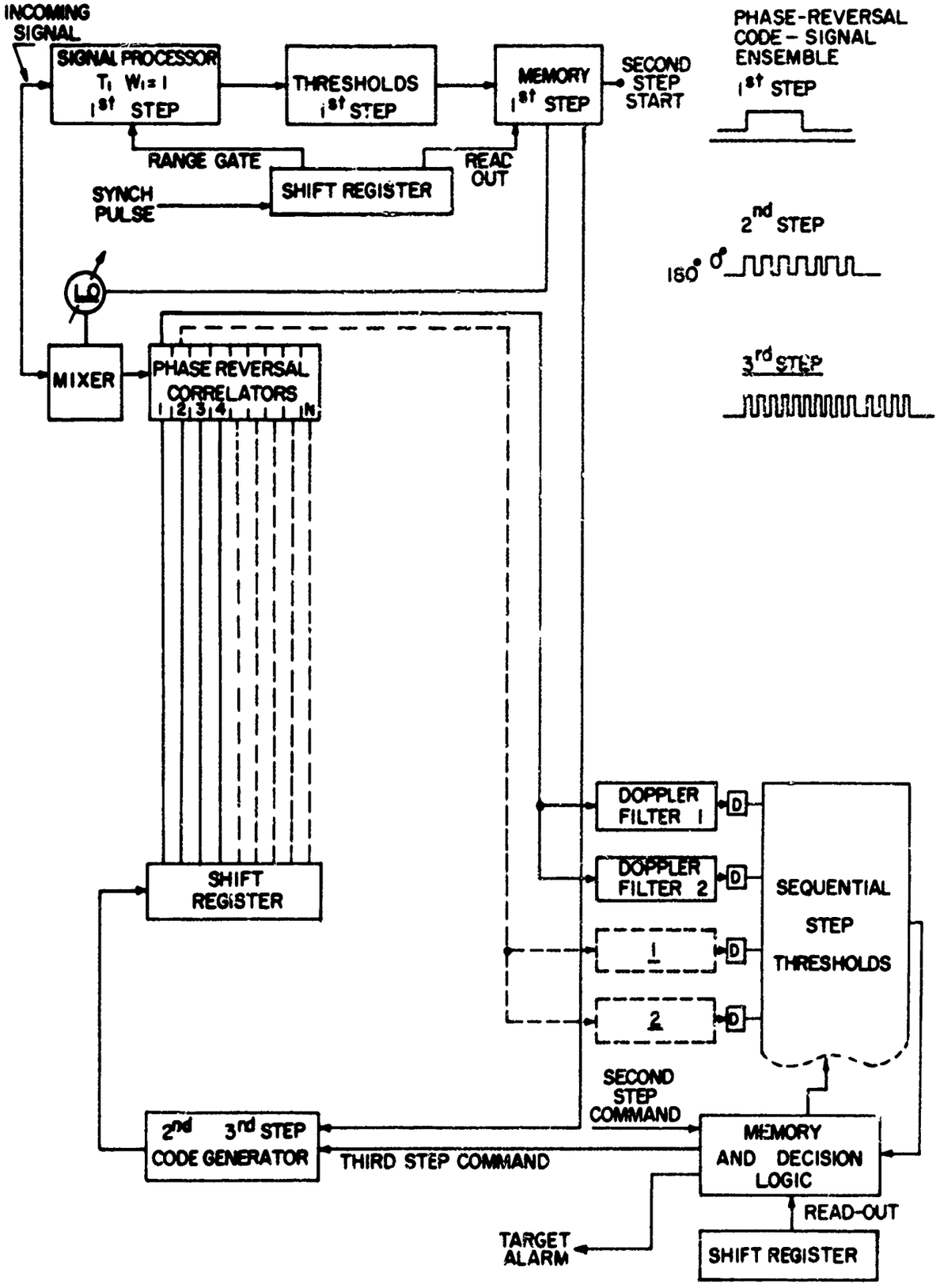

Figure 23. Resolution-Variant Signal Processor 13-Step Maximum EVSD

section. The pseudo-random code of the second step is generated using a 1.25 MC counting rate and the same code generator is employed at the 156 MC rate for the final step.

The output of the phase-reversal correlator is now a relatively narrow bandwidth signal and conventional filters matched to this unity-time bandwidth signal are employed. A linear detector and threshold follows each of these filters. Since the time duration of the transmitted signal is the same on the second and third stop, the doppler filters following the phase-reversal demodulators are also common for these latter two steps.

An important part of the scheme for reducing parallel signal processing requirements is accomplished by employing the coarse range and doppler coordinates of those cells exhibiting threshold crossings on the first step for reducing the range-doppler parameter space to be covered on the second step - and in turn, the parameters of the second step 'medium' size resolution cells exhibiting threshold crossings are communicated to the programmer for a third step use.

5.12 CRITICAL COMPONENT AND THIRD PHASE PROGRAM

The signal-processing system required for the implementation of a Resolution-Variant EVSD which is designed to meet a high resolution mission, where the bandwidth requirements are over 150 mc, is determined to be a critical component requiring further development. An active correlator system of the type discussed in Section 5.11 forms the basis of the resolution-variant signal processor which is designed to accommodate the changing time-bandwidth product signals on successive sequential steps, and approximate matched-filter processing on each of these steps.

Emphasizing the importance of the development of a resolution-variant signal processor of this type are the following considerations: 1) radar surveillance missions of the future are anticipated to be of the high resolution type, and, if these missions were performed in a conventional manner, system costs in many cases would be

excessive, 2) the Resolution-Variant EVSD offers the promise of economical performance of the high-resolution surveillance mission, 3) the signal processor flexibility requirements for a Resolution-Variant EVSD are similar in significant respects to those of other important high-resolution radar missions (terminal defense, hardpoint, and area defense) so that the development of the requirements for the space-surveillance class of mission will significantly extend the signal-processing art required for these other missions. The planned third phase of the subject contract consequently involves a preliminary design and development program leading to the development of such a multiple-stage resolution-variant signal processor capable of demonstrating: 1) the achievement of matched-filter conditions on successive sequential steps accommodating changes in the time-bandwidth product, energy, and fine-structure details of the waveform transmitted at each of these sequential steps, 2) power savings of the Resolution-Variant EVSD surveillance modes, 3) hardware economy accomplished by reducing the number of signal-processing channels required and, 4) the achievement of the typical large bandwidth requirement (achieved on the final sequential step) of over 150 MC.

5.13 HIGH SPEED DIGITAL CIRCUITS

A consideration of the high-speed digital circuits involved in the realization of a resolution-variant sequential detector with a maximum of three steps, and based on a system employment of a pseudo-random phase-reversal code waveform ensemble is presented in this and the following subsections. The pseudo-random phase-reversal code waveform ensemble, and the typical set of design parameters outlined in Section 5-10, are used as a basis for discussion of the high-speed technology involved in the active correlator system.

A block diagram of the high-speed logic portions of the system is presented in Figure 24. The same Shift Register Generator (SRG) and shift register are used for the second and third sequential steps.

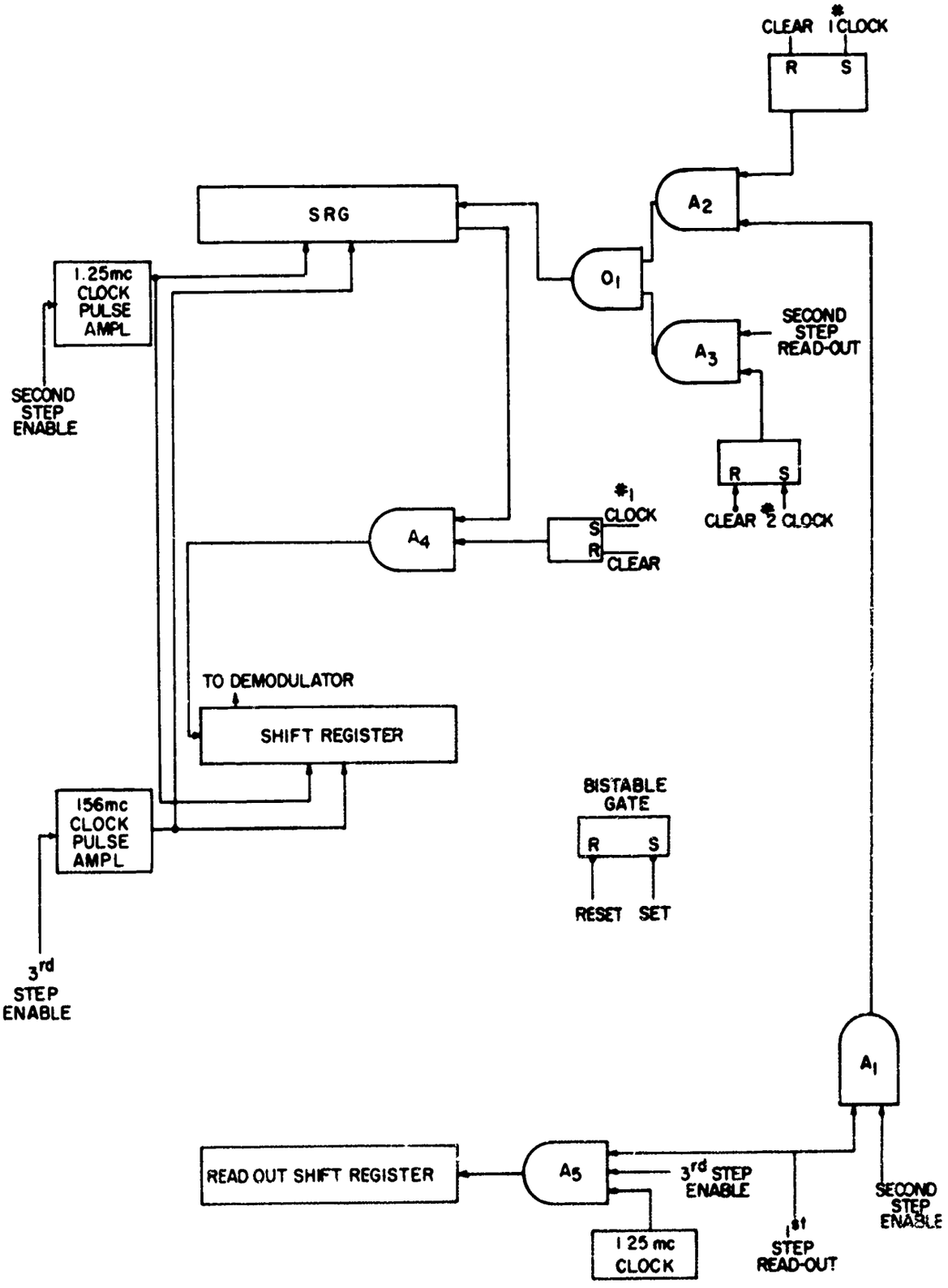

Figure 24. Block Diagram of High-Speed Logic

The system test for the presence of a target at a particular beam position is initiated with the transmission of a 100-microsecond uncoded pulse. Threshold crossings in any of the 125 range 'cells' assumed to cover the range uncertainty are 'memorized' in bi-stable elements. If at least one threshold crossing occurs in a range-doppler cell, a second-step 'enable' signal is generated.

The second-step 'enable' signal initiates the following sequence of events:

(a) The SRG taps, of Figure 24, are electronically connected to provide an 8-stage SRG for generating the second-step pseudo-random sequence of (2^8-1) bits,

(b) The 1.25-megacycle clock pulse amplifier and "AND" gate (A_1) are enabled,

(c) A second pulse, which is coded with the same sequence as that of (a), is transmitted, and

(d) A read-out of the first-step range-doppler bins exhibiting threshold crossings is initiated for use on the second sequential step.

The "second-step enable" and the read-out first-step range doppler bins produce an output from A_1 which enables A_2. "And" gate A_2 is, therefore, activated with the #1 clock pulse. This is a specially derived pulse which will control the starting of the SRG to within a clock pulse of the SRG running frequency. Thus, the SRG sequence starts at a precisely known time. The applied clock pulse has a rise time which is a fraction of a nanosecond. The clock pulse is obtained from high-speed counting circuits which are described in Section 5.14.

A scheme is now introduced to relieve the turn-on time requirement of the 1.25-megacycle clock, which supplies all stages of the SR and the SRG. The output of A_2 is applied to the 'OR' gate (0_1) and the output of this gate starts the SRG. The circuit and logic are so arranged that the SRG is not running even though it is being clocked, but must wait for the start command for the 'OR' gate (0_1). Similarly,

the shift register is in the reset state and receives no information from the SRG until A_4 is enabled by the #1 clock pulse. Consequently, the clock can be turned on in, say, milliseconds instead of 2 nanoseconds required for precise starting of the SRG. This provides a major simplification when so many stages need to be driven.

After the 1.25-megacycle clock is turned on, the SRG is ready for a command from the 'or' gate (0_1). Before receiving a start command, the SRG is not running but its stages are in a predetermined state of all "zeros" except for the next to the last stage which stores a "one". Thus, the start command always starts the sequence from the point which is required for proper correlation of a second-step return signal falling within one of the first-step 'coarse' range-doppler bins.

The second-step range-doppler bins exhibiting threshold crossings will set appropriate 'flip-flop' memory units. The occurrence of at least one admissable second-step threshold crossing initiates the following chain of events:

(a) The SRG taps are electronically reconnected to provide a 15-stage SRG for generating a non-repeating pseudo-random sequence of $2^{15}-1$ bits for use on the third sequential step.

(b) The 156-megacycle amplifier and "AND" gate A_5 are enabled while the 1.25-megacycle amplifier is disabled. The 1.25-megacycle clock is connected to the auxiliary shift register.

(c) A clear pulse is generated which clears the necessary gates.

(d) A third pulse, which is coded with the same sequence as that of (a), is transmitted.

(e) A read-out of the second-step range-doppler bins exhibiting threshold crossings is initiated for use for the third sequential step.

These read-out second-step range-doppler bins are used to start the SRG and SR which are now connected to operate at 156 MC. The #2 clock in conjunction with

the read-out range-doppler bins is employed to start the shift register for third-step operation in a manner similar to that used on the second step.

Admissable third-step range-doppler bins exhibiting threshold crossings are 'memorized', and if at least one of these threshold crossings occur, the target alarm is initiated.

5.14 CIRCUITS

Circuits which can be used to implement the gating, counting, and shift register logic of Section 5.13, are presented in Figure 25. The circuits have been previously subjected to tests at 100 MC over a temperature range of -30^{o} to $+85^{o}$ C. Single stages have been operated at 275 megacycles. The voltage swings are -50 millivolts and -500 millivolts, corresponding to a logical 'zero' and 'one' respectively.

In addition, the current-supply registers, R_8, have been removed from stages 14 and 15. Current to these stages is supplied by the transistor current switches comprising gates A_2, A_3 and 0_1 of Figure 24. The absence of any output from the "first step" and the "second step" makes $I_1 = 54$ milliamperes and $I_2 = 0$. This condition forces stage 14 to the "one" state and stage 15 to the "0" state. Since stage 15 provides the output for the feedback taps, all remaining stages go to zero. An output from the "first step" - in conjunction with #1 clock - or an output from the "second step" - in conjunction with #2 clock - makes $I_1 = I_2 = 27$ milliamperes, the normal operating current biases for stages 14 and 15. The shift-register generator becomes operative and the "one" stored in stage 14 starts the sequence. Note that clock #1 and clock #2 operate bi-stable tunnel diodes so that once the shift-register generator is activated, it will continue to generate the sequence until the bi-stable tunnel diodes are reset. Resetting is accomplished after the correlation has been detected.

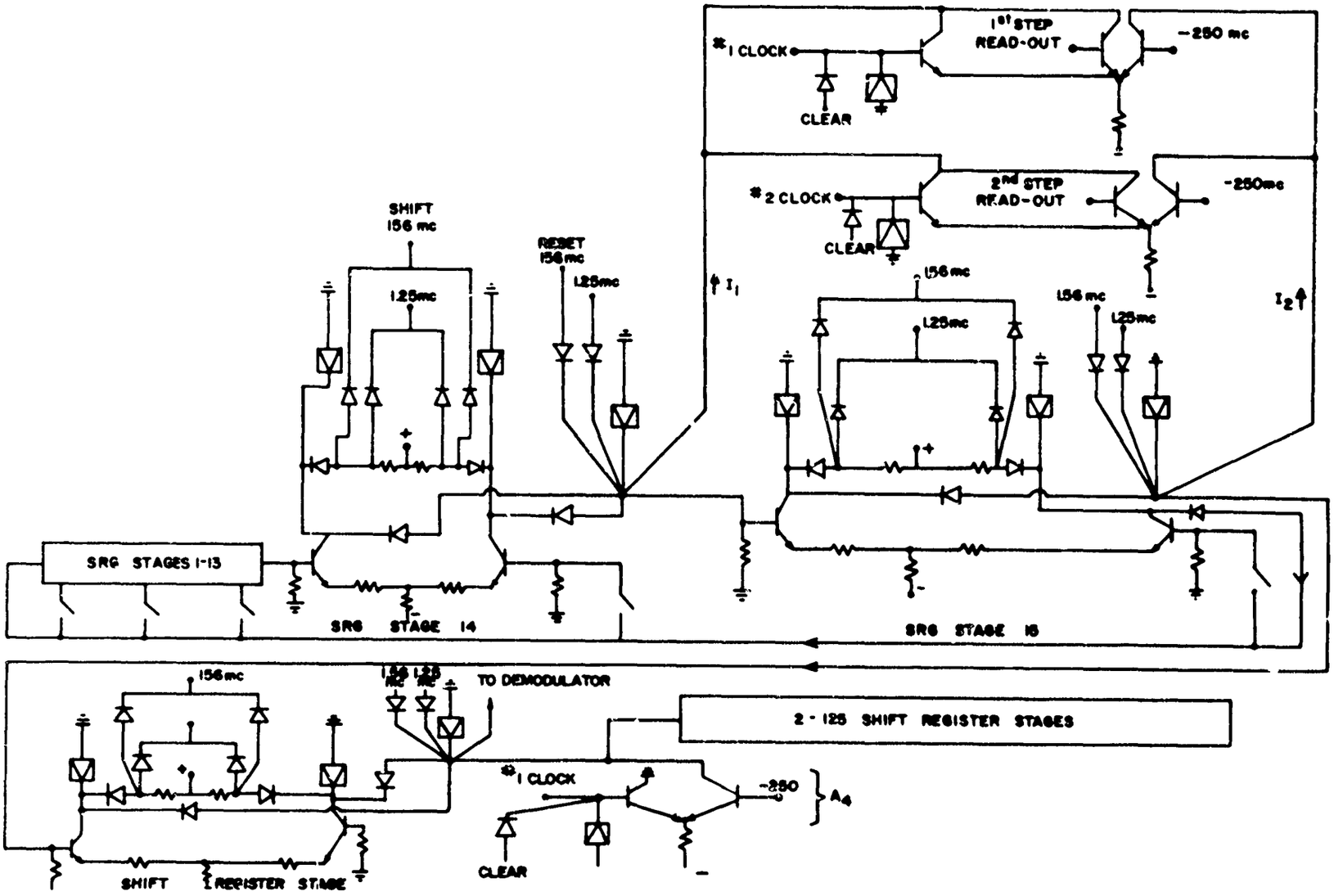

Figure 25. Circuit Diagram of High-Speed Digital Circuits

The generated sequence feeds the shift register. One of the shift-register stages is shown in detail. Here, a shift-register generator stage is converted to a shift-register stage since one of the inputs is permanently at "zero". This shift-register stage can be inhibited by the current switch comprising the "AND" gate, A_4, of Figure 25. This shift-register stage is enabled with the #1 clock which also switches a bi-stable tunnel diode, thus causing the shift register to receive information at a specified time and stop receiving information when the tunnel diode is cleared. Each shift-register stage has an output to drive the phase-shift demodulator.

5.15 ACCURATE CLOCK REFERENCE

In order to provide an accurate reference clock pulse for starting the shift-register generator, a counter is used to count down from 156 megacycles to 1.25 megacycles (giving the #2 clock) and then to 10 kilocycles (giving the #1 clock). In order to accomplish this, about fourteen binary counter stages will be required. For the required accuracy of starting the shift-register generator, it is important to keep the output jitter to a minimum (possibly less than 1 nanosecond). This requires counter stages having small jitter and, consequently, short delay. Even the fastest tunnel-diode counter stage will produce a jitter of about 0.5 nanosecond. Thus, the accumulated jitter of fourteen stages is 7 nanoseconds. This is not acceptable. The required jitter-free signal can be obtained with the tunnel-diode counter of Figure 26. Here, TD_1 and TD_2 make up a counter stage which supplies an output to TD_3. The input to TD_3 is differentiated by R and L. The bias of TD_3 is adjusted so that the output of TD_2, by itself, is not sufficient to cause firing. TD_3 is coincident with the 156-megacycle clock. Thus, the output of each counter stage is retimed by the 156-megacycle clock. This provides an output of the required time accuracy.

5.16 PHASE REVERSAL DEMODULATOR

Another critical portion of the signal processor, designed for a system transmitting a pseudo-random phase-reversal code waveform ensemble, is the cross-correlator

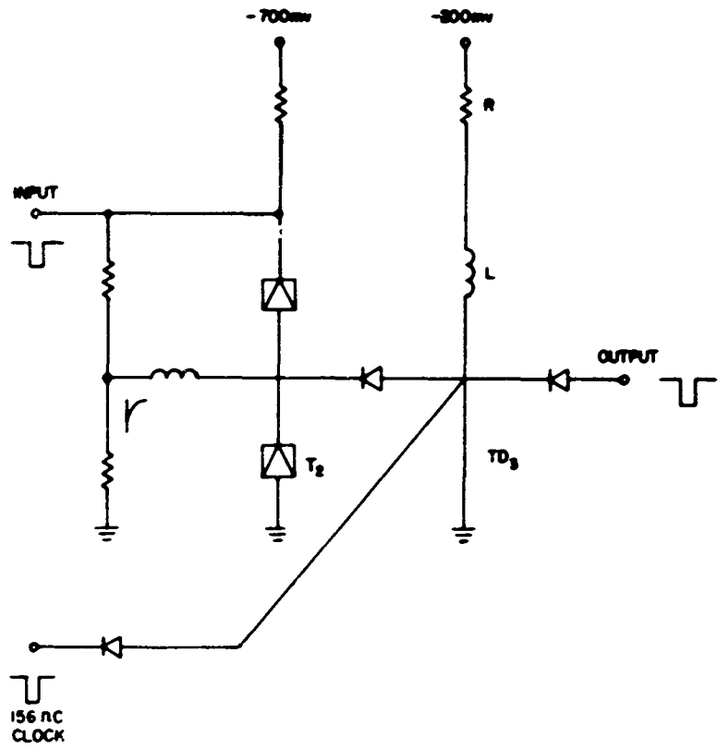

Figure 26. High-Speed Binary Counter

or phase-reversal demodulator unit. A phase-reversal demodulator is provided for each of the resolution cells and involves the removal of the 0-180° phase-reversal modulation for the return signal at the proper range bin. The range information is essentially extracted at this point and the resulting narrow band signal is now processed in narrow-band doppler filters. For example, for the 200-microsecond, 156-megacycle signal, the bandwidth at the output of the phase-reversal demodulator is reduced to 5 KC.

A realization of the demodulator circuit involving a selective phase reversal of some of the sequentially received pulses is described here. Semi-conductor diodes are considered for the switching elements. Switching by field effect devices, such as ferrites, is not appropriate because of the high switching speeds required.

The phase reversal is accomplished by a half cycle of delay, or by a mode twist, accomplished by, say, physically twisting a section of parallel wire transmission

line. The implementation of the extraction of the selected pulses may involve undesirable energy storages. A useful and well-tested form of demodulator using this idea is shown in Figure 27.

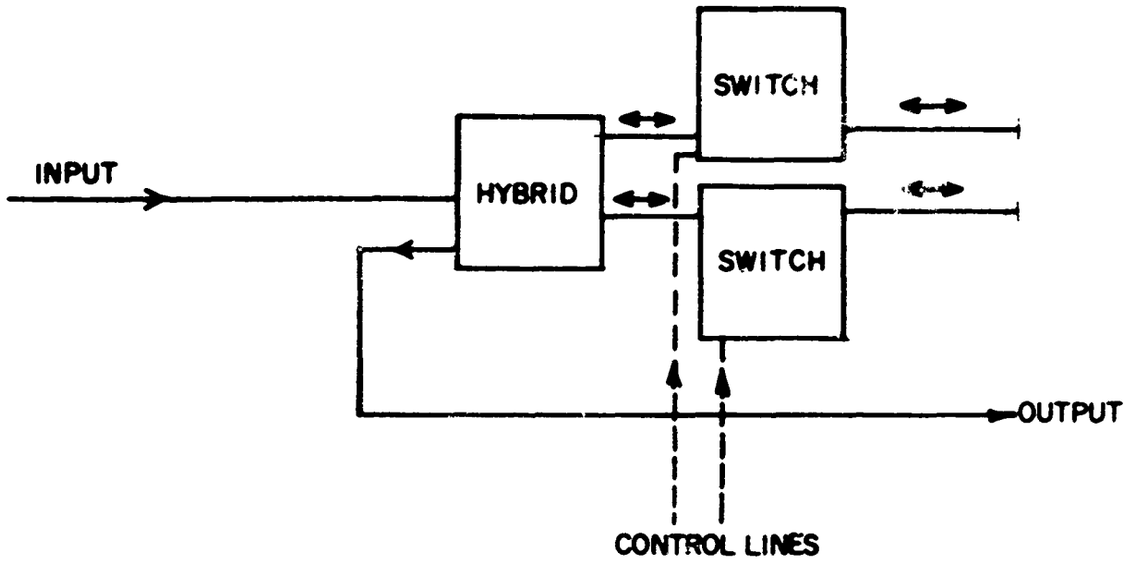

Figure 27. Sequential Demodulator

The input to the hybrid from the left divides equally between the two output ports at the right. Assuming both switches are in the step-mode, the two right outputs are reflected so as to add in the left output terminal. When both switches are in the pass-mode, the two right outputs are reflected by the shorts at the end of the transmission lines at the right, causing the output at the left to be delayed. Both switches are in the pass-mode at the same time and both are in the stop-mode at the same time. When the switches go into the stop-mode, a slug of energy is trapped between the switches and the shorted ends of the transmission line, causing a gap in the output. In an ideal sequential demodulator, no such energy would be lost.

The finite resistances of the switch cause a reduction of output level and, to achieve equal reduction for both the switch modes, trimming attenuators may be added to the configuration of Figure 27.

A second, and preferred, design approach which is somewhat more complicated, uses two parallel paths for processing the signal (Figure 28). The tapped energy resulting from either switch going into the stop-mode is lost in the attenuators, so it does not reverberate. The lost energy does not result in a gap in the output waveform. This attractive feature is purchased at the price of the output level being 6 db below the input level.

As the two switches alternate in being in the pass-mode, the absolute switch loss does not have a first-order effect on the uniformity of output level. A match in characteristics between the two switches will ensure a uniform output level into the hybrid for either phase. However, leakage through a switch in the stop-mode will affect the level of the final output. The phase inversion of Figure 28 arises from an inherent 90°-phase shift in each hybrid for the signal taking the lower route. This can be explained by the scattering matrix for the hybrid (Figure 29).

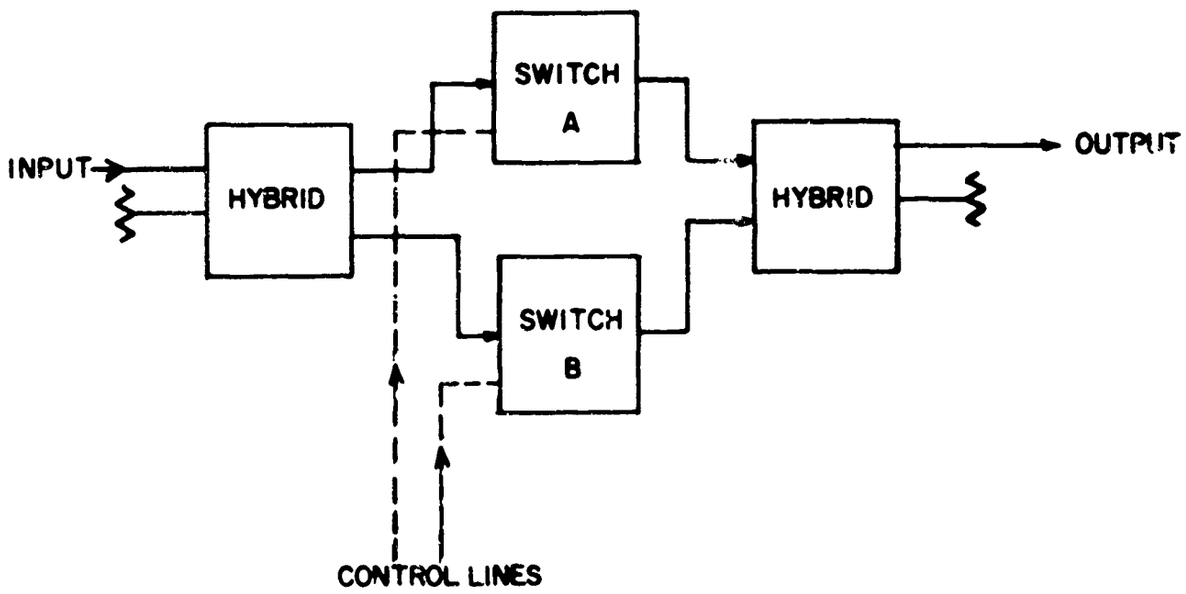

Figure 28. Parallel Demodulator

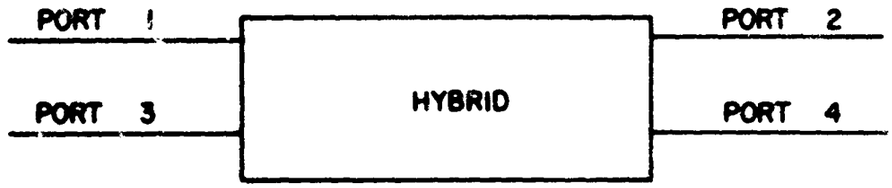

A HYBRID SCATTERING MATRIX CAN BE OF THE FORM :

$$S = \frac{1}{\sqrt{2}} \left[\begin{array}{cc|cc} 0 & 1 & 0 & j \\ 1 & 0 & j & 0 \\ \hline 0 & j & 0 & 1 \\ j & 0 & 1 & 0 \end{array}\right]$$

(1) THE ZEROS ON THE DIAGONAL INDICATE ALL TERMINALS ARE MATCHED.

(2) THE REMAINDER OF THE ZEROS SHOW ZERO COUPLING BETWEEN PORTS 1 AND 3, ALSO BETWEEN POSTS 2 AND 4.

(3) THE j TERMS SHOW A 90° SHIFT BETWEEN PORTS 1 AND 4, ALSO BETWEEN 2 AND 3.

Figure 29. Scattering Matrix for Hybrid

SECTION 6

SCAN TIME OPTIMIZATION WHERE CUMULATIVE DETECTION REQUIREMENTS EXIST

6.1 INTRODUCTION

An important radar surveillance situation is the one where a number of sequential detection mode scan "looks" of a target in the surveillance volume are premissible, and a minimization of the average power requirement is required for detecting the target on at least one of the scan looks with a prescribed cumulative detection probability (P_C), false alarm probability (P_{FA}), and number of resolution cells (N_F). In addition to the previously considered degrees of design freedom in EVSD modes, a new degree of design freedom introduced in the optimization problem at hand is the average single-scan time which determines directly, for a given trajectory, the average number of scan "looks" within the surveillance volume and the allowable coherent integration time for each beam position "look".

The optimization is necessarily intimately related to the cumulative detection probability, and this quantity is in turn a function of the target motion and its relative orientation to the search beam.

For example, if the target trajectory is pointed directly at the radar, the cumulative detection probability is a function of a sequence of progressively increasing signal-to-noise ratios encountered on individual scan "looks" as the radar range decreases.

On the other hand, if the target direction is perpendicular to the search beam, a different cumulative detection probability and necessarily a different scan time optimization is obtained since in this case the same average signal-to-noise ratio obtained from the target on each "look".

EVSD scan time optimizations have been accomplished in the subject study for both of these extreme cases of target trajectories. The otpimization for the case where the target vector is directed at the radar is applicable to the acquisition phase of an area-defense radar system, and, for a typical acquisition mode specification, the optimum ratio of the range interval between scan looks and the specified minimum range is 0.24. For this area-defense case, the required signal-to-noise ratio at each of the sequential steps for a scan look is specified at the minimum range. A scan-time optimization of this type for fixed sample size tests (uniform search modes) is also developed by Mallett and Brennan (Reference #14). A related optimization, also based on the use of EVSD's is discussed by Brennan and Hill (Reference #13).

The other class of surveillance optimizations for specified cumulative detection requirements is for the case where the average signal-to-noise ratio is the same on each scan look. This case is of interest for certain satellite surveillance situations. For this class, the desired strategy can be expressed in terms of the single-scan detection probability. It is noted that the optimum scan strategy is a function of the target type hypothesized.

6.2 NATURE OF SCAN TIME OPTIMIZATION

The object of the optimization procedure involves minimizing a cost function proportional to the average transmitter power requirements for a specified set of surveillance conditions. Roughly speaking, the EVSD scan time optimization involves a trade-off of the following effects on the average transmitter power requirements. Increasing the time interval between scans allows for longer coherent integration time in each sequential step, and therefore, has the effect of lowering the average power requirement for a prescribed receiver signal energy to noise power density requirement. However, this longer scan time reduces the number of scan looks at a target, and consequently, would have the opposing affect of increasing the average power requirements for a prescribed cumulative detection probability.

An important point to be made is that the EVSD's are essentially single-scan sequential detection modes (see Section 2), and their development involves minimizing a cost function proportional to the average transmitter energy requirement for the single-scan set of requirements. The optimization procedure, therefore, first involves expressing the cumulative detection probability and the average power requirement as a function of the EVSD single-scan detection probability and the single-scan average energy requirements. The cumulative requirements are also a function of a quantity proportional to the scan time and the value of this quantity, as well as the single-scan energy and threshold requirements, are determined to minimize the average transmitter power.

6.3 OPTIMIZATION FOR THE CASE WHERE TARGET IS DIRECTED AT RADAR

The scan time optimization is now described for those system requirements where 1) of the ensemble of admissable targets, the system requirements are specified for the target with the maximum constant velocity vector pointing at the radar, 2) a minimum of clutter targets exists during this phase of the mission so that the receiver thermal noise is the major false report inducing event, and 3) for the fluctuating target types, the target cross section is assumed independent for each scan "look". (For the cases #1 and #3 target types, the target cross section is assumed, for this analysis, to be completely correlated at each sequential step within the time duration of a scan look.)

6.4 FORMULATION OF THE CUMULATIVE DETECTION PROBABILITY

For this case, the cumulative detection probability at a prescribed minimum range may be expressed as:

$$P_C = \frac{1}{\Delta} \int_{R_{min}}^{R_{min}+\Delta} \left[1 - \prod_{m=0}^{\ell} \left[1 - P_D \left(\overline{X} \left(\frac{R_D}{R' + m\Delta} \right)^4, \beta_1, \beta_2 \right) \right] \right] dR' \tag{33}$$

The quantity $P_D\left(\bar{X}\left(\frac{R_D}{R'+m\Delta}\right)^4, \beta_1, \beta_2\right)$ is the single-scan probability of an EVSD mode detection, m scans from the last illumination of the target prior to the specified minimum range (R_{min}). This range of last illumination prior to R_{min} is designated R', and the spacing in range between scan looks is Δ. The single-scan EVSD detection probability $P_d\left(\bar{X}\left(\frac{R_D}{R'+m\Delta}\right)^4, \beta_1, \beta_2\right)$ is the same as those described in Section 2 for a 2-step maximum procedure with the exception that the received signal energy to noise power density $\bar{X}$, computed at the EVSD "design" range (R_D), must be multiplied by the factor $\left(\frac{R_D}{R'+m\Delta}\right)^4$ to determine its value at the range $R'+m\Delta$.

The integrand, therefore, represents the conditional probability of cumulative detection on the hypothesis that the last scan look occurs at the range R'. Since we are interested in the final cumulative detection probability at the range R_{min}, we must multiply this conditional probability by the a priori probability of R' and integrate over the domain of values of R'. This a priori probability is assumed uniform with the density function $1/\Delta\, dR'$ over the domain of values extending from R_{min} to $R_{min} + \Delta$.

This integral is approximated by a summation in equation (34), and by introducing the change in variables, $X' = R_{min}/R_D$ and $\delta = \Delta/R_D$, the final result of equation (33) is obtained.

$$P_C = \frac{1}{N}\sum_{J=1}^{N}\left[1 - \prod_{m=0}^{\ell}\left[1 - P_D\left(\bar{X}\left(\frac{R_D}{R_{min} + \frac{J\Delta}{N} + m\Delta}\right)^4, \beta_1, \beta_2\right)\right]\right] \quad (33)$$

$$P_C = \frac{1}{N}\sum_{J=1}^{N}\left[1 - \prod_{m=0}^{\ell}\left[1 - P_D\left(\bar{X}\left(\frac{1}{X' + J\frac{\delta}{N} + m\delta}\right)^4, \beta_1, \beta_2\right)\right]\right] \quad (34)$$

The first significant scan look is the parameter (ℓ). For the computations reported in this document, the first scan look (ℓ) was that look where the single-scan probability of detection was greater than 0.1.

Typical computations of P_C as a function of X' and δ are presented in Figures 30 and 31 for a non-fluctuating and a case #3 target respectively, where the single-scan EVSD design probability is 0.5, and the individual-cell false alarm probability is 10^{-8}, and 10 resolution cells are involved. It is noted in these figures that there is a set of values of X' and δ which yield the same cumulative detection probability. For example, the set of couples (X' and δ combinations) which yield a cumulative detection probability of 0.95 for the 10^{-8} false alarm probability case is presented in Figure 32 for the Case #3 target.

One aspect of the optimization problem involves determining the X' and δ combination minimizing power requirements for a specified set of error probabilities. The ratio $\frac{\delta}{X'} = \frac{\Delta}{R_{min}}$ then determines the scan rate.

6.5 DEVELOPMENT OF COST FUNCTION

The appropriate cost function for the final optimization is the average transmitter power requirement for achieving the specified cumulative detection probability per resolution cell. A quantity proportional to this cost is designated as $\bar{P}$ and is determined to be:

$$\bar{P} = \frac{\bar{C}(R_{min})^3}{X'^3 \, \delta} \tag{35}$$

where all of the quantities involved have been previously defined.

The kernel of the development of this cost function is the average received energy to noise power density of a single EVSD scan ($\bar{C}$). The quantity proportional to the transmitter energy requirement is $\bar{C}R_D^4$ where R_D is the 'design' range

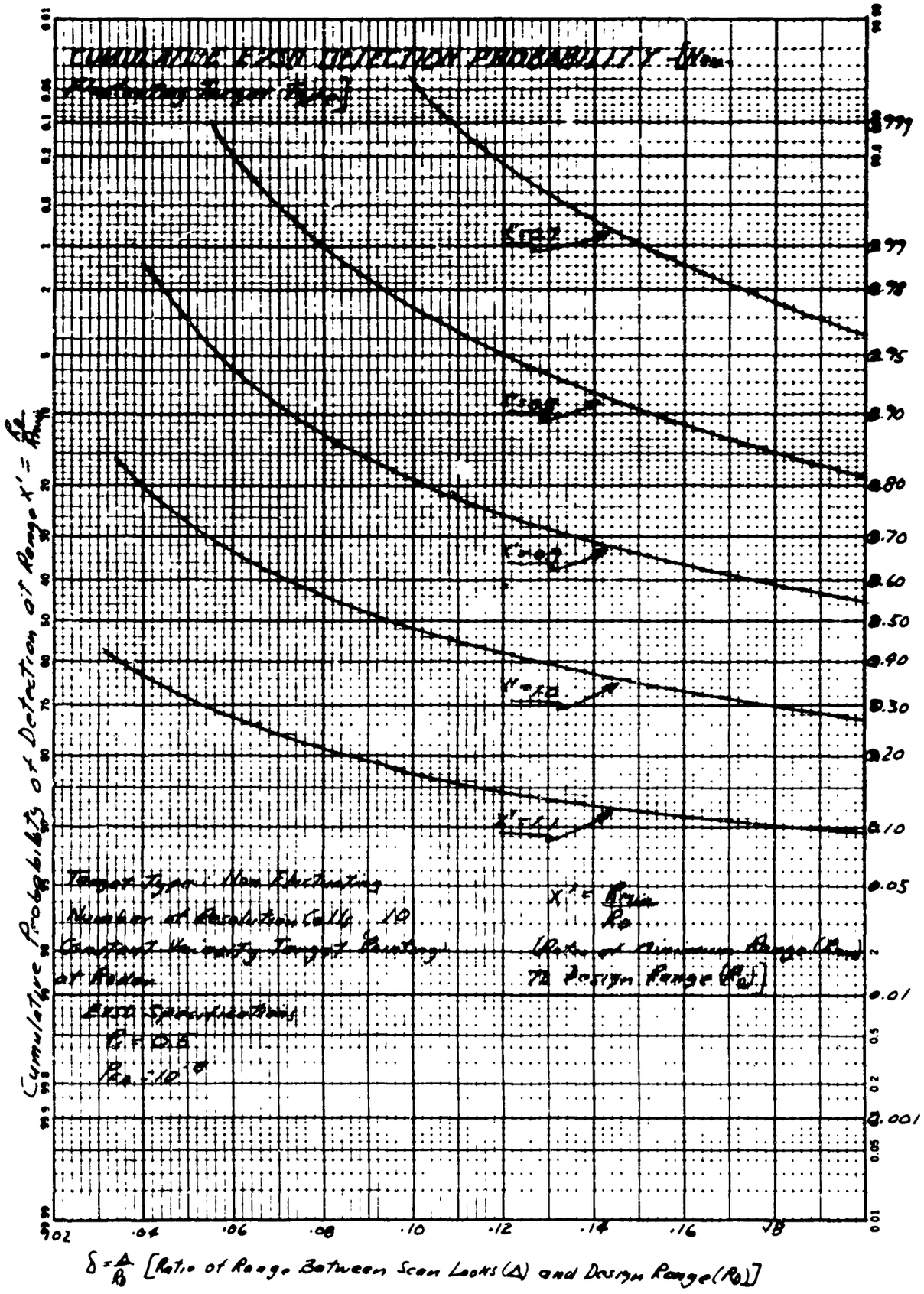

Figure 30. Cumulative EVSD Detection Probability (Non-Fluctuating Target Type)

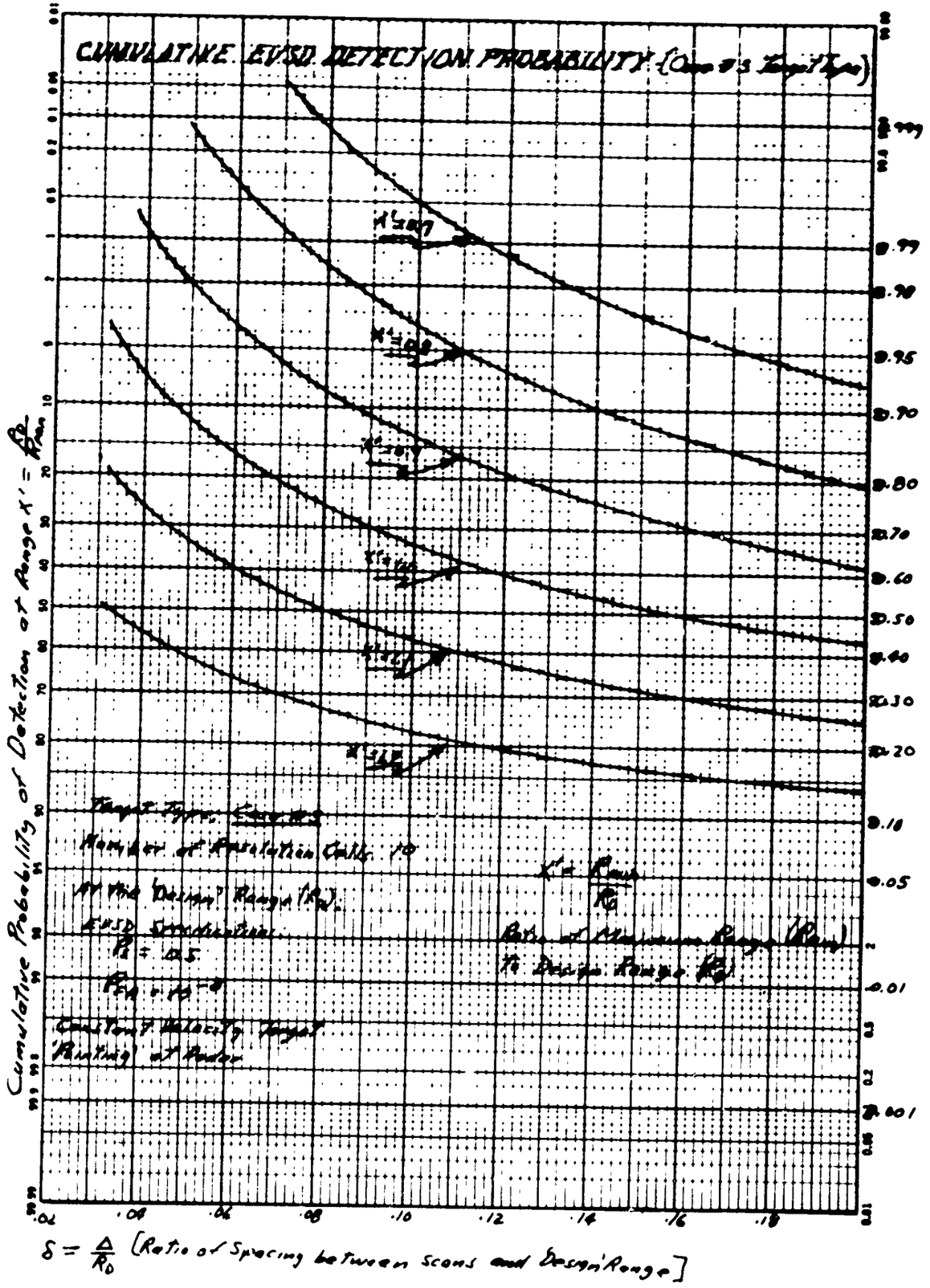

Figure 31. Cumulative EVSD Detection Probability (Case #3 Target Type)

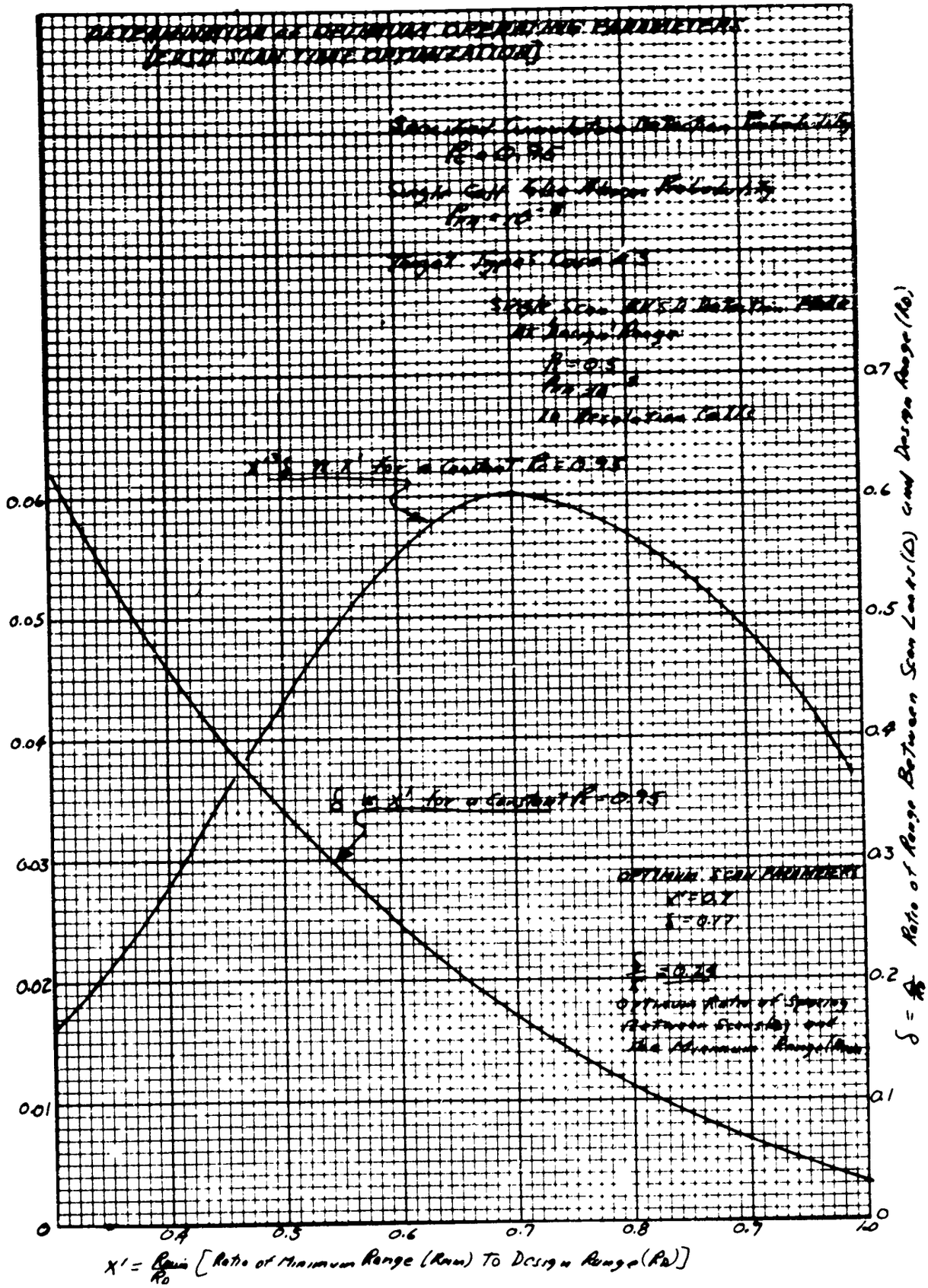

Figure 32. Determination of Optimum Parameters (EVSD Scan-Time Optimization)

for the specified received energy requirement. The average transmitter power requirement is this energy quantity divided by the average allowable correlation time τ for each scan look. For the constant velocity target, the average correlation time τ is a linear function of the range interval Δ between illuminations. It is now possible to formulate the desired cost function:

$$\bar{P} = \bar{C} \frac{R_D^4}{\Delta} \tag{36}$$

$\bar{P}$ is our desired cost, a quantity proportional to the average transmitter power requirement since the numerator $\bar{C}_D R_D^4$ is proportional to the average transmitter energy requirement, and the denominator Δ is proportional to the average time of a single beam position transmission on one scan. By introducing the relationships $X' = \frac{R_{min}}{R_D}$ and $\delta = \frac{\Delta}{R_D}$ into equation (10) we obtain the result of equation (35).

$$\bar{P} = \frac{\bar{C}(R_{min})^3}{X'^3 \delta} \tag{35}$$

For a given R_{min}, the quantity $\frac{\bar{C}}{X'^3 \delta}$ must be minimized. We have noted (see Figures 30, 31, and 32) that a number of couples (X', δ) satisfy the specified error probabilities. For a given single-scan design yielding a $\bar{C}$, the desired couple (X', δ) is the one maximizing the quantity X'^3. This step of the optimization procedure is illustrated in Figure 32. For this case, the optimum ratio of Δ to R_{min} (the ratio $\frac{\delta}{X'}$) is noted to be approximately 0.24. Since $\bar{C}$ is a function of the selected single-scan probability of detection, the conducted optimization procedure has involved the following steps:

(1) EVSD designs and the average energy requirement $\bar{C}$ are determined for a suitable range of specified single-scan detection probabilities. (The same false alarm probability is specified in each case.)

(2) For the specified cumulative detection probability, the sets of couples (X', δ) are determined for each of the EVSD designs of step #(1).

(3) For each EVSD design, the couple (X', δ) maximizing the quantity $X'^3 \delta$, is determined.

(4) The final step involves comparing the $\bar{P}$'s (or the quantity $\frac{\bar{C}}{X'^3 \delta}$) obtained for each EVSD design and selecting the EVSD design minimizing this cost function.

This optimization procedure has been followed for the case where the specified cumulative detection probability is 0.95, the false alarm probability in an individual resolution cell is 10^{-8} and the effective number of resolution cells is 10. EVSD designs for the cases where the single-scan detection probabilities ranged from 0.4 to 0.7 were considered and the optimum couples (X', δ) were determined for each case. A comparison of these costs showed the 0.5 single-scan probability design to result in a minimum power requirement. However, the minimum with respect to the selection of the EVSD design was a broad one. The (X', δ) combination minimizing the power seems to compensate for the single-scan detection probability specification, and yields essentially the same EVSD design relative to the specified minimum range. The optimum (X', δ) combination is $X'=0.7$ and $\delta = 0.17$, so that the desired ratio of interval between illuminations and minimum range is 0.24. The design and performance parameters for this EVSD are reproduced from reference #1 and are presented in Figures 33 and 34. To obtain the received signal energy to noise power density at the specified minimum range, the quantity 40 log X' must be added to the specified values in db at the 'design' range (see Figure 33). For the 10 resolution element case, the required average signal energy to noise power density at the minimum range is 14.11 db for the first step and 21.11 db for the second step. (At the 'design' range, these quantities are 8.04 db and 15.08 db respectively.)

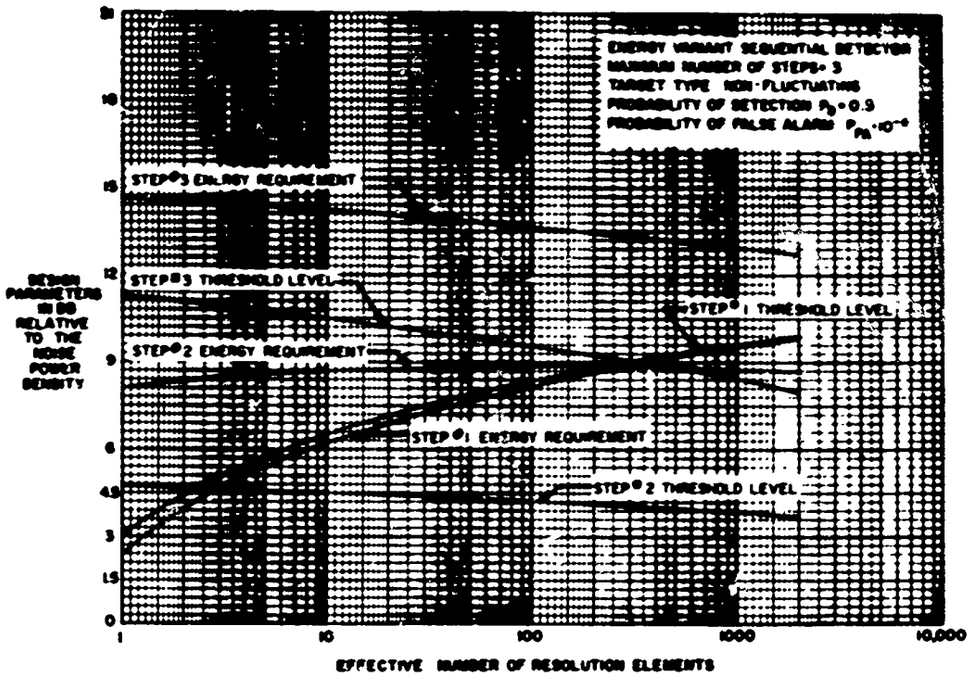

Figure 33. EVSD Design Parameters, Case #3 Target, $P_D = 0.5$, $P_{FA} = 10^{-9}$

The average power savings of the EVSD over the use of a fixed sample size test is presented in Figure 34, and it is noted that for the 10 resolution element case, the computed average power saving is approximately 4.5 db.

6.6 SURVEILLANCE OPTIMIZATION FOR THE CASE OF SAME AVERAGE RETURN SIGNAL ENERGY ON EACH SCAN LOOK

A simpler surveillance optimization task involves minimizing the average transmitter power for the surveillance situation where the average return signal energy does not change from one scan look to another. This case is of interest for certain space surveillance missions. A constant target-velocity vector 'pointing' perpendicular to the search beam is assumed (zero doppler case). The target is assumed to dwell in the surveillance volume for a prescribed time T, and the probability of detecting the target at least once during the scan time T is specified. In addition to a specification of this cumulative detection probability (P_C), the false alarm probability (P_{FA}) and the effective number of resolution cells (N_F) are also specified performance parameters.

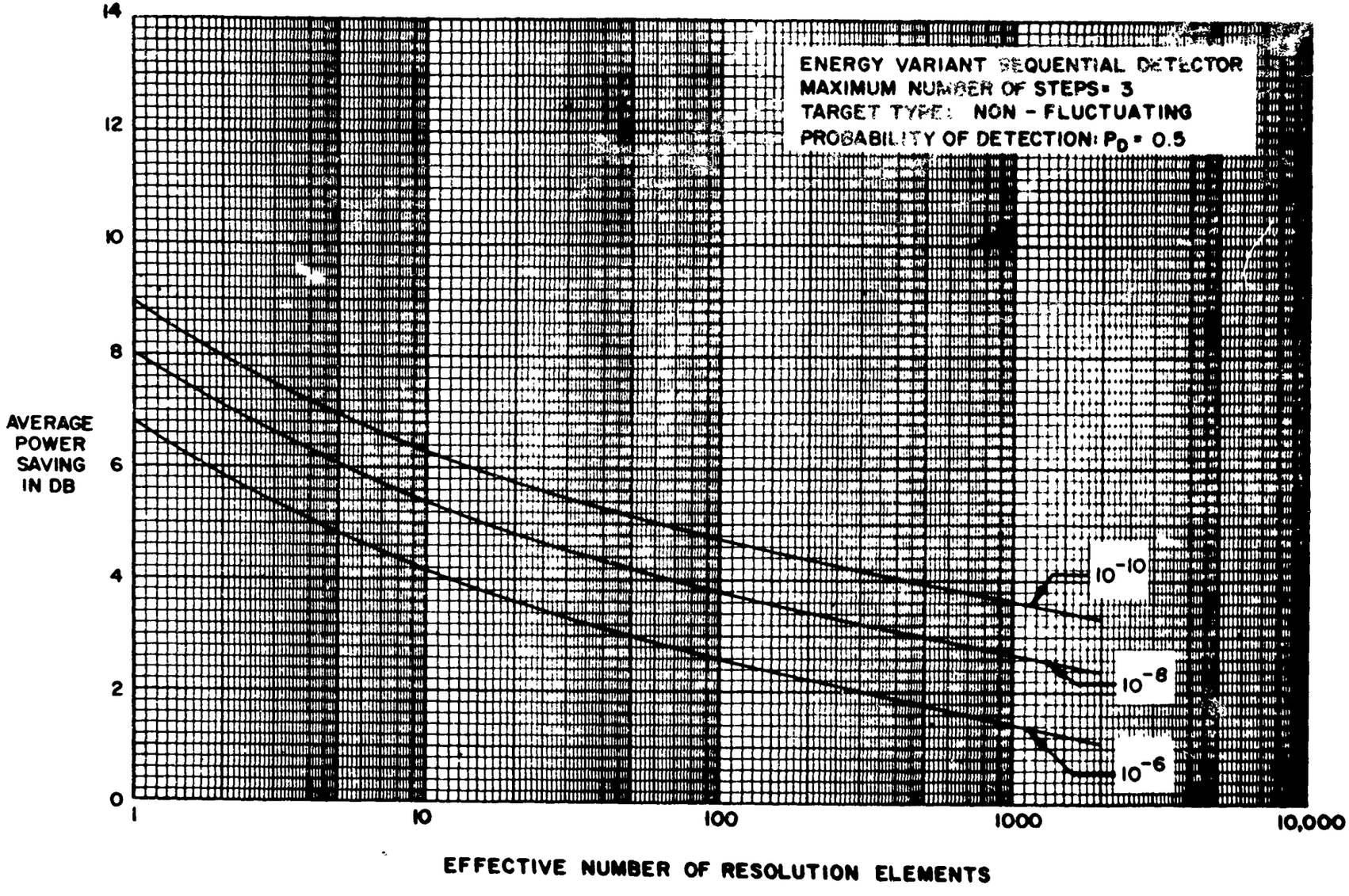

Figure 34. Average Power Saving, Case #3 Target, $P_D = 0.5$, $P_{FA} = 10^{-8}$

Each scan 'look' is effected with an EVSD mode, and the optimization problem involves determining the energy and threshold requirements on each sequential step, and the scan time, minimizing the average transmitter power.

6.7 COST FUNCTION AND FRAME TIME

The average frame time or the time between scan look (t) is $\bar{t} = T/\bar{n}$ where $\bar{n}$ is the average number of scan looks in the surveillance volume dwell time T. A quantity proportional to the average transmitter power requirement, therefore, is $\bar{P} = \frac{\bar{C}}{\bar{t}}$, or using $\bar{t} = \frac{T}{\bar{n}}$, the quantity $\bar{P}$ may be expressed as

$$\bar{P} = \frac{\bar{C}\,\bar{n}}{T} \tag{36}$$

$\bar{C}$ is the average EVSD cost (the quantity specified in equation (9) of Section 2.4, and is a function of the selected single-scan detection and false alarm probabilities (P_D and P_{FA}).

For a fixed time T, the cost function to be minimized, ($\bar{P}'$) is simply the product of the average received energy requirement to noise power density $\bar{C}$ and the average number of scan looks $\bar{n}$ or $\bar{P}' = \bar{C}\,\bar{n}$.

6.8 CUMULATIVE DETECTION PROBABILITY AND OPTIMIZATION

The cumulative detection probability (P_C) for this constant radar range case is expressed as

$$P_C = 1 - (1-P_D)^{\bar{n}} \tag{37}$$

where P_D is the single scan EVSD probability as described in equation (1) of Section 2.4.

The procedure for minimizing $\bar{P}' = \bar{C}\ \bar{n}$ first involves determining from equation 37, the number of scans $\bar{n}$ which yield the specified cumulative detection probability for a choice of single-scan detection probability. This number of looks $\bar{n}$ is plotted in Figure 35 as a function of the single-scan detection probability for the case where the cumulative detection probability is 0.95.

From the previously performed EVSD optimizations, the values of $\bar{C}$ are obtained and the products $\bar{C}\ \bar{n}$ are computed for a range of values of single-scan detection probability. The single-scan detection probability minimizing $\bar{C}\ \bar{n}$ for a specified cumulative detection probability and false alarm probability can then be determined. The cost function $\bar{C}\ \bar{n}$ for the case where $P_C = 0.95$ and $P_{FA} = 10^{-8}$ is plotted in Figure 35 as a function of the single-scan detection probability for the five target types considered in the study.

First, it is noted that there is no one scan strategy which is optimum for all target types. Secondly, it is clear from Figure 35, that the use of the wrong scan strategy for the target type of interest can lead to an unnecessarily high average transmitter power requirement. Another conclusion drawn from the analysis is that the EVSD costs for meeting a single-scan detection requirement vary widely for the target types considered. For example, in Figure 35, the difference in cost is noted to be approximately 7 db for detecting a Case #1 and Case #4 target type in a single scan with an EVSD mode and detection probability of 0.95. On the other hand, the difference in cost in achieving the cumulative detection probability of 0.95 with these two target types is reduced to approximately 2 db if the optimum scan strategy is employed for each target type.

For the fluctuating target types, and the constant target range assumption, it is noted that the case #2 and #4 targets, (target types which are assumed to yield statistically independent target cross-section samples within each sequential step) perform optimally for the cumulative detection requirement with approximately one EVSD scan look. On the other hand, the cases #1 and #3 target

types (target types which are assumed to present the same backscattering cross section to the radar for the duration of one EVSD scan look) require a number of such EVSD scan looks in order to minimize the average power for a cumulative detection requirement. For this constant-range case, it is also noted, as would be expected, that the non-fluctuating target requires only one EVSD scan look for optimum performance.

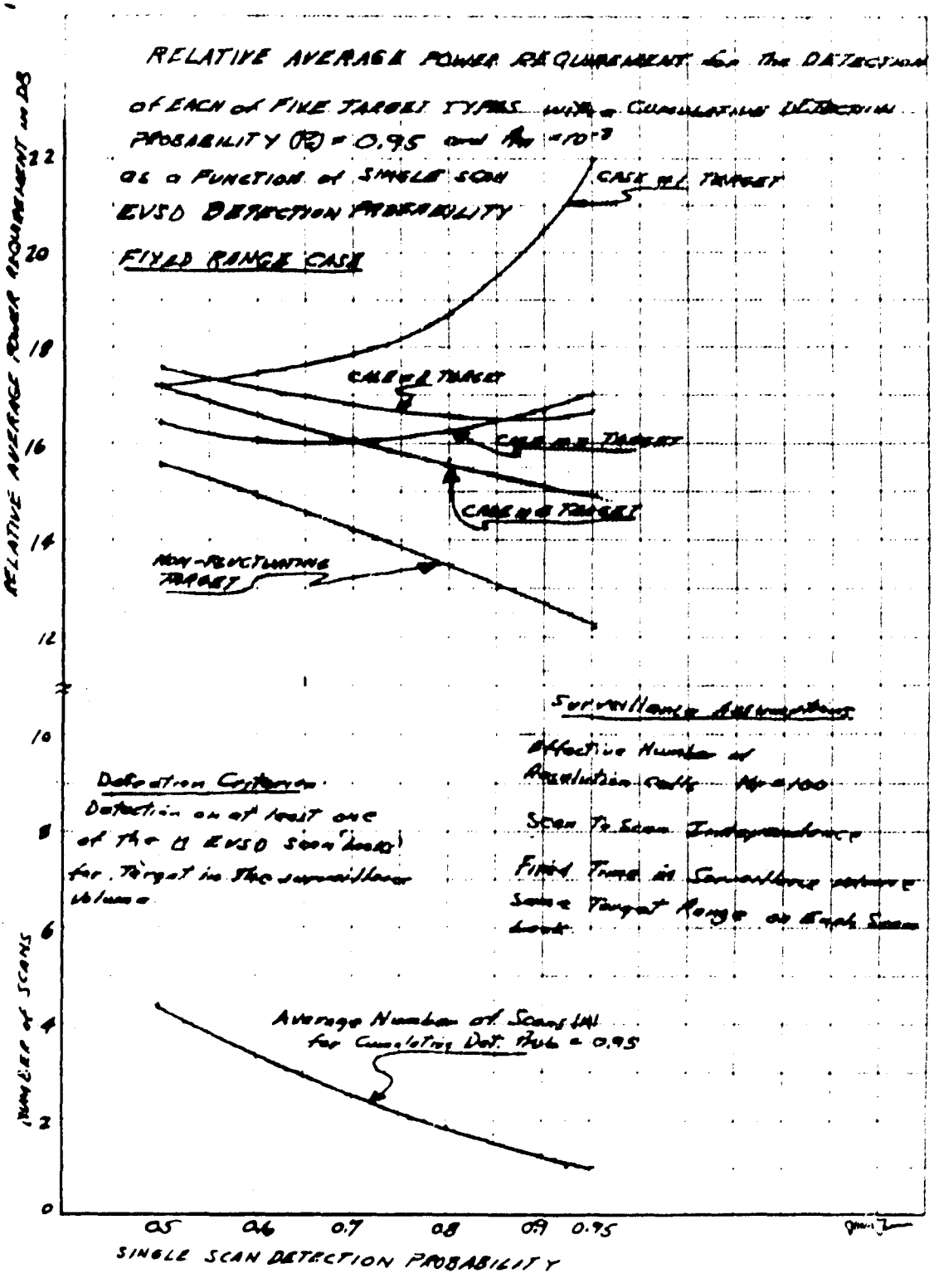

Figure 35. Relative Average Power Requirement for the Detection of Each of Five Target Types with a Cumulative Detection Probability $P_C = 0.95$ and $P_{FA} = 10^{-8}$ As A Function of Single-Scan EVSD Detection Probability, Fixed-Range Case

SECTION 7

DESIGN OF AN EVSD WITH A CONFIRMATION DELAY-TIME OPTION

An additional class of radar sequential detection mode developed during the program involves introducing an option on the time interval employed between the first and second sequential step of an EVSD with a maximum of two steps. This class of mode was developed for the high-fluctuating rate class of targets (such as the Case #2 and #4 target types represent) in an attempt at exploiting those first-step interrogation events which involve 'catching' and confirming the presence of the target at its more favorable target cross section.

The previously discussed optimization for this fluctuating target class involved including a number of statistically independent target cross section samples as degrees of freedom on each of the sequential steps. Typical optimizations included the use of three such pulse samples on the first step and six on the second step, and the decision statistic for a step was based on the sum of the square-law detected outputs of that step, with a single threshold for the sum decision statistic employed at each step.

Roughly speaking, the confirmation delay-time option mode combines the previously developed EVSD decision processor framework for Case #2 and #4 targets with an optional mode which is introduced when the observation at any of the N_1 first-step pulses is very large and the 'best' policy would involve 'packing' the second-step energy immediately into a single pulse on the second step since for this event, the probability is assumed to be large that a target is present at a favorable cross section.

Two thresholds are employed on the first step of this new mode — one is a single pulse threshold, and the second one is employed as a threshold of the sum of the

N_1 returns or the first step if none of these statistically independent returns exceeds the single-pulse threshold. If any one of the returns in the sequence of the N_1 first-step pulses exceeds the single-step threshold, the remainder of these first-step pulses are not transmitted, and instead the second or confirmation step with energy E_{22} is 'immediately' employed in a time interval (τ), relatively short when compared to the correlation time of the fluctuating target. A threshold β_{22} is employed for this 'quick' reaction second step. The cross section presented on the quick-reaction second step, if a target is present, is assumed to be the same target cross section sampled at the time of the immediately preceding pulse (the first-step pulse which crossed the single-step threshold.) The target is declared present if threshold crossings occur in a common-parameter space resolution cell.

If, after the N_1 first step pulses, the sum exceeds the first-step sum threshold β_{11} (but no single-pulse threshold has been exceeded) then a sequence of second-step pulses are used with energy E_{21}. The sum of this 'slow' reaction second-step group of pulses is then compared with threshold (β_{21}). A sketch of this confirmation time option mode and its relationship to the previously designed modes is presented in Figure 36.

Additional degrees of design freedom are noted to be included in the confirmation time option mode. An extra threshold is involved on each step, and, in addition, the second-step energy requirement for the 'quick' reaction mode is allowed to differ from that of the 'slow reaction' second step.

The optimization procedure is essentially the same as that used for the development of the previous EVSD's. However, for this case, the probability distributions (detection and false alarm probability) and the cost function to be minimized (the average energy requirement) must be modified to accommodate the more elaborate decision rule and mode strategy.

EVSD optimization employing this confirmation delay-time option were obtained for the Case #2 target type. Typical design and performance parameters for

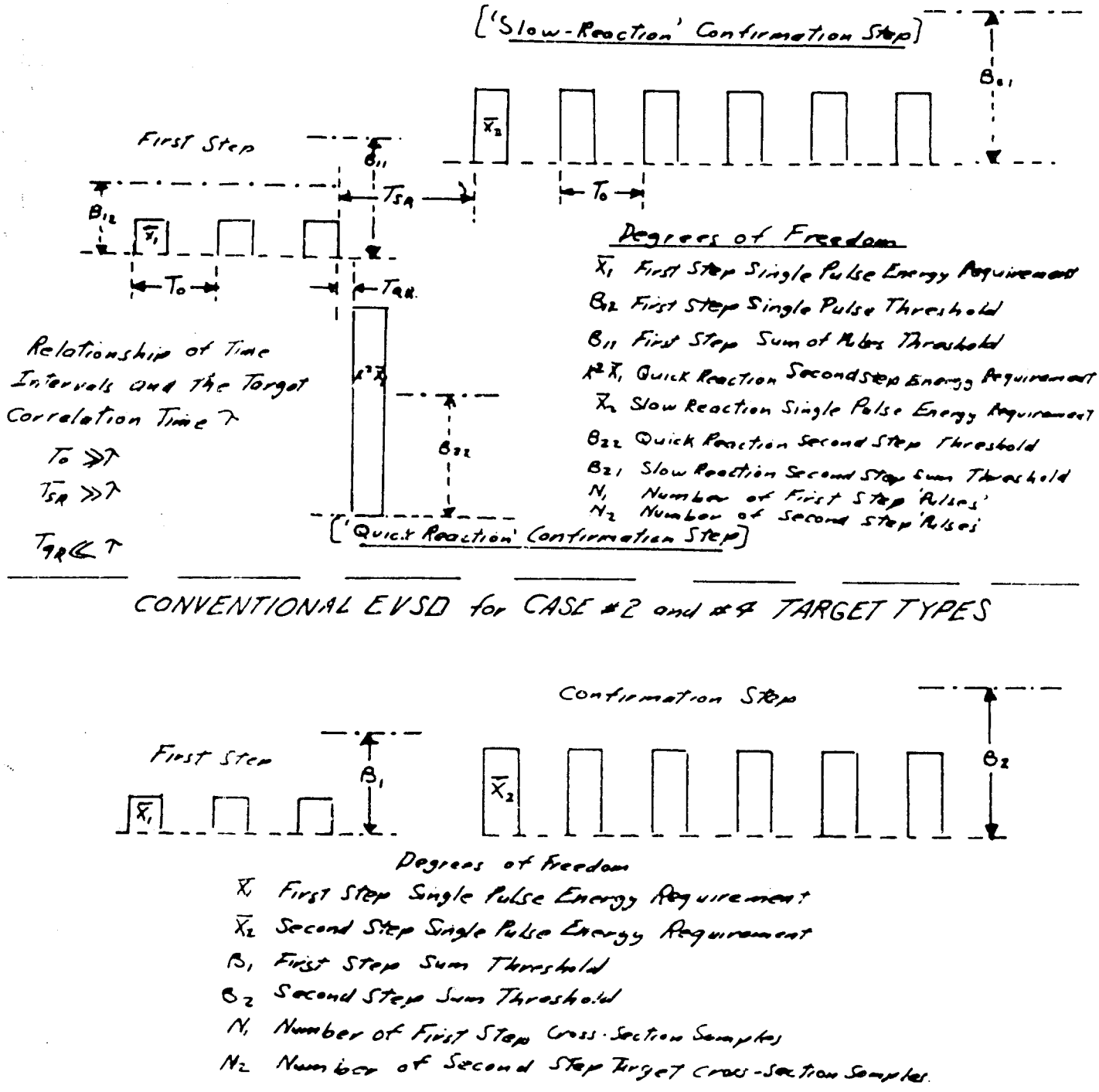

Figure 36. Degrees of Design Freedom in a Confirmation Time Option EVSD Mode

this mode are presented in Figures 37 and 38. For the surveillance conditions assumed, no significant increase in efficiency was obtained over the use of the conventional EVSD design for the Case #2 target. This more complex mode, therefore, cannot be recommended for this target type.

The mode, however, may yield a 'payoff' for other high-fluctuating rate targets but with first order probability density functions differing markedly from the exponential type represented by the Case #2 target. The optimization procedure for this more elaborate decision processor framework is felt to be of general interest, and demonstrates the flexibility of the analytical approach employed in accommodating imposed design constraints. For these reasons, the development of the detection probability, false alarm probability and cost function are described here, and details of this optimization procedure are presented in Appendix 3.

7.1 DECISION RULE AND DECISION PROCESSOR FRAMEWORK

A more formal description of the decision processor framework and in particular the decision rules and the radar policy to be employed on each sequential step follows:

First, the legend to be employed:

$X_{i,j,k}$ - The normalized matched-filter output followed by a square-law detector of the i^{th} sequential step, the j^{th} pulse, and the k^{th} resolution element.

(Only a two-step maximum sequential detection process is considered so that $i=1,2$.)

The quantities listed below constitute the degrees of design freedom of the optimization problem.

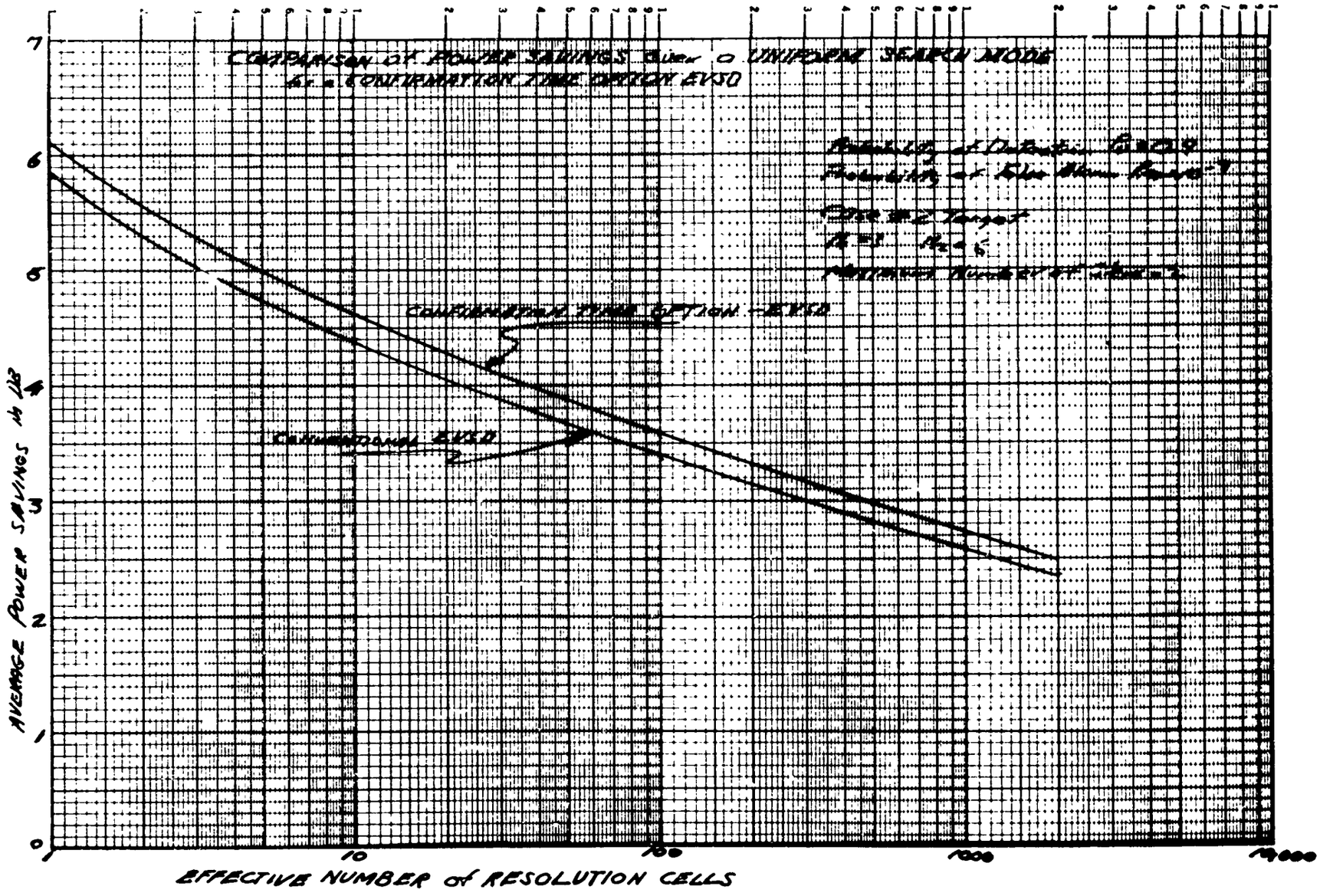

Figure 37. Comparison of Power Savings Over a Uniform Search Mode for a Confirmation Time Option EVSD

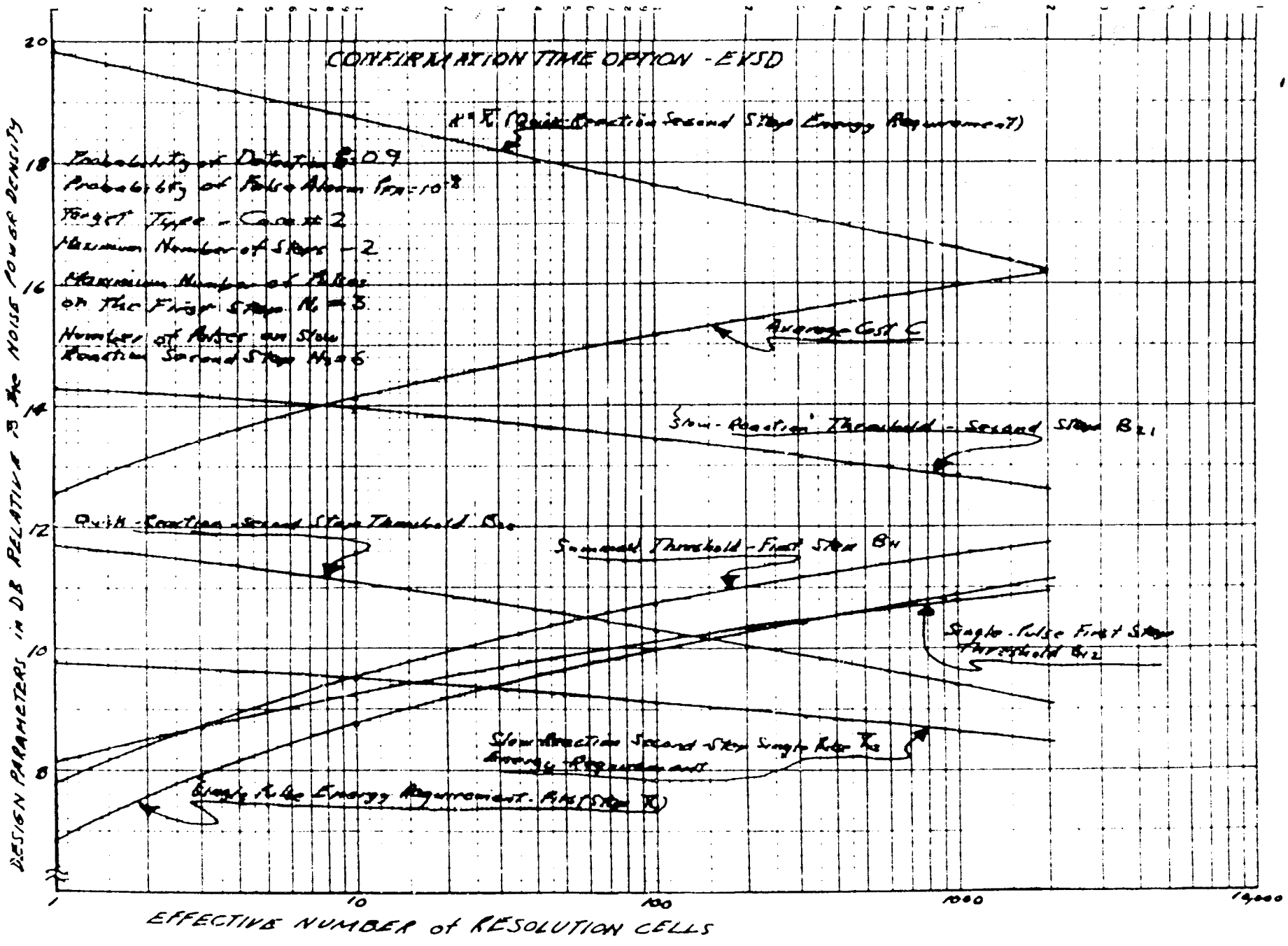

Figure 38. Confirmation Time Option EVSD-Design Parameters

N_i - The maximum number of pulses employed on the i^{th} step.

β_{12} - The single-pulse threshold of the first step.

β_{22} - The 'quick reaction' second-step threshold.

β_{11} - The sum threshold of the first step.

β_{21} - The 'slow reaction' second step summed output threshold.

X_1 - The single-pulse signal energy to noise power density of the first step.

K^2 - The ratio of the 'quick reaction' second-step signal energy to the single-pulse energy employed on the first step.

X_2 - The single-pulse signal energy to noise power density of the 'slow reaction' second sequential step.

$\bigcup_{\rho=1}^{M} E\rho$ - The union of events $E_1, E_2 \ldots E_M$.

$\bigcap_{\rho=1}^{M} E\rho$ - The intersection of events $E_1, E_2 \ldots E_M$.

N_F - The effective number of resolution cells.

A statistical hypothesis test is assumed to take place at each beam position where:

H_1 is the hypothesis of a target being present, and the acceptance of this hypothesis leads to an alarm reaction.

H_o is the alternate hypothesis of noise alone being present - and acceptance of this hypothesis terminates the test at the beam position.

If

$$\bigcup_{k=1}^{N_F} \left[(X_{1,\ell,k} > \beta_{12}) \bigcap_{J=1}^{\ell-1} (X_{\iota,j,k} < \beta_{12}) \right] \tag{38}$$

is true, then after the ℓ^{th} pulse of the first step, apply policy $R_{(QR)}$ 'Quick Reaction' Second Step for $\ell = 1,2,\ldots..N_1$.

$R_{(R)}$: Apply a single-pulse second step within a time $T_{(QR)}$ where $T_{(QR)} << \tau_T$. (τ_T is the target correlation time.) The energy of this second-step 'quick reaction' pulse is k^2 times the single-pulse energy employed on the first step.

If

$$\bigcup_{k=1}^{N_F} \left[X_{1\ell k} > \beta_{12} \bigcap_{J=1}^{\ell-1} X_{1Jk} < \beta_{12} \bigcap X_{2k}^{(Q \cdot R)} > \beta_{22} \right] \tag{39}$$

is true, accept H_1 hypothesis.

Alternatively, if

$$\bigcap_{k=1}^{N_F} \left[X_{1\ell k} > \beta_{12} \bigcap_{J=1}^{\ell-1} X_{1Jk} < \beta_{12} \bigcap X_{2k}^{(Q \cdot R)} < \beta_{22} \right] \tag{40}$$

is true, accept H_0 hypothesis.

If

$$\left[\bigcap_{\substack{J=1 \\ k=1}}^{\substack{k=N_F \\ J=N_1}} X_{1,J,k} < \beta_{12} \right] \bigcap \left[\bigcup_{k=1}^{N_F} \left(\sum_{J=1}^{N_1} X_{1,J,k} > \beta_{11} \right) \right] \tag{41}$$

is true, then use radar policy $R_{(SR)}$ (Slow-Reaction Second Step).

$R_{(SR)}$: Apply a train of N_2 pulses on the second step where the time interval between the start of the pulse train and between pulses within the train is at least T_{SR} where $T_{SR} > \tau_T$, and where the single-pulse signal energy to noise power density is $\bar{X}_2$.

If

$$\left[\bigcap_{\substack{K=1\\J=1}}^{\substack{K=N_F\\J=N_1}} X_{1,J,k} < \beta_{12}\right] \bigcap \left[\bigcap_{k=1}^{N_F}\left[\sum_{J=1}^{N_1} X_{1,J,k} > \beta_{11} \bigcap \sum_{J=1}^{N_2} X_{2Jk}^{(S \cdot R)} > \beta_{21}\right]\right] \quad (42)$$

is true, then accept the H_1 hypothesis.

Alternatively, if

$$\left(\sum_{J=1}^{N_2} X_{2Jk}^{(S \cdot R)} < \beta_{21}\right) \text{ is true}$$

in the above expression, then accept the H_o hypothesis.

The H_o hypothesis is also accepted if:

$$\bigcap_{k=1}^{N_F}\left[\bigcap_{\substack{K=1\\J=1}}^{\substack{K=N_F\\J=N_1}} (X_{1,J,k} < \beta_{12}) \bigcap \sum_{J=1}^{N_1} (X_{1,J,k} < \beta_{11})\right] \quad (43)$$

is true.

The probability of detecting a target 'lodged' in the k^{th} resolution cell may now be expressed as:

$$P_D = \sum_{\ell=0}^{N_1-1} P\left\{\bigcap_{J=1}^{\ell} X_{1,J,k} < \beta_{12}\right\} \int_{Z=0}^{\infty} P\left\{X_{1,\ell,k} > \beta_{12}; t\right\} P\left\{X_{2,k}^{(QR)} > \beta_{22}; kt\right\} f(t;\bar{x})dz$$

$$+P\left\{\sum_{J=1}^{N_2} X_{2,J,k} > \beta_{21}\right\} P\left\{\sum_{J=1}^{N_1} X_{1,J,k} > \beta_{11} \bigcap_{J=1}^{N_1} X_{1,J,k} < \beta_{12}\right\} \tag{44}$$

The above expression for P_D is shown to be:

$$P_D = F_1 F_2 + F_3 F_4 \tag{45}$$

where

$$F_1 = \sum_{J=0}^{N_1-1} \left(1 - \bar{e} \frac{\beta_{12}}{X_1 + 1}\right)^J \tag{46}$$

$$F_2 = Q\left(\sqrt{2\bar{x}, t}, \sqrt{2\beta_{12}}\right) \quad Q\left(K \sqrt{2\bar{x}, t}, \sqrt{2\beta_{22}}\right) e^{-t} \, dt \tag{47}$$

$$F_3 = \sum_{J=0}^{N_1=1} \frac{(-1)^J N_1! e^{-J \frac{\beta_{12}}{\bar{X}_1+1}}}{J!\,(N_1-J)!} \sum_{m=0}^{N_1-1} e^{-\frac{(\beta_{11}-J\beta_{12})}{\bar{X}_1+1}\left(\frac{\beta_{12}-J\,\beta_{12}\,m}{\bar{X}_1+1}\right)}}{m!} \tag{48}$$

and

$$F_4 = e^{-\frac{\beta_{21}}{\bar{X}_2+1}} \sum_{J=0}^{N_2-1} \frac{\left(\frac{\beta_{21}}{\bar{X}_2+1}\right)^J}{J!} \tag{49}$$

Similarly, the false alarm probability in an individual resolution cell may be expressed as:

$$P_{FA} = e^{-\beta_{12}} \, e^{-\beta_{22}} \, G_1 + G_3 \, G_4 \tag{50}$$

where:

$$G_1 = \sum_{J=0}^{N_1-1} (1-e^{-\beta_{12}})^J \tag{51}$$

$$G_3 = \sum_{J=0}^{N_1} \frac{(-1)^J N_1 ! e^{-J\beta_{12}}}{J! (N_1-J)!} \sum_{m=0}^{N_1-1} \frac{e^{-(\beta_{11}-J\beta_{12})} (\beta_{11}-J\beta_{12})^m}{m!} \tag{52}$$

and

$$G_4 = e^{-\beta_{21}} \sum_{J=0}^{N_2-1} \frac{\beta_{21}^J}{J!} \tag{53}$$

The cost function is made equal to the average required signal energy to noise power density for the no-target environment, and must include all possibilities of false chase with both the 'quick reaction' and the 'slow-reaction' second step.

This cost function may be expressed as:

$$C = \bar{X}_1 \left[\sum_{J=0}^{N_1-1} (1-e^{-\beta_{12}})^J N_F\right]\left[1+K^2\left[1-(1-e^{-\beta_{12}})^{N_F}\right]\right]$$

$$+ N_2\bar{X}\left[1-e^{-\beta_{12}}\right]^{N_1 N_F}\left[1-(1-G_3)^{N_F}\right] \tag{54}$$

The minimization is now accomplished by finding the minimum of the Lagrangian

$$L = C + \tau P_D + u \ln P_{FA} \tag{55}$$

subject to the conditions that $P_D = P_{DO}$ and $P_{FA} = P_{FO}$, where P_{DO} and P_{FO} are the specified detection and false alarm probability, respectively, and N_I is also specified.

The design parameters to be determined are N_1, N_2, β_{12}, β_{22}, β_{11}, β_{21}, $\bar{X}_1$, K, $\bar{K}_2$.

(The basic relationships for effecting this minimization are presented in Appendix 3.)

REFERENCES

1. Harold M. Finn, Missile and Surface Radar, RCA, Moorestown, N. J., "Optimum Radar Surveillance Mode Study, Technical Documentary Report No. RADC-TDR-64-122, July 1964." Prepared under Contract AF 30(602)-3152.

2. Harold M. Finn, "Energy-Variant Sequential Detectors for Fluctuating Targets," Proc. of Symposium on Electronically Scanned Array Techniques and Applications, RADC-TDR-64-225, Vol. I, July 1964, pp 444-468.

3. Harold M. Finn, "A New Approach to Sequential Detection in Phased-Array Radar Systems," Proceedings of the National Winter Convention on Military Electronics, 1963, Vol. II, pp 4-3 to 4-12.

4. A. Wald, "Sequential Analysis," John Wiley & Sons, Inc., New York, N. Y., 1947.

5. I. Bussgang and D. Middleton, "Optimum Sequential Detection of Signals in Noise," IRE Transactions on Information Theory, Vol. IT-1, pp 5-18.

6. G. Preston "The Search and Detection Efficiency of Surveillance and Communications Devices, Using Sequential Probability Ratio Analysis," Proc. of the Symposium on Decision Theory and Applications to Electronic Equipment Development," Vol. I, pp 100-117, May 1960.

7. Caspers, Simmon, Dillar, and Worley, Naval Electronics Laboratory, San Diego, Cal., NEL Reports 730, 963, 1021, and 1201.

8. C. Helstrom, "A Range-Sampled Sequential Detection System," IRE Transactions on Information Theory, Vol. IT-8 pp 43-47.

9. M. Marcus and P. Swerling, "Sequential Detection in Radar with Multiple Resolution Elements," IRE Transactions on Information Theory, Vol. IT-8 pp 237-245.

10. D. Blackwell and M. Girshick, "Theory of Games and Statistical Decisions," John Wiley & Sons, New York, N. Y., 1954.

11. A. Wald and J. Wolfowitz, "Optimum Character of the Sequential Probability Test," Ann. Math. Stat. 19, pp 326-339 (1948).

12. Elspace "A Radar System Based on Statistical Estimation and Resolution Considerations," Stanford University Applied Electronics Lab. Technical Report 361-1, August 1, 1955, AD-207896.

13. L. E. Brennan and F. S. Hill, Jr., "A Two-Step Sequential Procedure for Improving the Cumulative Probability of Detection in Radars," Rand Corp. Memorandum RM-4338, October 1964.

14. J. Mallette and L. Brennan "Cumulative Probability of Detection for Targets Approaching a Uniformly Search Radar," Proc. IEEE, Vol. 51, No. 4, April 1963, pp 596-601.

15. Harold Cramer, "Mathematical Methods of Statistics," Princeton University Press.

APPENDIX I

PROBABILITY OF DETECTION WHEN TARGET PRIORITY STRATEGY IS UTILIZED

The development of the expression

$$P_D = \prod_{i=1}^{N} P_{Di}, \tag{1}$$

where

$$P_{Di} = \sum_{P=0}^{n_i} (-1)^P \binom{n_i}{P} \frac{\rho^{-\frac{P^2}{2(P+1)}}}{P+1} \; Q\left(\frac{\alpha_i}{\sqrt{PH}}, \beta_i \sqrt{P+1}\right) \tag{2}$$

(Equation 30 of Section 5.5) is presented here.

$$P_{Di} = P\left\{Z > \underset{J}{\text{Max}} \left\{\xi_j\right\} \bigcap Z > \beta_i; \alpha_i\right\} \tag{3}$$

P_{Di} is the probability that of $n_i + 1$ channels, n_i of which contain noise alone (the same noise power density), the channel with a non-fluctuating target return plus noise will have a matched-filter output which is greater than both the outputs of the n noise-alone channels and the threshold β_i, and where the input signal energy to noise power density of the channel containing the signal is $\alpha_i^2/2$. The set of noise-alone outputs is designated as $\left\{\xi_j\right\}$ and the output of the signal channel is Z.

Equation 3 is a probability of extreme values (see Cramer, p. 370 Reference #15) and may be expressed as:

$$P_{Di} = \int_{\beta_i}^{\infty} G(Z) \; Z \, e^{-\frac{Z^2+\alpha_i^2}{2}} \; I_0(\alpha Z) \, dZ \tag{4}$$

where G(Z) is the probability that the maximum of all of the $\{\xi_j\}$ is less than Z, and:

$$G(Z) = \int_0^Z N_i \left[1 - e^{-\xi^2/2}\right]^{n_i - 1} \left\{e^{-\xi^2/2} \, d\right\} \tag{5}$$

The quantity

$$f_1(Z)dZ = Z \, e^{-\frac{Z^2 + \alpha_i^2}{2}} I_0(\alpha Z)dZ \tag{6}$$

of equation 4 is the probability density function of the matched filter output of the target channel, and

$$f_2\{\xi\} \, d\xi = \xi e^{-\xi^2/2} \, d\xi \tag{7}$$

of equation 5 is the probability density function of a noise-alone channel output.

We now introduce the change of variable

$$u = e^{-\xi^2/2} \tag{8}$$

and equation (5) becomes:

$$G = n_i \int_{e^{-Z^2/2}}^{1} (1-u)^{n_i - 1} \, du = (1-u)^n \Big|_{e^{-Z^2/2}}^{1} \tag{9}$$

and

$$G = \left(1 - e^{-Z^2/2}\right)^n \tag{10}$$

Now combining equation (10) and equation (4):

$$P_{Di} = \int_{\beta}^{\infty} \left[1 - e^{-Z^2/2}\right]^n Z e^{-\frac{Z^2 + \alpha^2}{2}} I_o(\alpha Z) dZ \qquad (11)$$

and employing the binomial expansion for the first term of the integrand:

$$P_{Di} = \sum_{P=0}^{n} (-1)^P \binom{n}{P} Z e^{-\frac{(P+1)\, Z^2 + \alpha^2}{2}} I_o(\alpha Z) dZ \qquad (12)$$

Factoring terms not involved in the integration:

$$P_{Di} = \sum_{P=0}^{n} (-1)^P \binom{n}{P} \frac{e^{-\frac{P\alpha_i^2}{Z(P+1)}}}{P+1} \int_{\beta_i}^{\infty} (P+1) Z e^{-\frac{(P+1)Z^2}{2}} e^{-\frac{\alpha^2}{2(P+1)}} I_o(\alpha Z) dZ \qquad (13)$$

Introducing the change of variables:

$$X = \sqrt{P+1}\ Z \text{ and } a = \frac{\alpha}{\sqrt{P+1}}$$

$$P_{Di} = \sum_{P=0}^{n} (-1)^P \binom{n}{P} \frac{e^{-\frac{P\alpha^2}{Z(P+1)}}}{P+1} \cdot \int_{\beta\sqrt{PH}}^{\infty} X e^{-\frac{X^2 + a^2}{2}} I_o(ax) dx \qquad (14)$$

and finally employing the definition of the Q function we arrive at our desired result:

$$P_{Di} = \sum_{P=0}^{n} (-1)^P \binom{n}{P} \frac{e^{-\frac{P^2}{2(P+1)}}}{(p+1)} Q\left(\frac{\alpha}{\sqrt{P+1}}, \beta\sqrt{P+1}\right) \qquad (15)$$

APPENDIX II

OPTIMIZATION OF A RESOLUTION-VARIANT EVSD — THREE STEP MAXIMUM PROCEDURE

The basic relationships involved in the optimization of a Resolution-Variant EVSD designed for the detection of a non-fluctuating target and employing a maximum of three steps is described below. (This procedure has been implemented on the IBM 7090 computer.)

When the equations for the detection probability (P_D), the equivalent single cell false alarm probability (P_{FA}), and the cost function (C) (equations 22, 28, and 29 respectively of Section 5.4) are specialized for a three step maximum procedure, they become:

$$P_D = Q(\alpha_1, \beta_1)\, Q(\alpha_2, \beta_2)\, Q(\alpha_3, \beta_3) \tag{2.1}$$

$$2 \ln \frac{1}{P_{FA}} = \beta_1^2 + \beta_2^2 + \beta_3^2 \tag{2.2}$$

$$C = \frac{1}{2}\left[\alpha_1^2 + n_1\left(\alpha_2^2\, e^{-\frac{\beta_1^2}{2}} + F_2\, \alpha_3^2\, e^{-\frac{\beta_1^2+\beta_2^2}{2}}\right)\right] \tag{2.3}$$

The specified quantities are the detection probability (P_D), the single cell false alarm probability (P_{FA}), the number of resolution cells on the first step (n_1), and the ratio of the time-bandwidth product on the second step to the time-bandwidth product of the first step $F_2 = (T_2 W_2)/(T_1 W_1)$. (For most cases of interest, the time-bandwidth product of the first step is made equal to unity.)

The six design degrees of freedom, then, are the required received energy to noise power density ratios at each of the three sequential steps $\left\{\alpha_1^2/2\right\}$, and the three normalized receiver thresholds $\left\{\beta_1\right\}$ where i = 1, 2, and 3.

The minimization of the cost function (equation 2.3) subject to the constraint relationships (equations 2.1 and 2.2), is most conveniently initiated by the introduction of the Lagrange multipliers τ and μ, and finding the extremum of the Lagrange function:

$$C + \tau (\varphi_1 \varphi_2 \varphi_3 - P_D) + \mu \left(\beta_1^2 + \beta_2^2 + \beta_3^2 - 2 \ln \frac{1}{P_{FA}} \right) \tag{2.4}$$

where

$$\varphi_i = Q (\alpha_i, \beta_i)$$

The partial derivatives of the Lagrange Function with respect to the six design degrees of freedom is next taken and each of these partial derivatives is equated to zero, yielding the six equations:

$$\alpha_1 + \tau \varphi_1' \varphi_2 \varphi_3 = 0 \tag{2.5}$$

$$n_1 \alpha_2 e^{-\frac{\beta_1^2}{2}} + \tau \varphi_1 \varphi_2' \varphi_3 = 0 \tag{2.6}$$

$$n_1 F_2 \alpha_3 e^{-\frac{\beta_1^2 + \beta_2^2}{2}} + \tau \varphi_1 \varphi_2 \varphi_3' = 0 \tag{2.7}$$

$$-\beta_1 n_1 \left(\frac{\alpha_2^2}{2} e^{-\frac{\beta_1^2}{2}} + F_2 \frac{\alpha_3^2}{2} e^{-\frac{\beta_1^2 + \beta_2^2}{2}} \right) + \tau \psi_1 \varphi_2 \varphi_3 + 2\mu\beta_1 = 0 \tag{2.8}$$

$$-\beta_2 n_1 F_2 \frac{\alpha_3^2}{2} e^{-\frac{\beta_1^2 + \beta_2^2}{2}} + \tau \varphi_1 \psi_2 \varphi_3 + 2\mu\beta_2 = 0 \tag{2.9}$$

$$\tau \varphi_1 \varphi_2 \psi_3 + 2\mu\beta_3 = 0 \tag{2.10}$$

where in (2.5) through (2.10) the notation used is:

$$\varphi_1 = Q(\alpha_1, \beta_1) \tag{2.11}$$

$$\frac{\partial \varphi_i}{\partial \beta_i} = \psi_i \tag{2.12}$$

$$\frac{\partial \varphi_i}{\partial \alpha_i} = \varphi_i' \tag{2.13}$$

Solving for the lagrange multipliers (with equations (2.5) and (2.10)):

$$\tau = \frac{\alpha_1}{\varphi_1' \varphi_2 \varphi_3} \tag{2.14}$$

and

$$2\mu = \frac{\alpha_1 \varphi_1 \psi_3}{\beta_3 \varphi_1' \varphi_3} \tag{2.15}$$

Six equations of interest for our solution are defined below:

$$f_1 = \frac{\alpha_2}{\alpha_1} n_1 e^{-\frac{\beta_1^2 + \beta_2^2}{2}} - \frac{\varphi_1 \varphi_3'}{\varphi_1' \varphi_3} = 0 \tag{2.16}$$

$$f_2 = \frac{\alpha_3}{\alpha_1} n_1 F_2 e^{-\frac{\beta_1^2 + \beta_2^2}{2}} - \frac{\varphi_1 \varphi_3'}{\varphi_1' \varphi_3} = 0 \tag{2.17}$$

$$f_3 = \frac{\beta_1 \beta_2}{\alpha_1} n_1 \left(\frac{\alpha_2^2}{2} e^{-\frac{\beta_1^2}{2}} + F_2 \frac{\alpha_3^2}{2} e^{-\frac{\beta_1^2 + \beta_2^2}{2}} \right) + \beta_3 \frac{\psi_1}{\varphi_1'} - \frac{\beta_1 \varphi_1 \psi_3}{\varphi_1' \varphi_3} = 0 \tag{2.18}$$

$$f_4 = \frac{\beta_2\,\beta_3}{\alpha}\, n_1\, F_2 \frac{\alpha_3^2}{2}\, e^{-\frac{\beta_1^2+\beta_2^2}{2}} + \beta_3 \frac{\varphi_1\,\psi_3}{\varphi_1'\,\varphi_2} - \beta_2 \frac{\varphi_1\,\psi_3}{\varphi_1'\,\varphi_3} = 0 \tag{2.19}$$

$$f_5 = \varphi_1\,\varphi_2\,\varphi_3 - P_D = 0 \tag{2.20}$$

$$f_6 = \beta_1^2 + \beta_2^2 - 2 \ln \frac{1}{P_{FA}} = 0 \tag{2.21}$$

A simultaneous solution of the six equations (2.16 through 2.21) is now required in order to find the desired vector (α_1, α_2, α_3, β_1, β_2, β_3) minimizing the cost C, subject to the P_D and P_{FA} specified.

A Newton's iteration is employed:

$$\left(\alpha_1^{(J+1)}, \alpha_2^{(J+1)}, \alpha_3^{(J+1)}, \beta_1^{(J+1)}, \beta_2^{(J+1)}, \beta_3^{(J+1)}\right) = \left(\alpha_1^{(J)}, \alpha_2^{(J)}, \alpha_3^{(J)}, \beta_1^{(J)}, \beta_2^{(J)}, \beta_3^{(J)}\right) + \left(\Delta\alpha_1^{(J)}, \Delta\alpha_2^{(J)}, \Delta\alpha_3^{(J)}, \Delta\beta_1^{(J)}, \Delta\beta_2^{(J)}, \Delta\beta_3^{(J)}\right) \tag{2.22}$$

and where:

$$\begin{bmatrix} \Delta\alpha_1 \\ \Delta\alpha_2 \\ \Delta\alpha_3 \\ \Delta\beta_1 \\ \Delta\beta_2 \\ \Delta\beta_3 \end{bmatrix} = \begin{bmatrix} f_1\alpha_1 & f_1\alpha_2 & f_1\alpha_3 & f_1\beta_1 & f_1\beta_2 & f_1\beta_3 \\ f_2\alpha_1 & f_2\alpha_2 & f_2\alpha_3 & f_2\beta_1 & f_2\beta_2 & f_2\beta_3 \\ f_3\alpha_1 & f_3\alpha_2 & f_3\alpha_3 & f_3\beta_1 & f_3\beta_3 & f_3\beta_3 \\ f_4\alpha_1 & f_4\alpha_2 & f_4\alpha_3 & f_4\beta_1 & f_4\beta_4 & f_4\beta_4 \\ f_5\alpha_1 & f_5\alpha_2 & f_5\alpha_3 & f_5\beta_1 & f_5\beta_5 & f_5\beta_5 \\ f_6\alpha_1 & f_6\alpha_2 & f_6\alpha_3 & f_6\beta_1 & f_6\beta_6 & f_6\beta_6 \end{bmatrix}^{-1} \begin{bmatrix} -f_1 \\ -f_2 \\ -f_3 \\ -f_4 \\ -f_5 \\ -f_6 \end{bmatrix} \tag{2.23}$$

The elements of the 6 x 6 matrix in equation (23) include the six partial derivatives required to be taken of each of the quantities f_1, f_2, f_3, f_4, f_5, and f_6. These 36 terms are not repeated here for the sake of brevity.

APPENDIX III

OPTIMIZATION OF THE CONFIRMATION DELAY-TIME OPTION EVSD

The development of the probability distributions involved in the design of a Confirmation Delay-Time Option EVSD for the detection of a Case #2 Target type and having a maximum of two steps is treated here in greater detail than in the discussion in Section 7.

First, the probability of detection (P_D), the single cell false alarm probability (P_{FA}), and the cost function (C) are listed below, and where the symbols used are the same as those defined in Section 7.

$$P_D = F_1 F_2 + F_3 F_4 \tag{3.1}$$

where

$$F_1 = \sum_{J=0}^{N_1-1} \left(1 - e^{-\frac{\beta_{12}}{\bar{X}_1 + 1}}\right)^J \tag{3.2}$$

$$F_2 = \int_0^\infty Q\left(\sqrt{2\bar{X}, t}, \sqrt{2\beta_{12}}\right) Q\left(K\sqrt{2\bar{X}, t}, \sqrt{2\beta_{22}}\right) e^{-t}\, dt \tag{3.3}$$

$$F_3 = \sum_{J=0}^{N_1-1} (-1)^J \frac{N_1!\, e^{-\frac{J\beta_{12}}{\bar{X}_1 + 1}}}{J!\ N_1 - J)!} \tag{3.4}$$

$$\bigotimes \sum_{m=0}^{N_1-1} e^{-\left(\frac{\beta_{11} - J\beta_{12}}{\bar{X}_1 + 1}\right) + \left(\frac{\beta_{11} - J\beta_{12}}{\bar{X}_1 + 1}\right)^m} - e^{-\frac{\beta_{12}(N_1 - J)}{\bar{X}_1 + 1}} \left(\frac{\beta_{12}(N_1 - J)}{\bar{X}_1 + 1}\right)^m \Bigg/ m!$$

$$F_4 = e^{-\frac{\beta_{21}}{\overline{X}_2 + 1}} \sum_{J=0}^{N_2 - 1} \frac{\left(\frac{\beta_{21}}{\overline{X}_2 + 1}\right)^J}{J!} \tag{3.5}$$

and

$$P_{FA} = e^{-\beta_{12}} e^{-\beta_{22}} G_1 + G_3 G_4 \tag{3.6}$$

$$G_1 = \sum_{J=0}^{N_1 - 1} \left(1 - e^{-\beta_{12}}\right)^J \tag{3.7}$$

$$G_4 = e^{-\beta_{21}} \sum_{J=0}^{N_2 - 1} \frac{\beta_{21}}{J_1}^J \tag{3.8}$$

$$G_3 = \sum_{J=0}^{N_1 - 1} (-1)^J \frac{N_1!\, e^{-J\beta_{12}}}{J!\,(N_1 - J)!} \sum_{m=0}^{N_1 - 1} e^{-(\beta_{11} - J\beta_{12})_+} (\beta_{11} - J\beta_{12})_+^m \tag{3.9}$$

$$- e^{-(N_1 - J)\,\beta_{12}} (\beta_{12}\,(N_1 - J)^m$$

and where

$$(Z)_+ = \begin{cases} 0, & Z < 0 \\ Z, & Z \geq 0 \end{cases} \tag{3.10}$$

the cost function

$$C = \overline{X}_1 C_1 C_2 + \overline{X}_2 C_3 C_4 \tag{3.11}$$

where

$$C_1 = \sum_{J=0}^{N_1 - 1} \left(1 - e^{-\beta_{12}}\right)^{JN_F} \tag{3.12}$$

$$C_2 = 1 + k^2 \left[1 - \left(1 - e^{-\beta_{12}}\right)\right]^{N_F} \tag{3.13}$$

$$C_3 = N_2 \left(1 - e^{-\beta_{12}}\right)^{N_1 N_F} \tag{3.14}$$

$$C_4 = 1 - \left(1 - G_3\right)^{N_F} \tag{3.15}$$

The optimization procedure, similar to those previously described involves finding the vector $[\overline{X}_1, \overline{X}_2, K, \beta_{11}, \beta_{12}, \beta_{21}, \beta_{22}]$ which satisfies the specified P_D and P_{FA} and minimizes the cost function C. The number of statistically independent target cross-section samples which are employed on each sequential step N_1, and N_2 are fixed inputs to the program. The optimization, then, with respect to N_1 and N_2 must be obtained by employing a sequence of selections N_1 and N_2, and comparing the minimum costs for each set.

The development of equation 3.1 is now treated in greater detail: (see also Section 7.1)

1. The product $F_1 F_2$ represents the contribution to the probability of detection due to the use of the quick-reaction second step, and the development of F_1 and F_2 follow directly from the decision rule employed.

2. $F_3 F_4$ is the contribution to the detection probability due to the event that the slow-reaction mode is employed and the detection criterion is satisfied.

F_4 is the probability that the sum of the N_2 (statistically independent) square law detected outputs of the slow-reaction second step exceeds the threshold β_{21}. The development of this quantity (equation 3.5) is the same as for the conventional EVSD, and it is presented in Appendix (V-B).

F_3 (equation 3.4) is the joint probability that no single-pulse threshold crossing occurs on any of the N_1 pulses of the first step but that the incoherent sum of these N_1 pulses is greater than the sum threshold β_{11}. It is this distribution which is most complex since it involves the convolution of truncated random variables. The development of equation 3.4, therefore, will be presented in the remainder of this appendix.

Let y be the square-law detected output of a single pulse; then define:

$$f(y) = \left\{ \begin{array}{l} \alpha e^{-\alpha y}, \quad 0 \le y \le \beta_{12} \\ 0, \quad y > \beta_{12}, \quad \alpha = \frac{1}{1 + [\text{illegible}]} \end{array} \right\} \tag{3.16}$$

Taking the Laplace transform:

$$f(s) = \int_0^{\beta_{12}} \alpha e^{-\alpha y} e^{-sy} \, dy = \alpha \int_0^{\beta_{12}} e^{-(\alpha + s)y} \, dy =$$

$$\left(\frac{\alpha}{\alpha + s}\right) \left(1 - e^{-(\alpha + s)\beta_{12}}\right) \tag{3.17}$$

and:

$$f_N(s) = \left(\frac{\alpha}{\alpha + s}\right)^N \left[1 - e^{-(\alpha + s)\beta_{12}}\right]^N =$$

$$\left(\frac{\alpha}{\alpha + s}\right)^N \sum_0^N (-1)^m \frac{N!\, e^{-m\alpha\beta_{12}} e^{-m\beta_{12} S}}{m!\,(N - m)!} \tag{3.18}$$

The quantity desired is

$$f_N(y) = L^{-1}\left(\bar{f}_N(s)\right) \tag{3.19}$$

and this inverse transform is effected by first noting:

$$L^{-1}\left\{e^{-sg}\,\bar{f}(s)\right\} = \begin{cases} 0, & x \le g \\ f(x-g), & x > g \end{cases} \tag{3.20}$$

and

$$\varphi_N(y) = L^{-1}\left\{\left(\frac{\alpha}{\alpha+s}\right)^N\right\} = \frac{\alpha^N y^{N-1} e^{-\alpha y}}{(N-1)!} \tag{3.21}$$

Therefore,

$$f_N(y) = \sum_{m=0}^{N} (-1)^m \frac{N!}{m!\,(N-m)!}\, e^{-m\alpha\beta_{12}}\, \varphi(y - m\beta_{12}) \tag{3.22}$$

$$f_N(y) = \frac{\alpha^N e^{-\alpha y}}{(N-1)!} \sum_{m=0}^{N} (-1)^m \frac{N!}{m!\,(N-m)!}\, (y - m\beta_{12})_+^{N-1} \tag{3.23}$$

where

$$(Z)_+ = \begin{cases} 0, & Z < 0 \\ Z, & Z \ge 0 \end{cases}$$

It can be seen that

$$f_N(x) \equiv 0 \quad \text{for } x \ge N\beta_{12}$$

and it can be shown that

$$\int_{\beta_{11}}^{\infty} f_N(v)\,dv = \sum_{J=0}^{N_1-1} (-1)^J \frac{N_1!\, e^{-\frac{J\beta_{12}}{\bar{X}_1+1}}}{J!\,(N_1-J)!} \sum_{m=0}^{N_1-1} \frac{e^{-\frac{(\beta_{11}-J\beta_{12})}{\bar{X}_1-1}} + \left(\frac{\beta_{11}-J\beta_{12}}{\bar{X}_1-11}\right)^m - e^{-\frac{\beta_{12}(N_1-J)}{\bar{X}_1+1}} \left(\frac{\beta_{12}(N_1-J)}{\bar{X}_1+1}\right)^m}{m!} \tag{3.4}$$

APPENDIX IV

DEVELOPMENT OF THE ENERGY-VARIANT SEQUENTIAL DETECTORS FOR THE CASE #2 AND #4 TARGET TYPES

Three EVSD types for the detection of the Case 2 and 4 target models have been developed (Reference #1). The basic system of equations employed in the development of each are considered in Parts A, B, and C below. In general, the optimization procedure involves finding the minimum of the cost function C by the method of Lagrange multipliers where the detection and false alarm probability equations are introduced as constraint relationships of the variables, and a Newton's iteration is employed to solve the resultant equations.

Part A - System of Equations for the Case where Independent Decision Statistics are Employed on Each Sequential Step, and $\bar{X}$'s are Design Degrees of Freedom.

$$P_D = F_1 F_2 \tag{IV.1}$$

$$P_{FA} = G_1 G_2 \tag{IV.2}$$

$$C = N_1 \bar{X}_1 + N_2 N_F \bar{X}_2 G_1 \tag{IV.3}$$

where $F_J = P\left\{Y_J > \beta_J;\ \bar{X}_J,\ N_J\right\}$ $J = 1,2$ (see Section 3-2, equation 22) (F_J is the probability of a threshold crossing in a single resolution cell on the J^{th} step).

For the Case #2 target:

$$F_J = e^{-\alpha_J \beta_J} \sum_{K=0}^{N_J - 1} \frac{(\alpha_J \beta_J)^K}{K!} \qquad \text{where } \alpha_J = \frac{1}{1 + \bar{X}_J} \tag{IV.4}$$

and for the Case #4 target:

$$F_J = \alpha_J^{N_J} e^{-\alpha_J \beta_J} \sum_{n=0}^{N_J} \frac{N_J ! \left(\frac{1}{\alpha_J}\right)^n}{n ! (N_J - n) !} \sum_{K=n}^{K+n-1} \frac{(\alpha_J \beta_J)^K}{K !} \qquad \text{(IV.5)}$$

(These distributions are developed in Appendix V.)

G_J refers to the probability of a threshold crossing of the decision statistic on the J^{th} step for the noise alone case in a single resolution cell. (Implicit in the statement $P_{FA} = G_1 G_2$ is that a common resolution cell is involved for the successive step threshold crossings.)

For the largest type G_J may be expressed as:

$$G_J = e^{-\beta_J} \sum_{K=0}^{N_J - 1} \frac{\beta_J^K}{K !} \qquad \text{(IV.6)}$$

The Lagrange function used is:

$$L = C + \lambda P_D + \mu \ln P_{FA} \qquad \text{(IV.7)}$$

and the partial derivatives with respect to the degrees of freedom $\bar{X}_1$, $\bar{X}_2$, β_1, β_2 are equated to zero, and constitute the minimizing equations.

$$\frac{\partial L}{\partial \bar{X}_1} = N_1 + \lambda \frac{\partial F_1}{\partial \bar{X}_1} F_2 = 0 \qquad \text{(IV.8)}$$

$$\frac{\partial L}{\partial \bar{X}_2} = N_2 N_F G_1 + \lambda F_1 \frac{\partial F_2}{\partial \bar{X}_2} = 0 \qquad \text{(IV.9)}$$

$$\frac{\partial L}{\partial \beta_1} = N_F N_2 \bar{X}_2 \frac{d G_1}{d \beta_1} + \lambda \frac{\partial F_1}{\partial \beta_1} F_2 + \frac{\mu}{G_1} \frac{d G_1}{d \beta_1} = 0 \qquad \text{(IV.10)}$$

$$\frac{\partial L}{\partial \beta_2} = \lambda_1 \frac{\partial F_2}{\partial \beta_2} + \frac{\mu}{G_2} \frac{dG_2}{d\beta_2} = 0 \qquad \text{(IV.11)}$$

Using (IV.8) and (IV.11) the Lagrange Multipliers are eliminated and the system of equations to be solved for $(X_1, X_2, \beta_1, \beta_2)$ are:

$$f_1 \quad \lambda_1 \frac{\partial F_2}{\partial \beta_1} - \lambda_2 \lambda_1 \frac{\partial F_1}{\partial X_1} F_2 \quad 0 \qquad \text{(IV.12)}$$

$$f_2 \quad \lambda_2 \frac{\partial G_1}{\partial \beta_1} \frac{1}{G_1} \frac{dG_1}{d\beta_1} \frac{\partial F_2}{\partial X_2} - \frac{1}{G_2} \frac{dG_2}{d\beta_2} \frac{\partial F_1}{\partial \beta_1} F_2$$

$$+ \frac{1}{G_1} \frac{dG_1}{d\beta_1} F_1 \frac{\partial F_2}{\partial \beta_2} \quad 0 \qquad \text{(IV.13)}$$

$$f_3 = F_1 F_2 - P_{DO} - 0 \qquad \text{(IV.14)}$$

$$f_4 = -\ln (G_1 G_2 / P_{DO}) - 0 \qquad \text{(IV.15)}$$

The simultaneous solution of these equations is accomplished by the Newton's iteration:

$$(X_1^{J+1}, X_2^{J+1}, \beta_1^{J+1}, \beta_2^{J+1}) = (X_1^J, X_2^J, \beta_1^J \beta_2^J) + (\Delta X_1^J, \Delta X_2^J, \Delta \beta_1^J, \Delta \beta_2^J)$$

where:

$$\begin{pmatrix} \Delta X_1^J \\ \Delta X_2^J \\ \Delta \beta_2^J \\ \Delta \beta_2^J \end{pmatrix} = \begin{pmatrix} \frac{\partial f_1^J}{\partial X_1} & \frac{\partial f_1^J}{\partial X_2} & \frac{\partial f_1^J}{\partial \beta_1} & \frac{\partial f_1^J}{\partial \beta_2} \\ \frac{\partial f_2^J}{\partial X_1} & \frac{\partial f_2^J}{\partial X_2} & \frac{\partial f_2^J}{\partial \beta_1} & \frac{\partial f_2^J}{\partial \beta_2} \\ \frac{\partial f_3^J}{\partial X_1} & \frac{\partial f_3^J}{\partial X_2} & \frac{\partial f_3^J}{\partial \beta_1} & \frac{\partial f_3^J}{\partial \beta_2} \\ \frac{\partial f_4^J}{\partial X_1} & \frac{\partial f_4^J}{\partial X_2} & \frac{\partial f_4^J}{\partial \beta_1} & \frac{\partial f_4^J}{\partial \beta_2} \end{pmatrix}^{-1} \begin{pmatrix} -f_1^J \\ -f_2^J \\ -f_3^J \\ -f_4^J \end{pmatrix} \qquad \text{(IV.16)}$$

The 16 equations of the partial derivatives of f_1, f_2, f_3, and f_4, as a function of $\bar{X}_1$, $\bar{X}_2$, β_1, and β_2 are then formed to be used in (IV.16). (These straightforward relationships are not repeated here for the sake of brevity.)

Fixed inputs to this minimization program are the number of statistically independent target cross-section samples employed on each step, N_1 and N_2. But since N_1 and N_2 are really integral valued variables to be selected, the optimization approach has involved repeating the minimization program for an ensemble of couples (N_1, N_2) and then selecting the minimum cost combinations.

Part B - System of Equations for the Case Where the Second Step Decision Statistic is Based on the Sum of the First and Second Step Outputs, and $\bar{X}$'s are Design Degrees of Freedom. (Maximum of Two Sequential Steps)

Let the single step, N-pulse detection density and distribution functions be $f_N(\bar{X},X)$ and $1-F_N(\bar{X},\beta)$.

If the random variables at the first and second steps are respectively $X = \sum_1^{N_1} X_1$ and $Y = X + \sum_1^{N_2} Y_1$, where $X_1,\ldots\ldots X_{N1}$, $Y_1,\ldots\ldots Y_{N2}$ are independent and represent the normalized square law detector outputs on each of the two steps.

The total probability of detection is:

$$\begin{cases} P_D = P\{X > \beta_1 \text{ and } X+Y > \beta_2\} = P\{X > \beta_1 \text{ and } Y > \beta_2 - X\} \\ P_D = \sum_{X_o > \beta_1} P\{X = X_o\}\ P\{Y > \beta_2 - X_o\} = \int_{\beta_1}^{\infty} f_{N1}(\bar{X}_1, X) F_{N2}(\bar{X}_2, \beta_2 - X)dX \end{cases} \qquad (IV.17)$$

We consider the two cases:

A. $\beta_2 \leq \beta_1$ Then $P_D = F_{N1}(\bar{X}_1, \beta_1)$

B. $\beta_2 > \beta_1$ Then $P_D = \int_{\beta_1}^{\beta_2} f_{N1}(\bar{X}_1, X)\ F_{N2}(\bar{X}_2, \beta_2 - X)dX + F_{N1}(\bar{X}_1, \beta_2)$

The false alarm probability in an individual resolution cell (P_{FA}) may be obtained from the above by setting $\bar{X}_1 = \bar{X}_2 = 0$

If we demand that $\bar{X}_1 = \bar{X}_2 = \bar{X}$, the formula of Part C will apply with P_D and P_{FA} defined as above. Otherwise, the required formulas are slight generalizations of those of Part A and are listed here:

$$f_1 = N_1 \frac{\partial P_D}{\partial \bar{X}_2} - N_2 N_P G_1 \frac{\partial P_D}{\partial \bar{X}_1} = 0 \qquad \text{(IV.18)}$$

$$f_2 = X_2 \frac{\partial P_D}{\partial \bar{X}_2} \frac{1}{G_1} \frac{dG_1}{d\beta_1} \frac{1}{P_{FA}} \frac{\partial P_{FA}}{\partial \beta_2} - \frac{\partial P_D}{\partial \beta_2} \frac{1}{P_{FA}} \frac{\partial P_{FA}}{\partial \beta_2} \qquad \text{(IV.19)}$$

$$+ \frac{\partial P_D}{\partial \beta_2} \frac{1}{P_{FA}} \frac{\partial P_{FA}}{\partial \beta_1} = 0$$

$$f_3 = P_D - P_{DO} = 0 \qquad \text{(IV.20)}$$

$$f_4 = \ln (P_{FA}/P_{FO}) = 0 \qquad \text{(IV.21)}$$

The simultaneous solution of these equations for $\bar{X}_1$, $\bar{X}_2$, β_1, and β_2 is now obtained by a Newton's iteration procedure as outlined in Part B.

The calculation of P_D and P_{FA} is now necessary. We consider the case for the Case 2 target where $\bar{X}_1 \neq \bar{X}_2$ and assuming $\beta_2 > \beta_1$, and let

$$\alpha_1 = \frac{1}{1 + \bar{X}_1}$$

Then
$$P_D = e^{-\alpha_1 \beta_2} \sum_{0}^{N_1 - 1} \frac{(\alpha_1 \beta_2)^K}{K!} + P_D^* \qquad \text{(IV.22)}$$

$$P_D^* = \int_{\beta_1}^{\beta_2} \frac{\alpha_1^{N_1} Y^{N_1 - 1} e^{-\alpha_1 Y}}{(N_1 - 1)!} e^{-\alpha_2 (\beta_2 - Y)} \sum_{K=0}^{N_2 - 1} \frac{\alpha_2^K (\beta_2 - Y)^K}{K!} \qquad \text{(IV.23)}$$

$$P_{FA} = e^{-\beta_2} \sum_{0}^{N_1 - 1} \frac{\beta_2 K}{K!} + P_F^* \qquad \text{(IV.24)}$$

$$P_F^* = \frac{e^{-\beta_2}}{(N_1-1)!} \sum_{0}^{N_2-1} \frac{1}{K!} \int_{\beta_1}^{\beta_2} Y^{N_1-1} (\beta_2 - Y)^K dY \qquad \text{(IV.25)}$$

Part C - System of Equations for the Case Where the First and Second Step Decision Statistics are independent but where a Constraint is introduced Requiring the Single Pulse Signal Energy to Noise Power Density X to be the same or Both Steps.

Initially we fix N_1, and N_2

$$P_D = F_{N1}(\alpha_1, \beta_1)\, F_{N2}(\alpha_1, \beta_2) \qquad \text{(IV.26)}$$

where for the Case 4 target model

$$\alpha = \frac{1}{1 + \frac{X}{2}}$$

$$P_{FA} = G_{N_1}(\beta_1)\, G_{N2}(\beta_2) \qquad \text{(IV.27)}$$

and the Lagrange function is $L = C + \lambda P_D + \mu \ln P_{FA}$ (IV.28)

$$\frac{\partial L}{\partial \bar{X}} = \frac{C}{\bar{x}} + \lambda \frac{\partial P_D}{\partial \bar{X}} = 0 \qquad \text{(IV.29)}$$

$$\frac{\partial L}{\partial \beta_1} = \frac{\partial C}{\partial \beta_1} + \lambda \frac{\partial P_D}{\partial \beta_1} + \frac{\mu}{P_{FA}} \frac{\partial P_{FA}}{\partial \beta_1} = 0 \qquad \text{(IV.30)}$$

$$\frac{\partial L}{\partial \beta_2} = \lambda \frac{\partial P_D}{\partial \beta_2} + \frac{\mu}{P_{FA}} \frac{\partial P_{FA}}{\partial \beta_2} = 0 \qquad \text{(IV.31)}$$

By eliminating the Lagrange multipliers, the following equations are obtained for minimizing C, subject to the conditions $P_D = P_{DO}$ and $P_{FA} = P_{FO}$ where P_{DO} and P_{FO} are the specified detection and false alarm probabilities respectively.

$$f_1 = \frac{\partial C}{\partial \beta_1} \frac{\partial P_D}{\partial X} \frac{1}{P_{FA}} \frac{\partial P_{FA}}{\partial \beta_2} + \frac{C}{X} \left(\frac{\partial P_D}{\partial \beta_2} \frac{1}{P_{FA}} \frac{\partial P_{FA}}{\partial \beta_1} \right.$$

$$\left. - \frac{\partial P_D}{\partial \beta_1} \frac{1}{P_{FA}} \frac{\partial P_{FA}}{\partial \beta_2} \right) = 0 \qquad \text{(IV.32)}$$

$$f_2 = P_D - P_{DO} = 0 \qquad \text{(IV.33)}$$

$$f_3 = P_{FA} - P_{FO} = 0 \qquad \text{(IV.34)}$$

Newton's method can now be used to solve these last three equations for X, β_1, and β_2. Here we notice that by requiring the same X on each step, the number of degrees of design freedoms have been reduced by one.

The nine equations of the partial derivatives of f_1, f_2, and f_3 with respect to X, β_1 and β_2 are also formulated for use in the Newton's procedure outlined in Part A. These equations, however, are not repeated here for the sake of brevity.

APPENDIX V

EVSD PROBABILITY DISTRIBUTIONS

Part A - EVSD Probability Distributions for Case #1 and #3 Target Models

As in equation (1) of Section 2.4 the probability of detection for the Case 1 and 3 target models may be expressed as

$$P_D = \int_{\alpha=0}^{\infty} \left[\prod_{J=1}^{N} Q(K_J \alpha, \beta_J) \right] f(\alpha; \bar{X}) d\alpha \qquad (V.1)$$

since the target cross-section is assumed to be constant for the maximum duration of the test of N steps.

In addition, the sampled output at the j^{th} step is based on having a filter matched to all of the energy of that step followed by a linear detector.

For the Case 1 Model $f(\alpha;\bar{X})d\alpha = \frac{\alpha}{\bar{X}} e^{-\alpha^2/2\bar{X}} d\alpha \qquad (V.2)$

and for the Case 3 Model $f(\alpha;\bar{X})d\alpha = \frac{2\alpha^3}{\bar{X}^2} e^{-\alpha^2/\bar{X}} d\alpha \qquad (V.3)$

It is convenient to introduce the change of variable $\alpha^2 = \bar{X}\zeta$, so that:

$$P_D = \int_{\zeta=0}^{\infty} \prod_{J=1}^{N} Q(K_J \sqrt{\bar{X}\zeta}, \beta_J) f(\zeta) d\zeta \qquad (V.4)$$

where for the Case 1 model $f(\zeta)d\zeta = \frac{1}{2} e^{-\zeta/2} d\zeta \qquad (V.5)$

and for the Case 3 model $f(\zeta)d\zeta = \zeta e^{-\zeta} d\zeta \qquad (V.6)$

The solution of P_D and the required derivatives of P_D with respect to the design degrees of freedom $\bar{X}$ and the sets $\{K_i\}$ and $\{\beta_i\}$, have been approximated by means of a 10 point quadrature formula. (The required derivatives for the optimization procedure are accomplished by first using the formal procedure of taking the derivatives of the integrand in equation (V.4).

The selection of a suitable quadrature formula has been influenced by the intuitively satisfying approach of representing the continuous probability density function $f(\xi)d\xi$ by a discrete distribution $\{f(\xi_i)\}$ formed in the following manner: For an N point schedule, the domain of the continuous distribution (positive real numbers) is divided into N sub-domains so that the probability of ξ appearing in any one of these sub-domains is $\frac{1}{N}$, and the value of ξ selected can be the local mean or median value. So for the case say where the local mean value is employed, and where the limits of the i^{th} subset are a and b,

$$\xi_i = \frac{\int_a^b \xi f(\xi)d\xi}{\int_a^b f(\xi)d\xi} \quad \text{(V.7) and where} \quad \int_a^b f(\xi)d\xi = \frac{1}{N} \qquad \text{(V.8)}$$

and $f\{\xi_i\}$ is selected as equal to $\frac{1}{N}$.

P_D for example is now approximated as follows:

$$P_D \approx \frac{1}{N} \sum_{i=1}^{N} \left[\prod_{J=1}^{N} Q(K_J \sqrt{\bar{X}\,\xi_i}) \right] \qquad \text{(V.9)}$$

An indication of the adequacy of the 10 point quadrature formula employed was obtained by duplicating the optimization procedure for some of the cases with a 20 point procedure. The differences in the computed parameters obtained with each of the two quadrature procedures were less than 0.1 db.

Part B - Probability Distribution for the Case 2 and 4 Target Model

For both the Case 2 and 4 target model EVSD's which are based on the use of independent decision statistics on each of the sequential steps, the probability of detection may be expressed as

$$P_D = \prod_{J=1}^{M} F_{N_J}(\bar{X}_J, \beta_J) \qquad (V.10)$$

M refers to the maximum number of sequential steps employed and $F_{N_J}(\bar{X}_J, \beta_J) = P\{Y_J > \beta_J; \bar{X}_J, N_J\}$ (See Equation 22 Section 3-2).

That is to say, $Y_J = \sum_{i=1}^{N_J} Y_i$ where Y_i is the normalized square law detector output. By making the change of variable $Y_i = \frac{X_i^2}{2}$ where X_i is the normalized linearly detected output of the matched filter and has the probability density function:

$$f(X)dX = X\, e^{\frac{-X^2 + \alpha^2}{2}}\, I_o(\alpha X)dX \qquad (V.11)$$

we arrive at (12) $f(Y_i)dY_i = \int_{Z=0}^{\infty} e^{-Y_i - Z_i}\, I_o(2\sqrt{Y_i Z_i}\, dY_i\, f(Z_i;\bar{X}_i)dZ_i$ (V.12)

where $Z_i = \frac{\alpha_i^2}{2}$ and $\bar{X}_i$ is the average value of Z_i.

The characteristic function for equation (V.12) for the case 2 target where $f(Z_i,\bar{X}_i)dZ_i = \frac{1}{\bar{X}}\, e^{-Z/X}\, dZ$ is $F_1(S) = \frac{1}{1 + S(1+\bar{X})}$, (see Reference 5) so that the characteristic function for the density function of the sum of N pulses is $F_N(S) = \left[\frac{1}{1 + S(1 + \bar{X})}\right]^N$, and $f_N(Y)dY$ is determined to be

$$f_N(Y)dY = \frac{\alpha^N Y^{N-1} e^{-\alpha Y}}{(N-1)!} dY \qquad (V.13)$$

where we let $\alpha = \frac{1}{1 + \bar{X}}$

Then $$F_N(\alpha,\beta) = \frac{\alpha^N}{(N-1)!} \int_{\alpha\beta}^{\infty} Y^{N-1} e^{-\alpha Y} dY \qquad (V.14)$$

$$F_N(\alpha,\beta) = \frac{1}{(N-1)!} \int_{\alpha\beta}^{\infty} Y^{N-1} e^{-Y} dy = \frac{\Gamma(N,\alpha\beta)}{\Gamma(N)} \qquad (V.15)$$

$$F_N(\alpha,\beta) = e^{-\alpha\beta} \sum_{K=0}^{N-1} \frac{(\alpha\beta)^K}{K!} \qquad (V.16)$$

For the Case 4 model, the characteristic function for equation (V.12) where in this case $f(Z_i,\bar{X}_i)dZ_i = \frac{4Z}{\bar{X}^2} e^{-2Z/X} dZ$ is

$$F_1(S) = \frac{1 + S}{\left[1 + S(1 + \frac{\bar{X}}{2})\right]^2} \qquad \text{(See reference 5)} \qquad (V.17)$$

and for the sum of N pulses $$F_N(S) = \frac{(1 + S)^N}{(1 + S/\alpha)^{2N}} \qquad (V.18)$$

where $\alpha = \frac{1}{1 + \bar{X}/2}$

The assertion is made that

$$f_N(Y)dy = \alpha^{2N} \sum_{n=0}^{N} \frac{N!(1 - \alpha)^n Y^{N+n-1} e^{-\alpha Y}}{(N+n-1)!\ (N-n)!\ n!} dY \qquad (V.19)$$

The proof follows from a calculation of $f_N(S) = \int_0^{\infty} f_N(Y)\, e^{-SY} dY$

$$f_N(S) = \alpha^{2N} \sum_{n=0}^{N} \frac{N!(1-\alpha)^n}{(N+n-1)!\,(N-n)!\,n!} \int_0^\infty Y^{N+n-1}\, e^{-(S+\alpha)}\, dY \qquad (V.20)$$

$$= \alpha^{2N} \sum_{n=0}^{N} \frac{N!\,(1-\alpha)^n}{(N-n)!\,n!\,(S+\alpha)^{N+n}} \qquad (V.21)$$

$$= \frac{\alpha^{2N}}{(S+\alpha)^N}\left[1 + \left(\frac{1-\alpha}{S+\alpha}\right)\right]^N = \frac{\alpha^{2N}\,(1+S)^N}{(\alpha+S)^{2N}} = \frac{(1+S)^N}{\left(1+\frac{S}{\alpha}\right)^{2N}} \qquad (V.22)$$

The computation of $F_N(\alpha,\beta) = \int_\beta^\infty f_N(Y)dY$ is based on considering:

$$\int_\beta^\infty t^m\, e^{-\alpha t}\, dt = \frac{1}{\alpha^{m+1}} \int_{\alpha\beta}^\infty X^m\, e^{-X}\, dX = \frac{m!}{\alpha^{m+1}} \Gamma(m+1,\alpha\beta) \qquad (V.23)$$

$$= \frac{m!}{\alpha^{m+1}}\, e^{-\alpha\beta} \sum_{K=0}^{m} \frac{(\alpha\beta)^K}{K!} \qquad (V.24)$$

and so $$\int_\beta^\infty f_n(Y)dY = \alpha^{2N} \sum_{n=0}^{N} \frac{N!\,(1-\alpha)\,(N+n-1)!\,e^{-\alpha\beta}}{(N+n-1)!\,(N-n)!\,n!\,\alpha^{n+M}} \sum_{K=0}^{N+n-1} \frac{(\alpha\beta)^K}{K!} \qquad (V.25)$$

and finally,

$$F_N(\alpha,\beta) = \int_\beta^\infty f_N(Y)dY = \alpha^N\, e^{-\alpha\beta} \sum_{n=0}^{N} \frac{N!\,\left(\frac{1-\alpha}{\alpha}\right)^n}{n!\,(N-n)!} \sum_{K=0}^{N+n-1} \frac{(\alpha\beta)^K}{K!} \qquad (V.26)$$

For both Equations (V.16) and (V.25), if α is set equal to 1 (that is the noise along case where $\bar{X} = 0$), the probability of a false report at a particular step $G_N(\beta)$ is obtained

$$G_N(\beta) = e^{-\beta} \sum_{n=0}^{N-1} \frac{\beta^K}{K!} \qquad (V.27)$$

APPENDIX VI

DETAILED ANALYTICAL PROCEDURE FOR THE DEVELOPMENT OF AN EWSD FOR THE NON-FLUCTUATING TARGET WITH A MAXIMUM OF TWO STEPS

Fluctuating Target with a Maximum of Two Steps

The surveillance mode optimization procedure detailed here for the detection of the non-fluctuating target, where a maximum of two steps are used, is typical of the procedure employed in the development of the EWSD's for the slowly fluctuating class of targets (the non-fluctuating and cases #1 and #3 target types).

The specified surveillance inputs are the probability of detection (P_{DO}), the probability of false alarm (P_{FO}), and the effective number of resolution elements (N_P).

The constraint relationships are:

$$P_D = Q(\alpha_1, \beta_1)\, Q(\alpha_2, \beta_2) = P_{DO} \tag{6.1}$$

$$\beta_1^2 + \beta_2^2 = 2 \ln \frac{1}{P_{FO}} \tag{6.2}$$

The cost function to be minimized is:

$$C = \frac{\alpha_1^2}{2} + \frac{\alpha_2^2}{2} N_P e^{-\beta_1^2/2} \tag{6.3}$$

We now set up the LaGrange function:

$$L = \left(\frac{\alpha_1^2}{2} + \frac{\alpha_2^2}{2} N_P e^{-\beta_1^2/2} \right) + \tau \left[Q(\alpha_1, \beta_1)\, Q(\alpha_2, \beta_2) \right] + \mu \left[\frac{\beta_1^2 + \beta_2^2}{2} \right] \tag{6.4}$$

and equate to zero the partial derivatives with respect to the design degrees of freedom $[\alpha_1, \alpha_2, \beta_1, \beta_2]$.

$$\frac{\partial L}{\partial \alpha_1} = 0 = \alpha_1 + \tau Q_1 \alpha Q_2 \tag{6.5}$$

$$\frac{\partial L}{\partial \alpha_2} = 0 = -\alpha_2 N_F e^{-\beta_1^2/2} + \lambda Q_1 Q_2 \alpha \tag{6.6}$$

$$\frac{\partial L}{\partial \beta_1} = 0 = -\beta_1 \frac{\alpha_2^2}{2} N_F e^{-\beta_1^2/2} + \lambda Q_1 \beta Q_2 + \mu \beta_1 \tag{6.7}$$

$$\frac{\partial L}{\partial \beta_2} = 0 = \lambda Q_1 Q_2 \beta + \mu \beta_2 \tag{6.8}$$

Now using (5) and (8) we relate the Lagrange multipliers μ and λ

$$\mu = -\lambda Q_1 Q_2 \beta \quad \text{and (10)} \quad \lambda = -\frac{\alpha_2 N_F e^{-\beta_1^2/2}}{Q_1 Q_2 \alpha} \tag{6.9}$$

We have introduced the following symbolism relating to the Q function and its derivatives:

$$Q_i = Q(\alpha_i, \beta_i) = \int_{\beta_i}^{\infty} X_i e^{-\frac{X_i^2 + \alpha_i^2}{2}} I_0(\alpha_i X_i) dX_i \quad i = 1,2 \tag{6.10}$$

$$Q_\alpha = \frac{\partial Q(\alpha, \beta)}{\partial \alpha} = \beta e^{-\frac{1}{2}(\alpha^2 + \beta^2)} I_1(\alpha \beta) \tag{6.11}$$

$$Q_\beta = \frac{\partial Q(\alpha, \beta)}{\partial \beta} = -\beta e^{-\frac{1}{2}(\alpha^2 + \beta^2)} I_0(\alpha \beta) \tag{6.12}$$

$$Q_{\alpha\alpha} = \frac{\partial^2 Q(\alpha, \beta)}{\partial \alpha^2} = -\left(\alpha + \frac{1}{\alpha}\right) Q_\alpha - \beta Q_\beta \tag{6.13}$$

$$Q_{\alpha\beta} = \frac{\partial^2 Q(\alpha, \beta)}{\partial \alpha \partial \beta} = -\alpha Q_\beta - \beta Q_\alpha \tag{6.14}$$

$$Q_{\beta\beta} = \frac{\partial^2 Q(\alpha, \beta)}{\partial \beta^2} = \left[\frac{1}{\beta} - \beta\right] Q_\beta - \alpha Q_\alpha \tag{6.15}$$

We now eliminate the Lagrange multipliers from 6.6 and 6.7 and define the quantities f_1, f_2, f_3 and f_4.

$$f_1 = \alpha_1 Q_1 Q_{2\alpha} - \alpha_2 N_F e^{-\beta_1^2/2} Q_{1\alpha} Q_2 = 0 \tag{6.16}$$

$$f_2 = \frac{\alpha_2}{2} Q_1 Q_{2\alpha} + \frac{1}{\beta_1} Q_{1\beta} Q_2 - \frac{1}{\beta_2} Q_1 Q_{2\beta} = 0 \tag{6.17}$$

$$f_3 = \beta_1^2 + \beta_2^2 - 2 \ln \frac{1}{P_{FO}} = 0 \tag{6.18}$$

$$f_4 = Q_1 Q_2 - P_{DO} = 0 \tag{6.19}$$

We now seek a solution to equations 6.16 through 6.19 for the variables $\alpha_1, \alpha_2, \beta_1$ and β_2 by means of the Newton's iteration

$$(\alpha_1^{J+1}, \alpha_2^{J+1}, \beta_1^{J+1}, \beta_2^{J+1}) = (\alpha_1^J, \alpha_2^J, \beta_1^J, \beta_2^J) + (\Delta\alpha_1^J, \Delta\alpha_2^J, \Delta\beta_1^J, \Delta\beta_2^J) \tag{6.20}$$

and where the starting values $(\alpha_1^0, \alpha_2^0, \beta_1^0, \beta_2^0)$ are suitably selected, and where:

$$\begin{pmatrix} \Delta\alpha_1^J \\ \Delta\alpha_2^J \\ \Delta\beta_1^J \\ \Delta\beta_2^J \end{pmatrix} = \begin{pmatrix} \frac{\partial f_1^J}{\partial\alpha_1} & \frac{\partial f_1^J}{\partial\alpha_2} & \frac{\partial f_1^J}{\partial\beta_2} & \frac{\partial f_1^J}{\partial\beta_2} \\ \frac{\partial f_2^J}{\partial\alpha_1} & \frac{\partial f_2^J}{\partial\alpha_2} & \frac{\partial f_2^J}{\partial\beta_1} & \frac{\partial f_2^J}{\partial\beta_2} \\ \frac{\partial f_3^J}{\partial\alpha_1} & \frac{\partial f_3^J}{\partial\alpha_2} & \frac{\partial f_3^J}{\partial\beta_1} & \frac{\partial f_3^J}{\partial\beta_2} \\ \frac{\partial f_4^J}{\partial\alpha_1} & \frac{\partial f_4^J}{\partial\alpha_2} & \frac{\partial f_4^J}{\partial\beta_1} & \frac{\partial f_4^J}{\partial\beta_2} \end{pmatrix}^{-1} \begin{pmatrix} -f_1^J \\ -f_2^J \\ -f_3^J \\ -f_4^J \end{pmatrix} \tag{6.21}$$

and where the 16 partial derivatives in the 4 x 4 matrix are defined as follows:

$$\frac{\partial f_1}{\partial \alpha_1} = Q_1 Q_{2\alpha} - \alpha_1 Q_{1\alpha} Q_{2\alpha} - \alpha_2 N_F e^{-\beta_1^2/2} Q_{1\alpha\alpha} Q_2 \tag{6.22}$$

$$\frac{\partial f_1}{\partial \alpha_2} = \alpha_1 Q_1 Q_{2\alpha\alpha} - N_F e^{-\beta_1^2/2} Q_{1\alpha} Q_2 - \alpha_2 N_F e^{-\beta_1^2/2} Q_{1\alpha} Q_{2\alpha} \tag{6.23}$$

$$\frac{\partial f_1}{\partial \beta_1} = \alpha_1 Q_{1\beta} Q_{2\alpha} + \beta_1 \alpha_2 N_F e^{-\beta_1^2/2} Q_{1\alpha} Q_2 - \alpha_2 N_F e^{-\beta_1^2/2} Q_{1\alpha\beta} Q_2 \tag{6.24}$$

$$\frac{\partial f_1}{\partial \beta_2} = \alpha_1 Q Q_{2\alpha\beta} - \alpha_2 N_F e^{-\beta_1^2/2} Q_{1\alpha} Q_{2\beta} \tag{6.25}$$

$$\frac{\partial f_2}{\partial \alpha_1} = \frac{\alpha_2}{2} Q_{1\alpha} Q_{2\alpha} + \frac{1}{\beta_1} Q_{1\alpha\beta} Q_2 - \frac{1}{\beta_2} Q_{1\alpha} Q_{2\beta} \tag{6.26}$$

$$\frac{\partial f_2}{\partial \alpha_2} = \frac{Q_1 Q_{2\alpha}}{2} + \frac{\alpha_2}{2} Q_1 Q_{2\alpha\alpha} + \frac{1}{\beta_1} Q_{1\beta} Q_{2\alpha} - \frac{1}{\beta_2} Q_1 Q_{2\alpha\beta} \tag{6.27}$$

$$\frac{\partial f_2}{\partial \beta_1} = \frac{\alpha_2}{2} Q_{1\beta} Q_{2\alpha} - \frac{1}{\beta_1^2} Q_{1\beta} Q_2 + \frac{1}{\beta_1} Q_{1\beta\beta} Q_2 - \frac{1}{\beta_2} Q_{1\beta} Q_{2\beta} \tag{6.28}$$

$$\frac{\partial f_2}{\partial \beta_2} = \frac{\alpha_2}{2} Q_1 Q_{2\alpha\beta} + \frac{1}{\beta_1} Q_{1\beta} Q_{2\beta} + \frac{1}{\beta_2^2} Q_1 Q_{2\beta} - \frac{1}{\beta_2} Q_1 Q_{2\beta\beta} \tag{6.29}$$

$$\frac{\partial f_3}{\partial \alpha_1} = 0 \tag{6.30}$$

$$\frac{\partial f_3}{\partial \alpha_2} = 0 \tag{6.31}$$

$$\frac{\partial f_3}{\partial \beta_1} = 2\beta_1 \tag{6.30}$$

(32)

$$\frac{\partial f_3}{\partial \beta_2} = 2\beta_2 \tag{6.33}$$

(33)

$$\frac{\partial \ell_4}{\partial \alpha_1} = Q_1 \alpha Q_2 \tag{6.34}$$

$$\frac{\partial \ell_4}{\partial \alpha_2} = Q_1 \quad Q_2 \alpha \tag{6.35}$$

$$\frac{\partial \ell_4}{\partial \beta_1} = Q_1 \beta Q_2 \tag{6.36}$$

$$\frac{\partial \ell_4}{\partial \beta_2} = Q_1 Q_2 \beta \tag{6.37}$$

UNCLASSIFIED
Security Classification

DOCUMENT CONTROL DATA - R&D
(Security classification of title, body of abstract and indexing annotation must be entered when the overall report is classified)

1 ORIGINATING ACTIVITY (Corporate author) Radio Corporation of America Missile and Surface Radar Division Moorestown, New Jersey	2a. REPORT SECURITY CLASSIFICATION Unclassified 2b GROUP

3 REPORT TITLE

Optimum Radar Surveillance Modes

4 DESCRIPTIVE NOTES (Type of report and inclusive dates)
Final Report - April 1964-February 1965

5 AUTHOR(S) (Last name, first name, initial)

Mr. Harold Finn

6 REPORT DATE	7a TOTAL NO. OF PAGES	7b. NO. OF REFS
September 1965	154	15

8a. CONTRACT OR GRANT NO. AF30(602)-3152 b. PROJECT NO. 4506 c. Task No. 450601 d System 760B	9a. ORIGINATOR'S REPORT NUMBER(S) 9b. OTHER REPORT NO(S) (Any other numbers that may be assigned this report) RADC-TR-65-77

10. AVAILABILITY/LIMITATION NOTICES

Available from DDC and CFSTI.

11. SUPPLEMENTARY NOTES	12. SPONSORING MILITARY ACTIVITY
	Rome Air Development Center Griffiss Air Force Base, New York

13 ABSTRACT A second-phase study of radar multiple-stage decision processors which minimize the average transmitter power and data processing costs for performing the surveillance mission are described. Energy Variant Sequential Detector (EVSD) theory is reviewed. Verification of theoretical performance predictions obtained with a digital computer simulation program reveals a deviation of simulated performance of less than 1% of predicted results. A sequential detection scheme for performing high-resolution surveillance missions where relatively large time-bandwidth products are involved is described. These modes (Resolution-Variant EVSD's) use the programmed control of the time-bandwidth product of the transmitted signal, the transmitted energy, and the receiver thresholds on the sequential steps employed in order to minimize both the transmitter power and the parallel signal processing costs. An active correlator system is concluded to be the most economical means for meeting the signal processor flexibility requirements for this mode, and the implementation of a Resolution-Variant EVSD where requirements include over a 150-MC bandwidth on the final sequential step is described. The resolution-variant signal processor required for efficient performance of future high-resolution surveillance missions is determined to be a critical component requiring further development. General implementation of EVSD's is reviewed. Only in the case of the high resolution surveillance mission is a critical component involved. In general, the radar implementation of EVSD's is concluded to be well within the state of the design art, and they are shown to avoid implementation problems associated with other sequential detection modes. The optimum scan time to be used when EVSD's are employed for each scan look is developed for both the case where the target is pointing directly at the radar, and the case where the target range is assumed relatively constant for the time duration in the surveillance volume. EVSD modes which include an option on the time interval between (over)

DD FORM 1 JAN 64 1473

UNCLASSIFIED
Security Classification

UNCLASSIFIED
Security Classification

14 KEY WORDS	LINK A		LINK B		LINK C	
	ROLE	WT	ROLE	WT	ROLE	WT
Phased Array Radar Sequential Detection						

Abstract (continued)
sequential steps are described, and the additional power savings over the use of a conventional EVSD are computed.

INSTRUCTIONS

1. ORIGINATING ACTIVITY: Enter the name and address of the contractor, subcontractor, grantee, Department of Defense activity or other organization *(corporate author)* issuing the report.

2a. REPORT SECURITY CLASSIFICATION: Enter the overall security classification of the report. Indicate whether "Restricted Data" is included. Marking is to be in accordance with appropriate security regulations.

2b. GROUP: Automatic downgrading is specified in DoD Directive 5200.10 and Armed Forces Industrial Manual. Enter the group number. Also, when applicable, show that optional markings have been used for Group 3 and Group 4 as authorized.

3. REPORT TITLE: Enter the complete report title in all capital letters. Titles in all cases should be unclassified. If a meaningful title cannot be selected without classification, show title classification in all capitals in parenthesis immediately following the title.

4. DESCRIPTIVE NOTES: If appropriate, enter the type of report, e.g., interim, progress, summary, annual, or final. Give the inclusive dates when a specific reporting period is covered.

5. AUTHOR(S): Enter the name(s) of author(s) as shown on or in the report. Enter last name, first name, middle initial. If military, show rank and branch of service. The name of the principal author is an absolute minimum requirement.

6. REPORT DATE: Enter the date of the report as day, month, year; or month, year. If more than one date appears on the report, use date of publication.

7a. TOTAL NUMBER OF PAGES: The total page count should follow normal pagination procedures, i.e., enter the number of pages containing information.

7b. NUMBER OF REFERENCES: Enter the total number of references cited in the report.

8a. CONTRACT OR GRANT NUMBER: If appropriate, enter the applicable number of the contract or grant under which the report was written.

8b, 8c, & 8d. PROJECT NUMBER: Enter the appropriate military department identification, such as project number, subproject number, system numbers, task number, etc.

9a. ORIGINATOR'S REPORT NUMBER(S): Enter the official report number by which the document will be identified and controlled by the originating activity. This number must be unique to this report.

9b. OTHER REPORT NUMBER(S): If the report has been assigned any other report numbers *(either by the originator or by the sponsor)*, also enter this number(s).

10. AVAILABILITY/LIMITATION NOTICES: Enter any limitations on further dissemination of the report, other than those imposed by security classification, using standard statements such as:

(1) "Qualified requesters may obtain copies of this report from DDC."

(2) "Foreign announcement and dissemination of this report by DDC is not authorized."

(3) "U. S. Government agencies may obtain copies of this report directly from DDC. Other qualified DDC users shall request through _____."

(4) "U. S. military agencies may obtain copies of this report directly from DDC. Other qualified users shall request through _____."

(5) "All distribution of this report is controlled. Qualified DDC users shall request through _____."

If the report has been furnished to the Office of Technical Services, Department of Commerce, for sale to the public, indicate this fact and enter the price, if known.

11. SUPPLEMENTARY NOTES: Use for additional explanatory notes.

12. SPONSORING MILITARY ACTIVITY: Enter the name of the departmental project office or laboratory sponsoring *(paying for)* the research and development. Include address.

13. ABSTRACT: Enter an abstract giving a brief and factual summary of the document indicative of the report, even though it may also appear elsewhere in the body of the technical report. If additional space is required, a continuation sheet shall be attached.

It is highly desirable that the abstract of classified reports be unclassified. Each paragraph of the abstract shall end with an indication of the military security classification of the information in the paragraph, represented as *(TS), (S), (C), or (U)*

There is no limitation on the length of the abstract. However, the suggested length is from 150 to 225 words.

14. KEY WORDS: Key words are technically meaningful terms or short phrases that characterize a report and may be used as index entries for cataloging the report. Key words must be selected so that no security classification is required. Identifiers, such as equipment model designation, trade name, military project code name, geographic location, may be used as key words but will be followed by an indication of technical context. The assignment of links, rules, and weights is optional.